Pathways to proteinuria

Khalil, R.

PATHWAYS TO PROTEINURIA

Ramzi Khalil

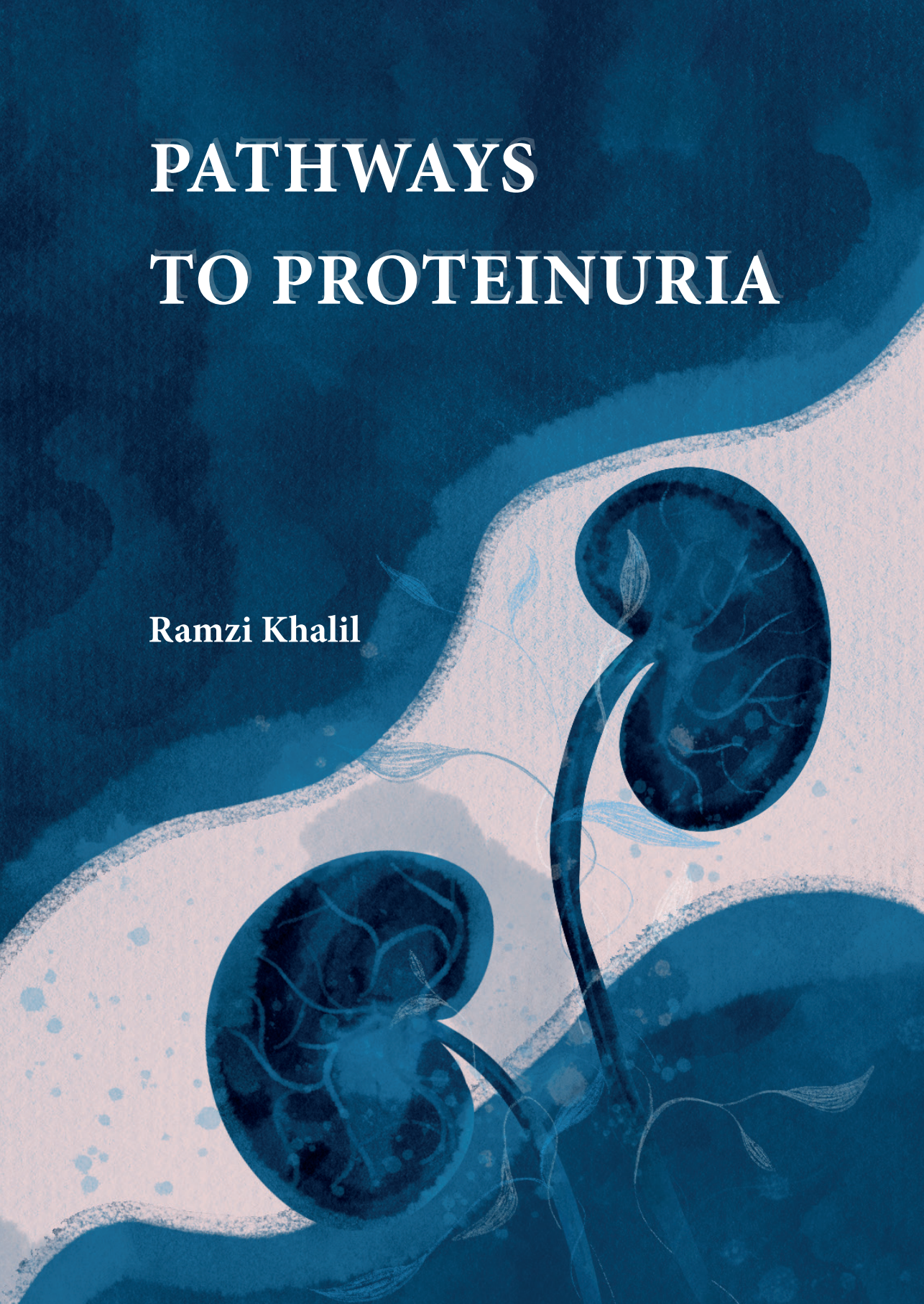

PATHWAYS TO PROTEINURIA

Ramzi Khalil

Pathways to proteinuria

ISBN: 978-94-6506-090-3
Cover design: Ramzi Khalil & Ridderprint | www.ridderprint.nl
Layout: Ridderprint | www.ridderprint.nl
Printing: Ridderprint | www.ridderprint.nl

PATHWAYS TO PROTEINURIA

Proefschrift

ter verkrijging van
de graad van doctor aan de Universiteit Leiden
op gezag van rector magnificus prof. dr. ir. H. Bijl,
volgens besluit van het college voor promoties
te verdedigen op dinsdag 4 juni 2024
klokke 13.45

door

Ramzi Khalil
geboren te Leiden
in 1991

Promotores

Prof. dr. P.C.W. Hogendoorn
Prof. dr. A.J. Rabelink

Co-promotor

Dr. J.J. Baelde

Promotiecommisie

Prof. dr. Y.K.O. Teng	
Dr. J. van den Born	*University Medical Center Groningen*
Prof. Dr. J. van der Vlag	*Radboud University Medical Center*
Prof. Dr. S. Florquin	*Amsterdam Medical Center*

Table of Contents

Chapter 1.	General introduction and outline	7
Chapter 2.	Cystinosis (ctns) zebrafish mutant shows pronephric glomerular and tubular dysfunction	17
Chapter 3.	Glomerular permeability is not affected by heparan sulfate glycosaminoglycan deficiency in zebrafish embryos	47
Chapter 4.	Mutations in the heparan sulfate backbone elongating enzymes EXT1 and EXT2 have no major effect on endothelial glycocalyx and the glomerular filtration barrier	65
Chapter 5.	Increased dynamin expression precedes proteinuria in glomerular disease	83
Chapter 6.	Transmembrane Protein 14A protects glomerular filtration barrier integrity	103
Chapter 7.	General discussion and future perspectives	121
Appendices	Nederlandse samenvatting	138
	Curriculum vitae	144
	List of publications	145
	Dankwoord	146

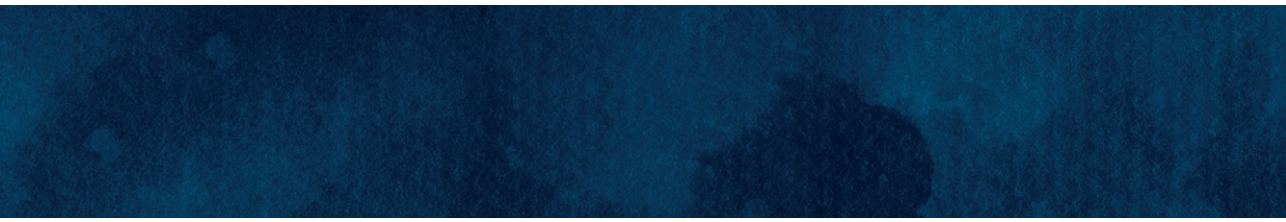

CHAPTER 1

General introduction and outline

Proteinuria and chronic kidney disease

Proteinuria is an independent predictor of the progression of kidney injury, cardiovascular morbidity, and overall mortality (1). Under physiological circumstances, no sustained proteinuria is present. Proteinuria only occurs when serum proteins are able to pass the glomerular filtration barrier and when tubular reabsorption mechanisms are saturated or fail. Damage to any of these components can result in proteinuria. Moreover, although the mechanisms of damage and disease vary across the different types of renal diseases, many still lead to proteinuria and can result in chronic kidney disease (CKD). CKD is classified according to the remaining glomerular filtration rate and the amount of proteinuria in the Kidney Disease Improving Global Outcomes (KDIGO) guidelines (2).

The prevalence of CKD is expected to rise further due to an aging population. The 2019 'Global burden of disease study' reports that chronic kidney disease rose from rank 29 to 18 between 1990 and 2019 as a cause for disease-adjusted life years (3). In the Netherlands, an estimated 12% of the population suffers from chronic kidney disease (CBS/nierstichting). Treatment of underlying disease and general cardiovascular risk management such as treating hypertension and dyslipidaemia are still the cornerstone of management of chronic kidney disease (CKD) and attenuating proteinuria. A specific treatment for proteinuria might become feasible when the pathways leading to proteinuria are elucidated further. For this, a closer investigation of the structures and mechanisms that normally prevent proteinuria from occurring is required.

The glomerular filtration barrier

Figure 1 shows an overview of human renal anatomy with each image going into more detail. Most humans have two kidneys as seen in the top left image. They are located in the retroperitoneal space. The parenchyma of the kidney is usually divided in the outer cortex and inner medulla. Each human kidney contains around one million functional units called nephrons. Each nephron consists of a glomerulus and a tubular apparatus, shown in the detail of the sagittal image of the human kidney. The glomerulus, seen in the top right, is a specialized capillary bed that starts with the afferent arteriole which comes from the renal artery, which in turn directly sprouts from the abdominal aorta. 20 to 25% of cardiac output is routed to the kidneys, where it first passes the glomerulus. There, around 20% of passing serum is filtered by passing the glomerular filtration barrier, and the other 80% continues through the efferent arteriole to the peritubular capillaries where both active and passive secretion and reabsorption take place. The entire glomerular capillary bed is lined by the glomerular filtration barrier, shown in the middle image. Below, the detail shows a schematic overview of the distinct structures

of the glomerular filtration barrier. The glomerular filtration barrier is made up of the glomerular endothelial glycocalyx layer (purple), fenestrated endothelial cells (red), glomerular basement membrane (grey), and the visceral epithelial cells (yellow) – or podocytes – with interdigitating foot processes (green).

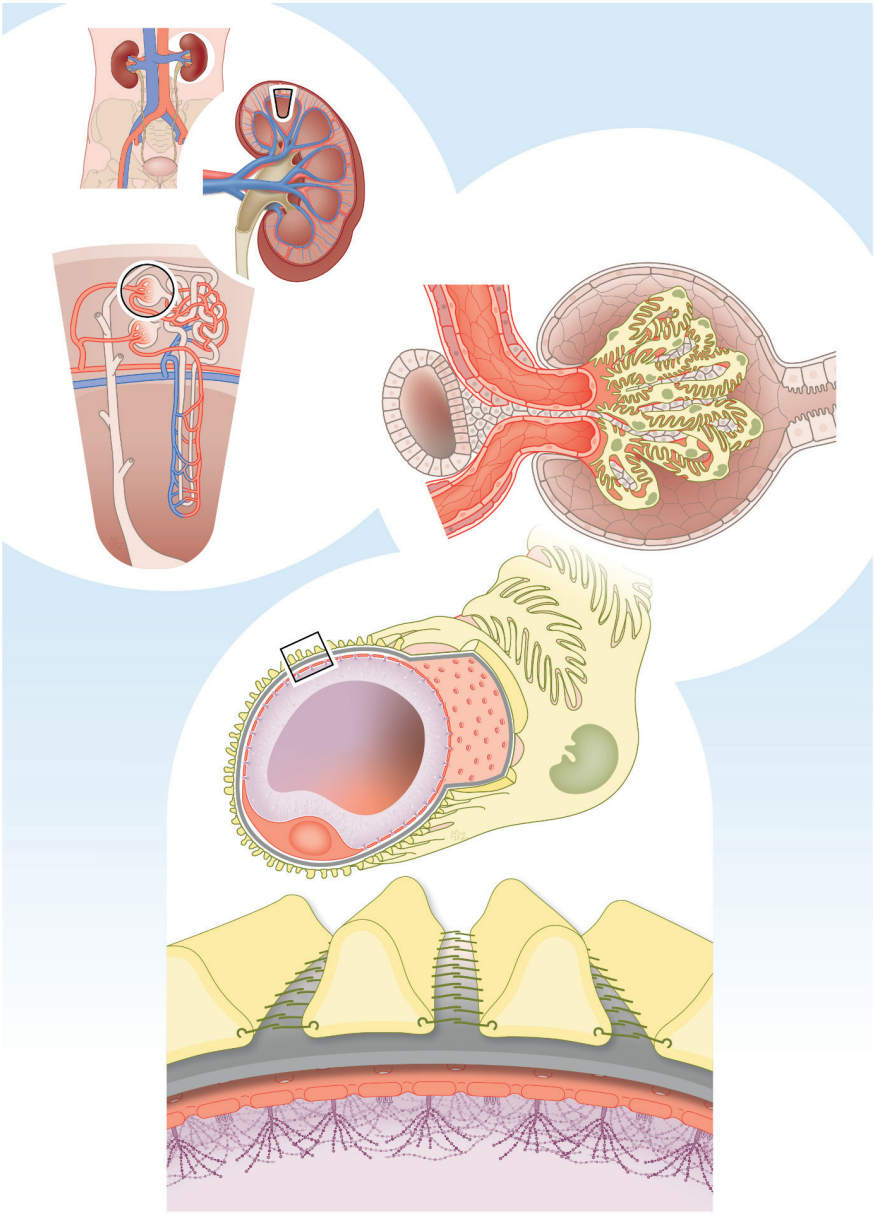

Figure 1. The human kidney, nephron, glomerulus, glomerular capillary, and glomerular filtration barrier

Glycocalyx and fenestrated endothelial cell

The first layer of the glomerular filtration barrier is the glycocalyx. As the name implies, it consists mostly of various 'sugary' chains, which consist of negatively charged heparan sulphate glycosaminoglycan chains attached to heparan sulphate core proteins and hyaluronan. The glycocalyx has a role in mitigating inflammation, and coagulation.(4) The glycocalyx lines the specialized endothelial cells of the glomerulus. These endothelial cells have the distinguishing feature of being fenestrated with 60 nm pores. The negatively charged glycocalyx covering these pores is considered to be the first barrier between the vascular lumen and the ultrafiltrate that serum proteins such as albumin encounter. In end-stage renal disease, damage to the structural integrity and composition of the glycocalyx is observed.(5) Also, in experimental models where damage to the glycocalyx is induced, proteinuria occurs. As such, it is thought to be a vital part of the glomerular filtration barrier in the protection against proteinuria.

Glomerular basement membrane

The next layer is the glomerular basement membrane (GBM). It is an extracellular matrix that is proximally deposited by the glomerular endothelial cells and the visceral epithelial cell on the distal end. On electron microscopy, three GBM layers can be distinguished. These are the lamina rara interna on the vascular side, the lamina densa, and the lamina rara externa adjacent to the epithelial side. The GBM mainly contains laminin, collagen type IV, and heparan sulphate proteoglycans. It normally has a thickness between 300 and 400 nm. The GBM has an overall negative charge due to the sulphated glycosaminoglycan chains of the heparan sulphate proteoglycan aggregates.

Heparan sulphate glycosaminoglycans

Glomerular filtration occurs with both size and charge selectivity (6). Maintaining this selectivity and GFB integrity has long been attributed to heparan sulphate glycosaminoglycans (7, 8). As stated above, they are localized in both the glycocalyx and GBM. Heparan sulphate glycosaminoglycan chains consist of repeating disaccharide motifs that contain a uronic acid and a glucosamine derivative. Theoretically, up to 48 different motifs can be formed. Heparan sulphate synthesis starts with chain initiation, where a tetrasaccharide linkage region is formed and is covalently bound to a core protein. The next phase of HS synthesis consists of chain polymerization, which is dependent on enzymes encoded by the *EXT1* and *EXT2* genes. These enzymes form a co-polymerase that adds repeating disaccharide units consisting of D-glucuronic acid (GlcAβ4) and *N*-acetyl-glucosamine (GlcNAcα4). During chain polymerization, the polymer is also modified

by various sulfotransferases and an epimerase leading to GlcNAc N-deacetylation/N-sulfation, epimerization of GlcA to L-iduronic acid (IdoA), and 2, 3, and 6-O-sulfation. These modifications not only result in an overall negative charge, but also the formation of ligand binding sites, such as FGF-2, antithrombin, chemokines, and cytokines. Thus, when chain polymerization is impaired due to a lack of EXT1 or EXT2, no modification can take place and hence the heparan sulphate is functionally impaired.(9)

Podocyte and slit diaphragm

Lastly, the distal end of the GFB is covered by visceral epithelial cells or podocytes. Podocytes gained their name from the Greek words podos (ποδος), which means foot, and kutos (κύτος), meaning jar or vessel, and used as a term to describe cells. One of the characteristics of podocytes is the presence of interdigitating foot processes called pedicles. The remaining space between these processes creates so-called filtration pores or slit diaphragms. The diaphragm is not an open connection to Bowman's space. Adjacent foot processes are connected by nephrin (*NPHS1*) and NEPH1 (*KIRREL1*).(10) These proteins connect adjacent foot processes by spanning the slit diaphragm and attaching to the actin cytoskeleton of podocytes.

The actin cytoskeleton and dynamin

When podocytes are damaged, loss of architectural organization of the cytoskeleton occurs, which leads to retraction and effacement of the podocyte and its foot processes. The pathways and proteins responsible for podocyte cytoskeletal organization are steadily being uncovered. One of these proteins is dynamin, a small GTPase that is primarily known for its role clathrin-coated vesicle budding in neurons. It has now been described to be involved in the turnover of nephrin, regulation of actin, and endocytosis of albumin by podocytes, making it a potential future therapeutical target for preventing proteinuria. (11-14)

Tubular reabsorption mechanisms

After passing the glomerular filtration barrier, the ultrafiltrate enters Bowman's space. Afterwards, the ultrafiltrate passes various parts of the tubule, where its content is altered through re-absorption and secretion which occur in both active and passive manners. Normally, when serum proteins such as albumin are indeed able to pass the glomerular filtration barrier, they are re-absorbed by proximal tubular epithelial cells. Tubular reabsorption mechanisms are not only responsible for the re-absorption of filtered protein, but also that of for example urea, bicarbonate, phosphate, glucose, and

sodium. The first part of ultrafiltrate is isotonic to serum, and as such, active processes are required to reabsorb these solutes. Hence, the proximal tubule epithelial cells possess many mitochondria to facilitate these active processes. On the tubular luminal side, these cells are lined with microvilli which form the brush border, which significantly increases the luminal surface area. It is here that solutes and colloids are reabsorbed. Some groups have provided evidence that albumin does in fact pass the glomerular filtration barrier in much greater quantities than previously thought. They claim that tubular reabsorption mechanisms thus play a larger role in preventing proteinuria than has been attributed to them before.(15) Although the relative contribution to preventing proteinuria is controversial, there is a general consensus that adequate tubular reabsorption mechanisms are required to prevent, at least in part, the loss of protein in the urine. A complete loss of tubular reabsorption function results in Fanconi syndrome. This syndrome is characterized by proteinuria and severe acid-base and electrolyte disorders. In children, the most common cause of Fanconi syndrome is nephropathic cystinosis. Nephropathic cystinosis is a lysosomal storage disorder that results in cystine crystal deposition in various tissues. The proximal tubule is usually the first affected site.

As stated above, pathological processes in any one of the GFB layers can lead to proteinuria. Although this has long been attributed to the individually affected layer, it is now deemed more likely that the glomerular filtration barrier functions as a whole unit and requires all components to properly function. Moreover, the GFB can be seen as a dynamic barrier with various repair and compensation mechanisms rather than a static barrier that only sieves particles based on size, weight, and hydrostatic pressure.

Identifying new targets

Identifying which components of the glomerular filtration barrier are needed to maintain proper barrier function is essential to identifying potential therapeutic options. Historically, the function of the various components of the glomerular filtration barrier has been discovered in patients with genetic defects leading to proteinuria.(16) More recently, experimental animal models have been used to identify genes and their encoded products that might be important in GFB function. For example, genetic association studies in proteinuric rats have identified a panel of various genes potentially involved in the development of proteinuria.(17) After identifying these genes in a previously described array, the candidate genes and their encoded proteins were then investigated further to establish whether a direct relation to the development of proteinuria is present. In multiple studies presented here, the method to examine whether a protein has a significant role in the development of proteinuria consisted of assessing whether knocking down mRNA

translation resulted in proteinuria in a zebrafish embryo model. Next, differential mRNA and protein expression are investigated in spontaneously proteinuric rats. In this step, the temporal relationship between the onset of proteinuria and relative loss of expression is assessed. Furthermore, the translation to human proteinuric kidney disease is made by examining the protein expression of the investigated targets in kidney biopsies from patients with proteinuric renal diseases.

These methods were used both to investigate known proteins, such as dynamin, but has also uncovered previously unknown proteins to be involved in the development of proteinuria, such as transmembrane protein 14A.

Aim and outline of the thesis

In this thesis, the pathways leading to proteinuria are explored. To identify potential pathways, elements considered essential are revisited, known pathways are explored further, and new players in the field of proteinuria are identified.

First, a zebrafish embryo model to assess both glomerular filtration barrier function and tubular reabsorption mechanisms is presented in **Chapter 2**. The use of this model for developing new therapeutic options for the rare but devastating disease of nephropathic cystinosis is presented.

In **Chapters 3** and **4**, the loss of heparan sulphate glycosaminoglycans is investigated. Heparan sulphate glycosaminoglycans have long been considered essential for adequate glomerular filtration function. In **Chapter 3,** a global heparan sulphate glycosaminoglycan deficiency on the development of proteinuria was shown to not affect glomerular filtration barrier function nor tubular reabsorption mechanisms. The used *dackel* zebrafish embryo mutant has a biallelic germline mutation in the zebrafish homologue of *EXT2*, resulting in truncated and functionally impaired heparan sulphate glycosaminoglycan chains. **Chapter 4** continues with investigating the loss of heparan sulphate glycosaminoglycans in multiple osteochondroma patients, who have a heterozygous mutation in either EXT1 or EXT2. Here, no proteinuria, a specific renal phenotype, or changes to the glomerular endothelial glycocalyx were observed.

In **Chapter 5**, the role of dynamin in proteinuric conditions and human disease is explored. Dynamin has been identified to play an important role in maintaining glomerular filtration barrier structure and function. In this chapter, this role is further specified as a dynamically regulated protective mechanism against the development of proteinuria.

A previously unknown factor in the development of proteinuria is transmembrane protein 14A, which is discussed in **Chapter 6**. It is described as a protective element in the development of proteinuria through experiments in cell culture, a zebrafish embryo model, proteinuric rats, and human proteinuric kidney diseases.

References

1. Matsushita K, van d, V, Astor BC, Woodward M, Levey AS, de Jong PE, et al. Association of estimated glomerular filtration rate and albuminuria with all-cause and cardiovascular mortality in general population cohorts: a collaborative meta-analysis. Lancet. 2010;375(9731):2073-81.
2. Group CW. KDIGO clinical practice guideline for the evaluation and management of chronic kidney disease. Kidney Int Suppl. 2013.
3. Diseases GBD, Injuries C. Global burden of 369 diseases and injuries in 204 countries and territories, 1990-2019: a systematic analysis for the Global Burden of Disease Study 2019. Lancet. 2020;396(10258):1204-22.
4. Dane MJ, van den Berg BM, Lee DH, Boels MG, Tiemeier GL, Avramut MC, et al. A microscopic view on the renal endothelial glycocalyx. Am J Physiol Renal Physiol. 2015;308(9):F956-66.
5. Dane MJ, Khairoun M, Lee DH, van den Berg BM, Eskens BJ, Boels MG, et al. Association of kidney function with changes in the endothelial surface layer. Clin J Am Soc Nephrol. 2014;9(4):698-704.
6. Rennke HG, Patel Y, Venkatachalam MA. Glomerular filtration of proteins: clearance of anionic, neutral, and cationic horseradish peroxidase in the rat. Kidney Int. 1978;13(4):278-88.
7. Kanwar YS, Farquhar MG. Presence of heparan sulfate in the glomerular basement membrane. Proc Natl Acad Sci U S A. 1979;76(3):1303-7.
8. Kanwar YS, Linker A, Farquhar MG. Increased permeability of the glomerular basement membrane to ferritin after removal of glycosaminoglycans (heparan sulfate) by enzyme digestion. J Cell Biol. 1980;86(2):688-93.
9. Esko JD, Selleck SB. Order out of chaos: assembly of ligand binding sites in heparan sulfate. Annu Rev Biochem. 2002;71:435-71.
10. Miner JH. Glomerular basement membrane composition and the filtration barrier. Pediatr Nephrol. 2011;26(9):1413-7.
11. Gu C, Chang J, Shchedrina VA, Pham VA, Hartwig JH, Suphamungmee W, et al. Regulation of dynamin oligomerization in cells: the role of dynamin-actin interactions and its GTPase activity. Traffic. 2014;15(8):819-38.
12. Gu C, Yaddanapudi S, Weins A, Osborn T, Reiser J, Pollak M, et al. Direct dynamin-actin interactions regulate the actin cytoskeleton. EMBO J. 2010;29(21):3593-606.
13. Sever S, Altintas MM, Nankoe SR, Moller CC, Ko D, Wei C, et al. Proteolytic processing of dynamin by cytoplasmic cathepsin L is a mechanism for proteinuric kidney disease. J Clin Invest. 2007;117(8):2095-104.
14. Soda K, Balkin DM, Ferguson SM, Paradise S, Milosevic I, Giovedi S, et al. Role of dynamin, synaptojanin, and endophilin in podocyte foot processes. J Clin Invest. 2012;122(12):4401-11.
15. Comper WD, Hilliard LM, Nikolic-Paterson DJ, Russo LM. Disease-dependent mechanisms of albuminuria. Am J Physiol Renal Physiol. 2008;295(6):F1589-600.
16. Tryggvason K, Patrakka J, Wartiovaara J. Hereditary proteinuria syndromes and mechanisms of proteinuria. N Engl J Med. 2006;354(13):1387-401.
17. Koop K, Eikmans M, Wehland M, Baelde H, Ijpelaar D, Kreutz R, et al. Selective loss of podoplanin protein expression accompanies proteinuria and precedes alterations in podocyte morphology in a spontaneous proteinuric rat model. Am J Pathol. 2008;173(2):315-26.

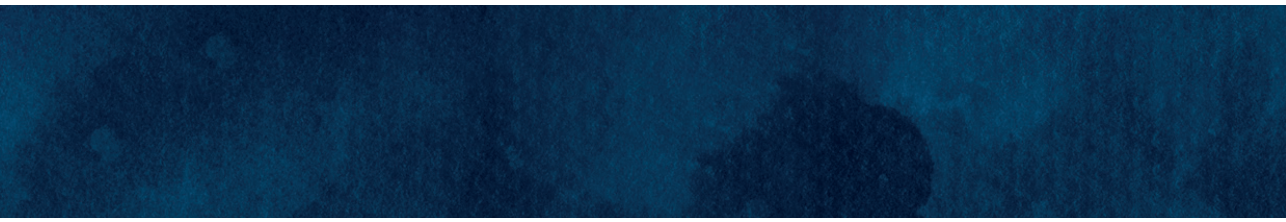

CHAPTER 2

Cystinosis (ctns) zebrafish mutant shows pronephric glomerular and tubular dysfunction

Scientific Reports 2017, 7, 42583

Mohamed A. Elmonem[1,2], Ramzi Khalil[3], Ladan Khodaparast[4], Laleh Khodaparast[4], Fanny O. Arcolino[1], Joseph Morgan[5], Anna Pastore[6], Przemko Tylzanowski[7,8], Annelii Ny[9], Martin Lowe[5], Peter A. de Witte[9], Hans J. Baelde[3],Lambertus P. van den Heuvel[1,10], Elena Levtchenko[1]*

[1] Department of Paediatric Nephrology & Growth and Regeneration, University Hospitals Leuven, KU Leuven, Leuven, Belgium

[2] Department of Clinical and Chemical Pathology, Faculty of Medicine, Cairo University, Cairo, Egypt

[3]Department of Pathology, Leiden University Medical Centre, the Netherlands

[4] Department of Cellular and Molecular Medicine, Switch Laboratory, VIB, University Hospitals Leuven, KU Leuven, Leuven, Belgium

[5]Faculty of Biology, Medicine and Health, University of Manchester, Manchester, United Kingdom

[6]Laboratory of Proteomics and Metabolomics, Children's Hospital and Research Institute "Bambino Gesù" IRCCS, Rome, Italy

[7]Department of Development and Regeneration, Laboratory for Developmental and Stem Cell Biology, Skeletal Biology and Engineering Research Centre, University of Leuven, Leuven, Belgium

[8]Department of Biochemistry and Molecular Biology, Medical University, Lublin, Poland

[9]Laboratory for Molecular Bio-discovery, Department of Pharmaceutical and Pharmacological Sciences, KU Leuven, Leuven, Belgium

[10]Department of Paediatric Nephrology, Radboud University Medical Centre, Nijmegen, the Netherlands

Abstract

The human ubiquitous protein cystinosin is responsible for transporting the disulphide amino acid cystine from the lysosomal compartment into the cytosol. In humans, Pathogenic mutations of *CTNS* lead to defective cystinosin function, intralysosomal cystine accumulation and the development of cystinosis. Kidneys are initially affected with generalized proximal tubular dysfunction (renal Fanconi syndrome), then the disease rapidly affects glomeruli and progresses towards end stage renal failure and multiple organ dysfunction. Animal models of cystinosis are limited, with only a *Ctns* knockout mouse reported, showing cystine accumulation and late signs of tubular dysfunction but lacking the glomerular phenotype. We established and characterized a mutant zebrafish model with a homozygous nonsense mutation (c.706C>T; p.Q236X) in exon 8 of *ctns*. Cystinotic mutant larvae showed cystine accumulation, delayed development, and signs of pronephric glomerular and tubular dysfunction mimicking the early phenotype of human cystinotic patients. Furthermore, cystinotic larvae showed a significantly increased rate of apoptosis that could be ameliorated with cysteamine, the human cystine depleting therapy. Our data demonstrate that, *ctns* gene is essential for zebrafish pronephric podocyte and proximal tubular function and that the *ctns*-mutant can be used for studying the disease pathogenic mechanisms and for testing novel therapies for cystinosis.

Introduction

Nephropathic cystinosis (MIM 219800) is an autosomal recessive lysosomal storage disorder characterized by the accumulation of the amino-acid cystine in the lysosomes of different body cells. It is caused by pathogenic mutations in the human *CTNS* gene encoding for cystinosin, the protein transporting cystine out of lysosomes[1]. In humans, cystinotic infants are born asymptomatic and stay healthy with normal growth parameters until approximately 6 months of life. After 6 months, infants manifest with dehydration, polyuria, polydipsia and rickets. The kidneys are initially affected in the form of defective proximal tubular reabsorption and increased urinary losses of amino-acids, glucose, phosphate, bicarbonate and proteins, or what is known as the renal Fanconi syndrome; however, this is usually rapidly followed by progressive glomerular damage, stunted growth and multiple organ dysfunction[2]. The aminothiol cysteamine, currently used as a specific treatment for cystinosis, can successfully deplete cystine in the lysosomal compartment and can delay the progression of the disease; however, it does not prevent the renal Fanconi syndrome and does not restore the lost renal function[3].

Over the past decade much interest has been given to study different pathogenic mechanisms of nephropathic cystinosis in an attempt to find better therapeutic agents targeting mechanisms other than cystine accumulation like autophagy[4,5], oxidative stress[6,7] and inflammation[8,9]. A successful mouse model for cystinosis was developed recently[10] and was beneficial in revealing many pathogenic aspects of the disease[11-15]. However, the experimentation on mammalian models is usually time consuming, expensive and limited to a small number of test subjects[16]. Moreover, the murine model of cystinosis has a milder renal phenotype compared to humans and does not show signs of glomerular dysfunction starting in humans in early childhood[17].

Zebrafish *(Danio rerio)* was introduced as an attractive alternative to study pathogenic aspects in many genetic diseases[18-23]. This isdue to their rapid *in vitro* development, high fecundity, lower maintenance cost, optical transparency of the fertilized embryo, sequenced genome and the availability of gene down-regulation and gene editing technologies[24]. Furthermore, they emerged as a promising vertebrate model to study renal biology and associated medical conditions, especially in the fish embryonic and larval stages[25,26]. The zebrafish embryonic kidney, which is a functional pronephros, consists of a pair of segmented nephrons sharing a single glomerulus and showing astonishing histologic and functional similarities to the human nephron. This structure is formed approximately 24 hours post fertilization (24 hpf) and actual blood filtration starts approximately at 48 hpf[27] offering a rapid and simple anatomical model for nephron

patterning[28], disease modeling[29,30], identification of new genes affecting glomerular function and tubulogenesis[16,31,32]and drug testing[33].

In the current study, we investigated the pathological and functional characteristics of the first zebrafish mutant model of nephropathic cystinosis. We elucidated the main pathophysiological defects causing the diseased phenotype, which can be used for targeting novel therapeutic approaches.

Results

Zebrafish ctns gene

The zebrafish *ctns*(ENSDARG00000008890) is a 10 exon gene in chromosome 11. It corresponds to the coding 10 out of 12 exons of the human *CTNS*(ENSG00000040531,17p13.2)[34]. The zebrafish Ctns protein (UniProt F1QM07, 384 aa) has a 60.2% amino-acid identity and 78.5% similarity to the human cystine transporter cystinosin (UniProt O60931, 367 aa), with 75.6% identity and 88.8% similarity in the regions of the seven transmembrane domains (Fig. 1a). The genetic zebrafish mutant line (*ctns*-/-) used in the current study is homozygous for the nonsense mutation c.706C>T (at the 10th base position of exon 8 of the zebrafish *ctns* gene) leading to a premature stop codon (TAA) and truncated protein at glutamine 236 (p.Q236X). The translation product is thus devoid of the last four transmembrane domains and both lysosomal targeting motifs at the 5th cytosolic loop and the C terminal tail, which is expected to render the protein non-functional (Fig. 1a, b). Up to date, no paralogue gene to *ctns* has been reported in zebrafish.

Morphology of ctns-/- zebrafish larvae

We initially evaluated the morphological phenotype of morphant and *ctns*-/- larvae at 4 days post fertilization (4 dpf) (N=191 and 334, respectively) in comparison to wild-type (wt) larvae (N=152) according to the grading system of Hanke et al., 2013[16]. Here, oedema was graded in four stages. Stage I: no signs of oedema; stage II: mild oedema; stage III: intermediate oedema; and stage IV: severe total body oedema. Seven percent of living morphant larvae showed stage IV oedema and extreme body curvature, while 16% and 24% showed milder oedema (stages III and II, respectively). The morphological changes were less severe in the genetic *ctns*-/- larvae, as they showed milder pericardial oedema and body curvature (stage II) in 14% of larvae. More severe forms of oedema (Stages III-IV) were very rare (3 and 1%, respectively), while the majority (82%) were not deformed (Fig. 2a and Supplementary Fig. S1 online).

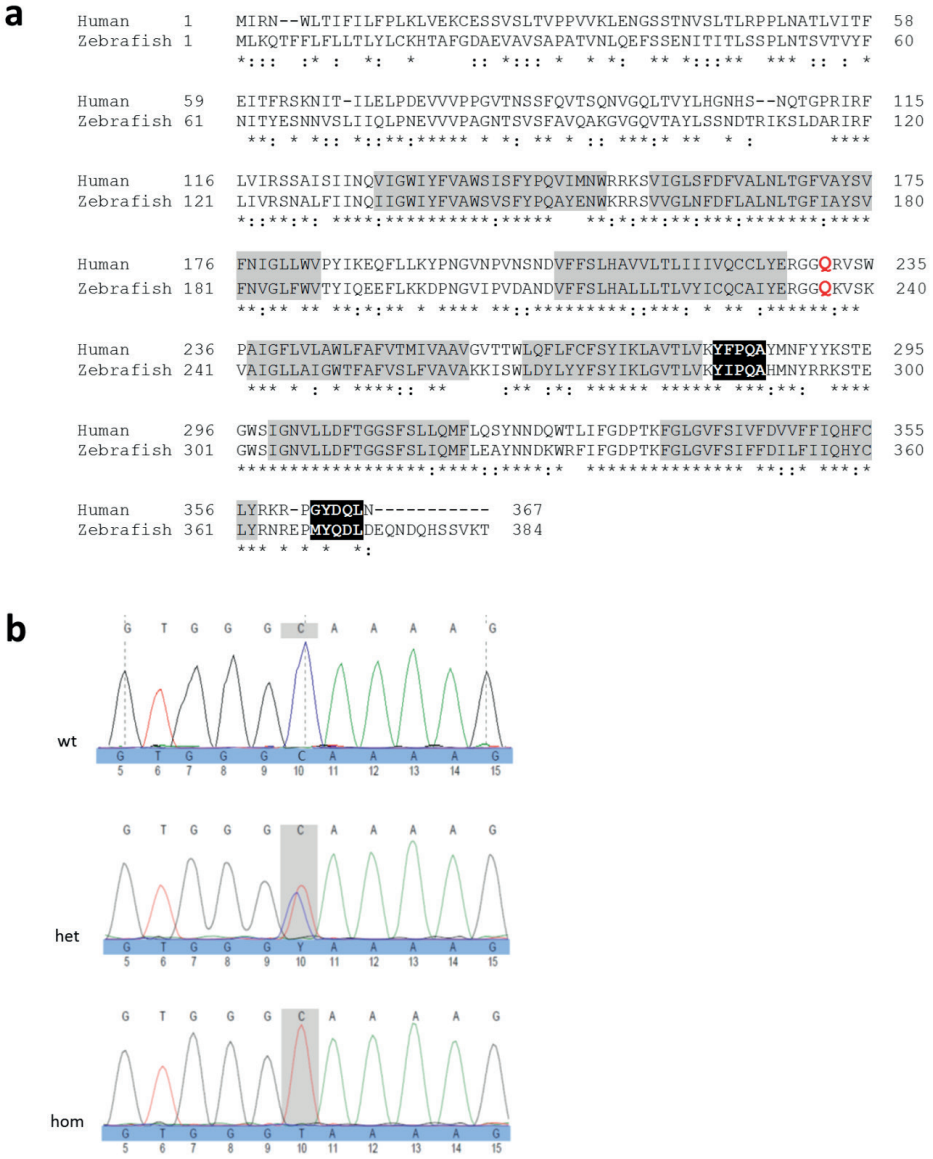

Figure 1. Alignment of zebrafish Ctns protein and human cystinosin.

(**a**) Amino-acid sequence alignment of the zebrafish Ctns protein and human cystinosin. The site of the genetic zebrafish model truncating mutation (c.706C>T; p.Q236X) is marked in red. Identical amino-acids are denoted by asterisks and similar amino acids by double dots. The seven transmembrane domains are highlighted in grey and the two lysosomal targeting motifs in black. (**b**) Exon 8 of the zebrafish *ctns* gene showing the wild-type (wt), the heterozygous (het) and the homozygous (hom)sequences for the c.706C>T mutation. Typical base sequence is marked above each electrophoretogram, while altered sequence is marked below.

Cystine accumulation in ctns −/− larvae and organs of adult ctns −/− zebrafish

Being a major pathologic feature of cystinosis, we measured cystine levels in both homogenized larvae and adult organs of mutant fish compared to the wt. *ctns*−/− larvae at 6 dpf accumulated cystine about ten times higher compared to wt larvae (Fig. 2b). We also had a similar increase in homogenates of morphant larvae (data not shown). Furthermore, cystine levels in *ctns*−/− larvae gradually decreased in response to increasing concentrations of cysteamine in the swimming water (Fig. 2b). Other thiol compounds related to cystine metabolism such as oxidized glutathione (GSSG), total glutathione (GSH) and free cysteine were also evaluated in homogenates of wt and mutant larvae (Fig. 2c-e). *ctns*−/− larvae showed significantly higher levels of both GSSG and free cysteine compared to the wt; however, GSH was not significantly different. Cysteamine treatment significantly reduced abnormally high GSSG levels.

In adult fish, the kidneys of 8 months *ctns*−/− zebrafish demonstrated cystine concentrationsover 50 times of that detected in wt kidneys. Similarly, the *ctns*−/− brain accumulated 10 times higher cystine, while the liver and heart accumulated double the amount of cystine in the wt (Fig. 2f-i). Thus, the results show that the inactivation of *ctns*gene in zebrafish leads to the failure of cystine metabolism, recapitulating the human phenotype.

ctns−/− zebrafish show growth retardation and higher rates of embryonic mortality

Next, we investigated if the defects in cystine metabolism had other effects on zebrafish. Therefore, we monitored the developmental stages of both *ctns*−/− and wt zebrafish embryos in four independent crossings over the first three days of maturation at predetermined time points (3h, 6h, 24h, 48h and 72 hpf). *ctns*−/− embryos showed significant delay in development at all time points investigated, although the difference was more striking at early time points (≤ 24h)(Fig. 3). Additionally, the percentage of dead embryos during the first 3 days post fertilization was significantly higher in *ctns*−/− zebrafish (101/363 (27.8%)), when compared to wt (33/322 (10.2%)), $P<0.001$. Hatching was also relatively delayed in *ctns*−/− embryos at both 48hpf and 72hpf time points. In a different set of experiments, mortality rates were improved with therapeutic doses of cysteamine (Fig. 3f). Hatching rates were also partially normalized by cysteamine therapy (Supplementary Fig. S2 online). Thus, the deregulation of *ctns* gene led to overall developmental delay, and increased embryonic mortality that are partially restored by cysteamine.

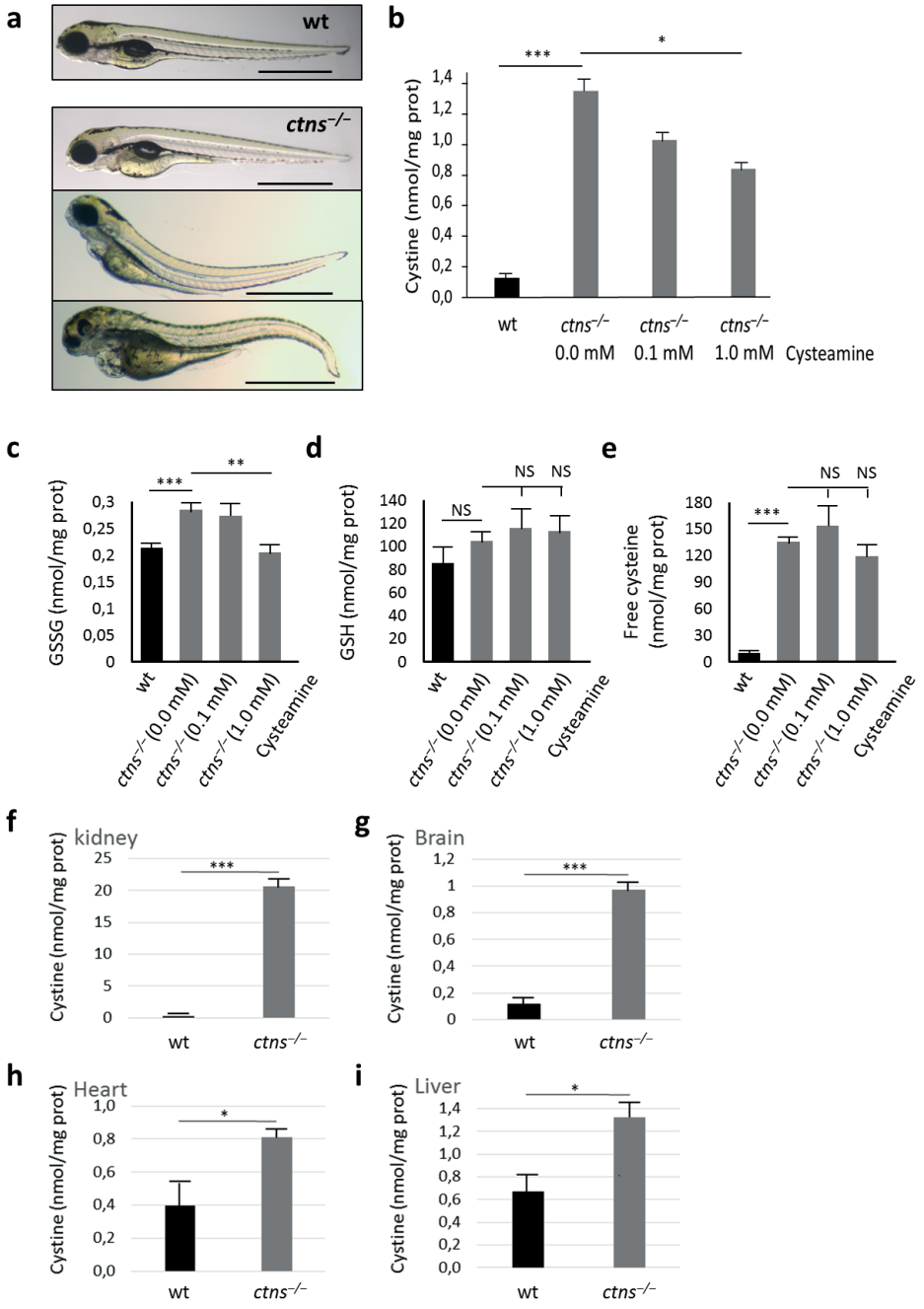

Figure 2. Morphology and cystine measurements.

(**a**) Morphology of wild-type and *ctns*−/− larvae at 4 dpf. Wild-type larva shows normal morphology, while mutant *ctns*−/− larvae show various degrees of developmental delay and deformity: upper larva show signs of growth retardation in the form of slightly bigger yolk, bulging heart and bent-down head, while the middle and lower larvae show mild and severe deformity, respectively

Figure 2. Continued

(bars=1 mm). (**b**) Cystine content in homogenates of 6 dpf wt or *ctns*-/- zebrafish larvae. *ctns*-/- larvae were either free of treatment (N=133) or subjected to 0.1 or 1.0 mM of cysteamine in the swimming water (N=111 and 121 larvae, respectively). Comparison was performed with wt larvae (N=191). (**c**) Oxidized glutathione (GSSG) content in homogenates of 6 dpf wt or *ctns*-/- zebrafish larvae (same conditions and larval numbers as cystine). (**d**) Total glutathione (GSH) content in homogenates of 6 dpf wt or *ctns*-/- zebrafish larvae.*ctns*-/- larvae were either free of treatment (N=80) or subjected to 0.1 or 1.0 mM of cysteamine in the swimming water (N=108 and 104 larvae, respectively). Comparison was performed with wt larvae (N=158). (**e**) Free cysteine content in homogenates of 6 dpf wt or *ctns*-/-zebrafish larvae (same conditions and larval numbers as GSH). (**f-i**) Cystine content in homogenates of 8-month-old adults (Kidney, brain, heart and liver, respectively) (N=3 of each genotype). Concentrations of cystine and other thiol compounds were expressed as nmol/mg protein. * P<0.05, ** P<0.01, *** P<0.001.

ctns-/- zebrafish larvae have increased apoptosis rate that can be ameliorated by cysteamine

We further addressed whether, as reported previously in human and mouse tissues,[7,11,12] cystinosis triggered apoptosis in zebrafish larvae. Apoptosis was investigated in surviving wt and *ctns*-/- larvae at 5 dpf using the Acridine Orange (AO) fluorescent dye which binds to DNA of apoptotic cells and spares necrotic cells. Cystinotic larvae were naïve to treatment or treated with 0.1 mM of cysteamine (N=10 for each condition). The apoptotic spots in the untreated *ctns*-/- larvae were clearly visible and significantly increased compared to wt larvae. Interestingly, the low dose of cysteamine significantly reduced both number and intensity of apoptotic spots, P<0.001 (Fig. 4a-d). We further confirmed the increased rate of apoptosis through the detection of positive staining for caspase-3 by immunohistochemistry in 5 dpf *ctns*-/- larvae. Apoptotic signals in immunohistochemistry were not restricted to skeletal structures but were also present in internal organs especially in proximal tubules and in the liver (Fig. 4e,f). A higher caspase-3 enzyme activity performed by a luciferase based assay was detected in the homogenates of *ctns*-/- larvae compared to the wt at 5 dpf, P<0.001 (Fig. 4g).

ctns-/- zebrafish larvae have normal locomotor activity

In order to evaluate if there are any early behavioural or kinetic abnormalities in the cystinotic zebrafish larvae, we monitored the locomotor activity of 5 dpf *ctns*-/- larvae (N=56) in comparison to wt larvae (N=52) under light and dark conditions. The quantification of locomotor activity (in actinteg units) did not reveal any significant difference between the two genotypes regardless of the lighting conditions (P=0.416 in light and P=0.279 in dark) (Supplementary Fig. S3 online).

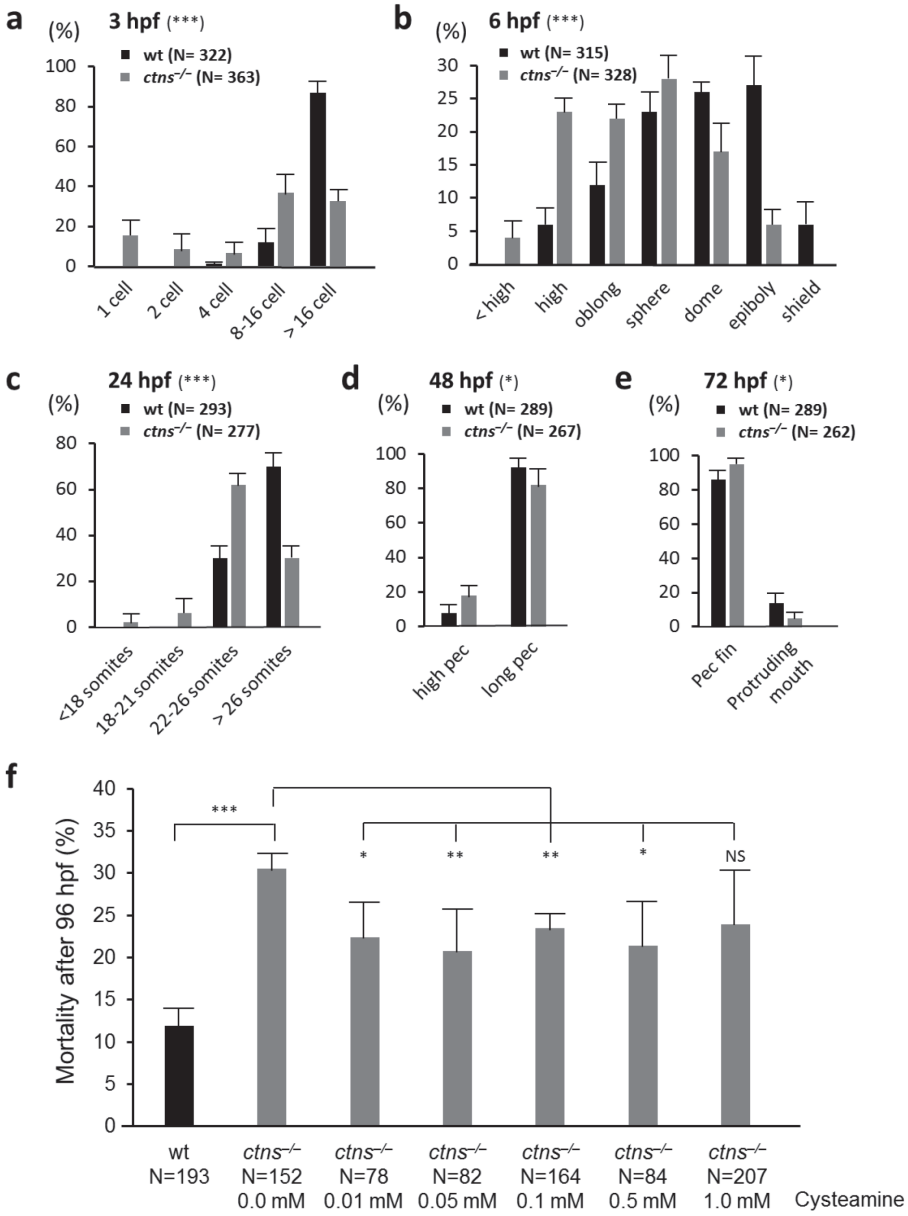

Figure 3. Early developmental stages of zebrafish ctns−/− embryos and response to cysteamine therapy. Embryonic development was monitored over the first 3 days of life at predetermined time points: (a) 3hpf, (b) 6hpf, (c) 24hpf, (d) 48hpf and (e) 72hpf. The outcomes of four different mating settings, 16 females and eight males from each genotype were used (363 *ctns*−/− and 322 wt embryos). Percentages of different developmental stages at each time point were calculated per the total number of living embryos for each genotype at each time point. * P<0.05, *** P<0.001 against wild-type percentages using Pearson chi-square test. (f) Effect of different doses of cysteamine therapy on mortality rates of *ctns*−/− larvae during the first 96 hpf. * P<0.05, ** P<0.01, *** P<0.001 against untreated *ctns*−/− larvae using student's *t* test.

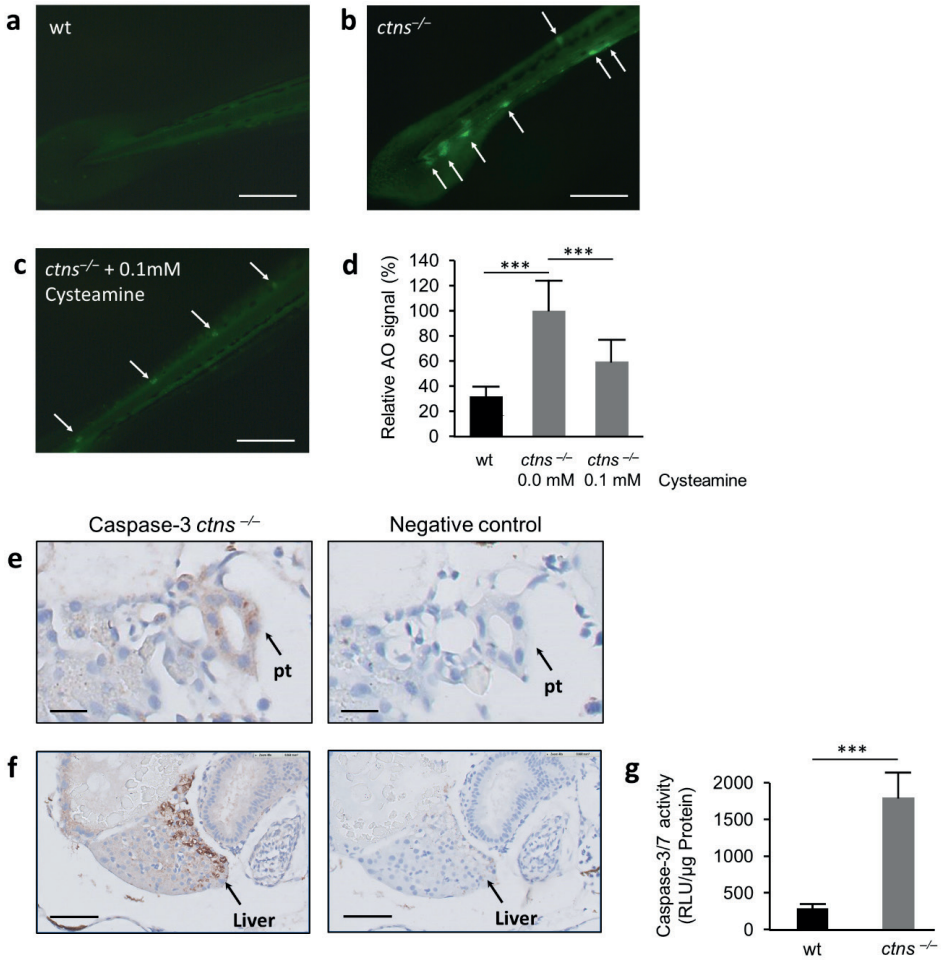

Figure 4. Apoptosis in ctns−/− larvae.

(**a**-**d**) Acridine orange: Five dpf wt larvae and *ctns*−/−larvae, naïve to treatment or treated with 0.1 mM of cysteamine (N=10 for each group), were incubated with Acridine Orange (AO). Fluorescent spots(white arrows) were delineated in high magnification mode and quantified by ImageJ software. (**a**) A representative tail segment of 5 dpf wt larva (bar= 200µm). (**b**) A representative tail segment of 5 dpf *ctns*−/−untreated larva (bar= 200µm). (**c**) A representative tail segment of 5 dpf *ctns*−/− larva treated with 0.1 mM cysteamine (bar= 200µm). (**d**) Quantitation of the relative fluorescence intensity of apoptotic spots. Average intensity of untreated *ctns*−/−larvae was set at 100%.*** P<0.001 against untreated *ctns*−/−larvae. (**e,f**) Caspase-3 immunohistochemistry. (**e**) Representative images showing increased apoptotic signal over the proximal tubule in 5 dpf *ctns*−/− larva (left) compared to the negative control (right), bar= 10µm. pt, proximal tubule. (**f**)Representative images showing increased apoptotic signal over the liver in 5 dpf *ctns*−/− larva (left) compared to the negative control (right), bar= 30µm. Rabbit serum was used for the negative control sections instead of 1ry Ab.(**g**) Caspase-3/7 enzyme activity. Quantitation of Caspase-3/7 enzyme activity by a luciferase based assay in the homogenates of 5 dpf wt and *ctns*−/−larvae (On average 60 larvae over 3 separate homogenates for each genotype were used). Results were expressed in luminescence units (RLU)/ µg protein of each homogenate. *** P<0.001.

ctns−/− zebrafish pronephros shows enlarged lysosomes in proximal tubular cells and partial podocyte foot process effacement

Analysis by light microscopy showed no apparent glomerular or tubular abnormalities compared to wt (Fig. 5a, b). Analysis by block face scanning electron microscopy revealed however that proximal tubular epithelial cells (PTECs) in *ctns*−/− pronephros had numerous and enlarged lysosomes compared to wt (Fig. 5c, d). We calculated the numbers and average surface area of lysosomes in complete cut-sections of wt and *ctns*−/− larvae at the level of proximal tubules (n= 10 each). Per cut-section lysosomal numbers were higher in the proximal tubules of *ctns*−/− larvae (68.4±4.7) compared to wt larvae (24.5±3.8), $P<0.001$. Average lysosomal surface area was also higher in the *ctns*−/− larvae (1.38±0.1 μm^2) compared to the wt (0.51±0.03 μm^2), $P<0.001$ (Fig.5e). On the other hand, cystinotic PTECs did not show cystine crystal accumulation or brush border flattening.

The ultrastructural analysis of podocytes of *ctns*−/− larvae showed partial foot process effacement and narrowed slit diaphragmatic spaces when compared to wt larvae, while glomerular basement membrane appeared to be of normal thickness (Fig. 5f, g). To assess podocyte foot process effacement in a quantitative manner, average podocyte foot process width (FPW) was measured. A previously described formula was used to perform this analysis[35]. *ctns*−/−larvae showed higher podocyte FPW (0.62±0.09 μm) when compared to wt larvae (0.51±0.05 μm), $P=0.033$ (Fig.5h). Thus, at the cellular level the *ctns*−/− larvae also showed some of the human pathological features of the disease.

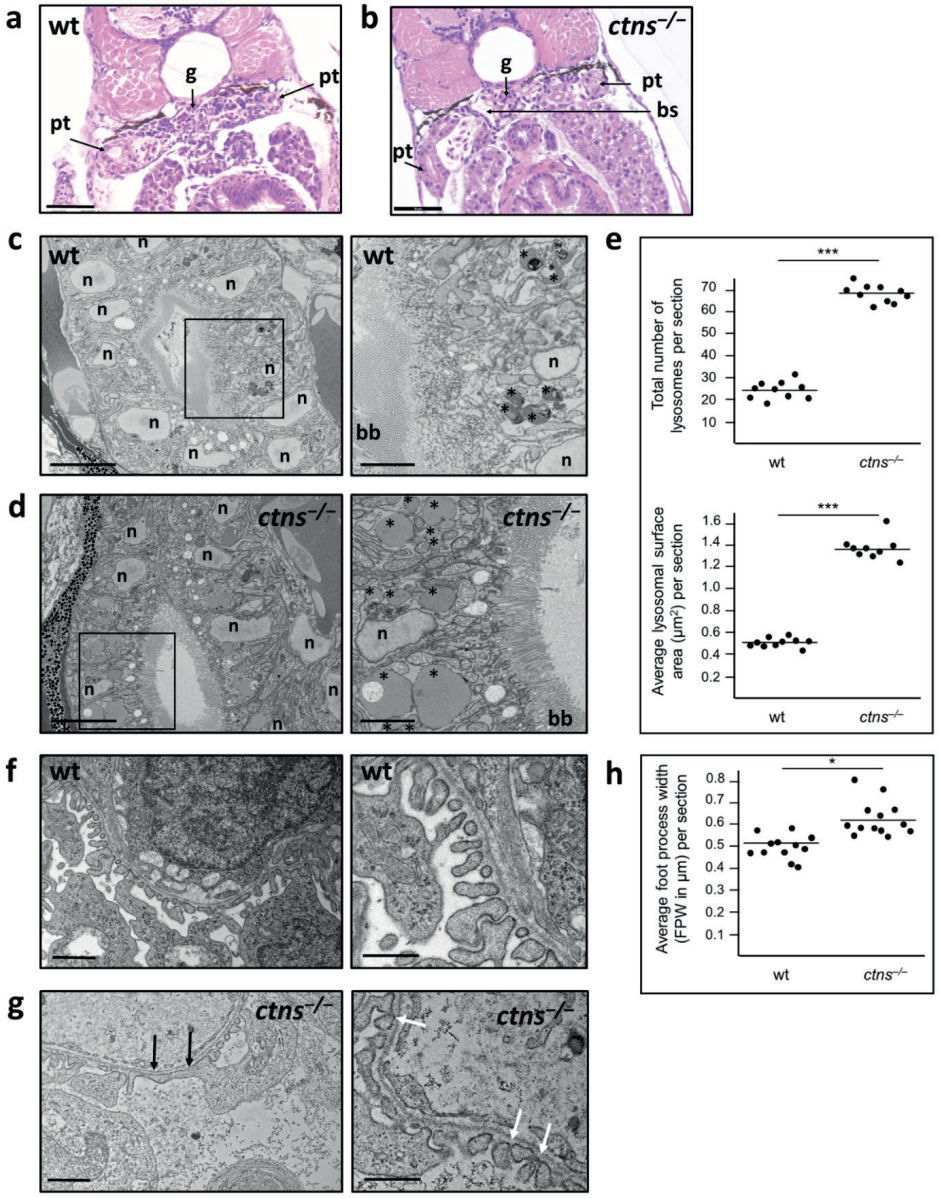

Figure 5. Morphology of the pronephros of ctns−/− larvae compared to the wt.

(**a**) H&E stained cut-section of a 6 dpf wt larva at the level of the glomerulus and proximal tubules(bar=50μm). (**b**) H&E stained cut-section of a 6 dpf *ctns*−/− larva at the level of the glomerulus and proximal tubules showing no apparent abnormality (bar=50 μm). (**c**) Block face scanning EM image of the proximal tubule of a 4 dpf wt larva (bar=5 μm).Demarcated area was magnified (right) to show size and distribution of lysosomes (asterisks) in the wt (bar=2 μm).(**d**) Scanning EM image of the proximal tubule of a 4 dpf *ctns*−/− larva showing intact brush border (bar=5 μm). Demarcated area was magnified (right) to show larger number of lysosomes (asterisks) many of which were significantly enlarged in size compared to the wt (bar=2 μm). (**e**) Quantitation of the number and surface area of lysosomes in cut sections at the level of proximal tubules in

Figure 5. Continued

both genotypes. (**f**) Transmission EM image of the glomerulus of a 6 dpf wt larva showing normal foot processes (bar=2 μm). A magnified EM image (right) of podocytes of 6 dpf wt larva showing preserved podocytes slit diaphragms (bar=1 μm). (**g**) Transmission EM image of the glomerulus of a 6 dpf *ctns*−/− larva showing partial foot process effacement (black arrows) (bar=2 μm). A magnified EM image (right) of podocytes of 6 dpf *ctns*−/− larva showing narrowed podocyte slit diaphragmatic spaces (white arrows) (bar=1 μm). (**h**) Quantitation of podocyte foot process width (FPW) in cut sections at the level of the glomerulus in both genotypes. bb, brush border; bs, Bowman's space; g, glomerulus; n, nucleus; pt, proximal tubule. * P<0.05, *** P<0.001 between the 2 genotypes using student's *t* test.

ctns−/− *zebrafish pronephros shows signs of glomerular disease*

defective glomerular permselectivity

Since many aspects of human and zebrafish cystinosis were similar, we investigated the functional consequences of the disruption of *ctns* gene in zebrafish larvae. One of the functional tests for the zebrafish kidney is measuring the time required for dextran clearance from the pronephros. In case of a glomerular defect, high molecular weight(HMW)dextran is expected to be lost more rapidly from the vasculature due to impaired glomerular filtration barrier (GFB). Thus, we injected fluorescent labelled 70-kDa dextran into the vascular system of 72 hpf larvae (N=20 of each genotype). After 24 hours we monitored the fluorescence intensity of each larva over the retinal vascular bed[16]. The fluorescence intensity in *ctns*−/− larvae was significantly lower compared to wt larvae, P<0.001 (Fig. 6a-c). Furthermore, the number of 70-kDa dextran droplets visualized passing through the proximal tubular wall of 72 hpf *ctns*−/− larvae fixed in 4% paraformaldehyde (PF) 1h after injection was significantly higher when compared to wt larvae denoting also the increased passage of the 70-kDa dextran in the glomerular filtrate (N=10 of each genotype), P=0.031 (Fig. 6).

decreased glomerular filtration rate (GFR)

Human cystinosis patients develop a slow and gradual decrease in GFR usually starting during childhood. Hence we evaluated the GFR of mutant *ctns*−/− larvae compared to that of the wt by injecting FITC-inulin into the vascular system of larvae at 96 hpf[36]. Inulin is freely passing through the glomerular membrane, not reabsorbed and not excreted from the tubular cells, thus is widely used for the assessment of GFR. We monitored the percent of fluorescence intensity decline over 3 fixed anatomical positions in the caudal artery of each larva after 4 hours of injection (Supplementary Fig. S4 online). The percentage of decline of fluorescent intensity in *ctns*−/− larvae (65.3±5.1%, N=43) was slightly but significantly reduced compared to wt larvae (68.7±4.2%, N=45), P<0.001 denoting the early affection of GFR in *ctns*−/− zebrafish larvae. The difference was significant in two

independent experiments, P=0.01 and 0.032. These results emphasize the similarity between zebrafish and human cystinosis patients.

ctns−/− zebrafish pronephros show impaired proximal tubular function

impaired endocytosis of low molecular weight dextran

Another functional aspect that we investigated was the tubular reabsorption. Here we carried out a histological evaluation of the number of dextran droplets in the proximal tubular cell wall of fixed larvae after the injection of a fluorescent labelled low molecular weight (LMW) dextran (4-kDa) into the vascular system of 72 hpf larvae in both *ctns*−/− and wt (N=10 of each genotype). The low molecular weight dextran freely passes the glomerular filtration barrier and is efficiently reabsorbed by the proximal tubular endosomal machinery. Interestingly, the fluorescence over the proximal tubule of *ctns*−/− larvae was virtually absent compared to the injected wt larvae (P<0.001, Fig. 6), suggesting that proximal tubular reabsorption was defective in the *ctns*−/− larvae.

altered abundance and localization of the endocytic receptor megalin

Altered apical abundance of the multi-ligand receptor megalin has been linked with the abnormal endocytosis and defective function of cystinotic PTECs in both mice and human cells[11,37]. We evaluated the abundance and localization of megalin in the proximal tubules in both 5 dpf *ctns*−/− and wt larvae, as described previously[38]. The overall level of megalin present in *ctns*−/− larvae was about half of that in the wt (Fig. 7a-e); however, the most striking feature was the altered distribution of megalin in the cystinotic PTECs where it accumulated in sub-apical punctate rings or cytoplasmic vacuoles when compared to the wt, where it was more evenly distributed in the apical brush border. This altered localization denotes a defective recycling of megalin from apical endosomes, which may explain, at least partially, the disturbed endocytosis in cystinotic larvae. We also evaluated the overall megalin gene (*lrp2a*) expression in homogenized 3 dpf and 6 dpf *ctns*−/− and wt larvae. At the RNA level, there was no statistical significant difference detected between both genotypes(Fig. 7f) similar to zebrafish models of other genetic disorders with impaired proximal tubular endocytosis, such as Lowe syndrome[38]. The reduced abundance of megalin protein at the proximal tubular brush border in the absence of decreased transcript levels is consistent with the abnormal recycling of the protein rather than a decreased transcription and is similar to the findings in humans[37,39].

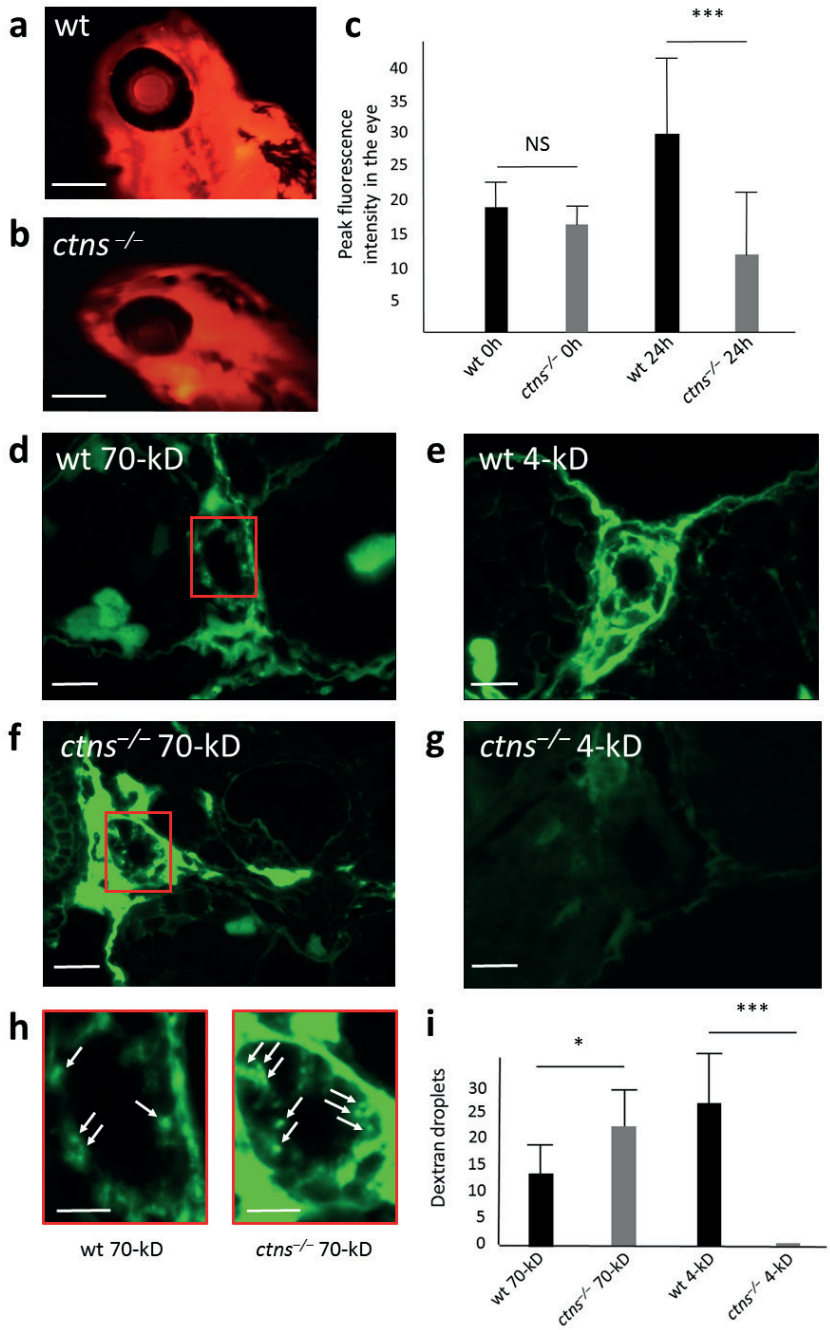

Figure 6. Functional evaluation of glomerular permeability and tubular reabsorption of ctns−/− larvae. (**a-c**) Eye fluorescence assay: peak fluorescence intensity in the retinal vascular bed of *ctns−/−* zebrafish larvae and wild-type larvae (N=20 each). Fluorescence intensities were evaluated using fixed diameter circles by the ImageJ software. (**a**) A representative wild-type 4 dpf larva(24h post-injection) (bar=200 μm). (**b**) A representative *ctns−/−*4 pdf larva(24h post-injection)(bar=200 μm). (**c**) A diagrammatic

Figure 6. Continued

representation of peak fluorescence intensities in the retinal vascular bed of both genotypes. (**d-i**) Histopathological functional evaluation: (**d**) A representative proximal tubule of wt larva injected with the 70-kDa labelled dextran(bar=10 μm). (**e**) A representative proximal tubule of wt larva injected with the 4-kDa labelled dextran (bar=10 μm). (**f**) A representative proximal tubule of *ctns*−/− larva injected with the 70-kDa labelled dextran(bar=10 μm).(**g**) A representative proximal tubule of *ctns*−/− larva injected with the 4-kDa labelled dextran (bar=10 μm). (**h**) A higher magnification of the proximal tubules of both genotypes showing internalized 70-kDa dextran within cytosolic puncta that likely correspond to endocytic compartments (marked areas in panels **d** and **f**) (bars=5 μm). (**i**) Quantitation of the number of dextran puncta in both high and low molecular weight dextran injections in both genotypes (N=10 for each genotype and each condition). * P<0.05, *** P<0.001.

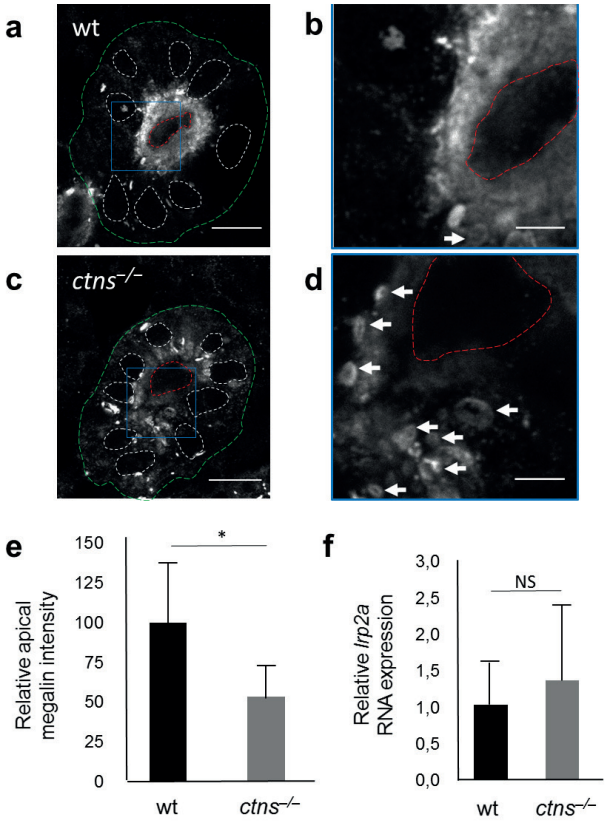

Figure 7. Megalin expression in proximal tubular cells.

(**a**) Transverse fluorescent image of the proximal pronephric region of wt 5 dpf larva labelled with anti-megalin antibody (bar=10 μm). (**b**) Higher magnification image of wt proximal tubule (square in panel a) showing mainly the diffuse distribution of megalin at the cellular brush border (bar=3 μm). (**c**) The proximal pronephric region of *ctns*−/− 5 dpf larva labelled with anti-megalin antibody (bar=10 μm). (**d**) Higher magnification image of *ctns*−/− proximal tubule (square in panel **c**) showing majority of megalin staining in sub-apical intracytoplasmic vacuoles (white arrows) (bar=3 μm). Outer boundaries of proximal tubules were delineated with green, lumen with red, and nuclear boundaries were delineated with white. (**e**) Quantitation of megalin protein abundance in proximal tubules of wt and *ctns*−/−larvae (N=5 for each genotype). (**f**) Quantitation of the megalin encoding *lrp2a* RNA expression in homogenized larvae of 6 dpf wt vs *ctns*−/−larvae (N= 5 individually separated RNA samples for each genotype). * P<0.05.

Discussion

The last common ancestor of humans and zebrafish was a marine vertebrate that lived approximately 450 million years ago; however, 70% of protein-coding human genes are related to genes found in the zebrafish and 84% of genes known to be associated with human disease have a zebrafish counterpart[40,41]. In the current study we established and characterized a*ctns*-/-zebrafish mutant and uncovered many important aspects of the renal pathophysiology resulting in the functional abnormalities of the early larval stage of the *ctns*-/- zebrafish. The key-findings of the study are: 1) significant cystine accumulation, increased mortality and increased rate of apoptosis in the *ctns*-/- zebrafish which are partially responsive to cysteamine treatment. 2) early impairment of pronephros affecting both glomerular and proximal tubular function.

Significant accumulation of cystine, the main pathologic landmark of nephropathic cystinosis, validated our model and confirmed the pathogenic nature of the mutation. Both morphant and *ctns*-/- zebrafish larvae showed comparable phenotypes. We preferred to proceed with embryos and larvae of the genetic *ctns*-/- model, as it is well known that the phenotype severity and toxicity of morphant models are dependent on the morpholino dose injected[42], which is not an issue in the genetic model.

Although cystinosin in humans is ubiquitously expressed, the expression is especially high in the kidneys[43]. Interestingly, the adult *ctns*-/-zebrafish kidneys accumulated the highest concentrations of cystine (>50 times the wt) contrasting the murine model of cystinosis in which the highest cystine accumulations were observed in adult liver and spleen[10,44]. Interestingly, similar to our data in zebrafish homogenates, Wilmer et al., 2011 detected a significant increase in GSSG in cystinotic PTECs compared to wt without alterations in GSH levels[45]. In their *in vitro* study PTECs in culture responded to the antioxidant cysteamine treatment by decreasing GSSG and increasing GSH[45] while *in vivo* in fish only a significant fall in GSSG was observed.

Cystine accumulation has been shown to cause increased apoptosis rate inhuman tissues and in the mouse model of cystinosis[7,11,12]. The suggested mechanism is enhanced cysteinylation of pro-apoptotic enzyme protein kinase C delta due to the lysosomal overload and increased lysosomal membrane permeability[46]. Moreover, oxidative mitochondrial stress and ER stress have been attributed to enhanced apoptosis in cystinotic cells[7,12].Similarly, in our zebrafish model the AO rapid screening technique revealed increased number of apoptotic signals in whole larvae. These data were confirmed by caspase-3 immunohistochemistry and enzyme activity in homogenates of the *ctns*-/- larvae. Importantly, AO apoptotic signals were significantly reduced by therapeutic doses

of cysteamine (0.1 mM) confirming the importance of cystine depletion in the correction of cystinotic phenotype.

Another key finding of our study is that the *ctns*-/- zebrafish model exhibits the early renal phenotype. Resorption of the 4-kDa dextran, which readily passes the GFB, was virtually absent in the *ctns*-/- larvae, indicating perturbed proximal tubular reabsorption. The 70-kDa tracer, which does not readily pass the GFB, was lost more rapidly in the *ctns*-/- larvae than in the wt. Moreover, the loss of glomerular permeability was probably underestimated in the tubular reabsorption analysis, as the 4-kDa experiment has shown that tubular reabsorption capacity was reduced. This phenotype closely mimics the human disease which usually manifests with both tubular and glomerular impairment during infancy and childhood, at a much earlier age than in its mouse counterpart. Although the functional glomerular defect in the *ctns*-/- larvae with the HMW dextran is evident at this early stage, the data on partial podocyte effacement and minimal loss of inulin clearance were not that impressive. Thus, these data should be further evaluated at later time points which may be more representative for the podocyte damage. On the other hand, unlike in mammals, podocytes can regenerate in the adult zebrafish[47] which can mitigate renal disease progression.

Interestingly, the presence of the renal phenotype in the *Ctns*-/- mouse depended on its genetic background. While the first cystinosis mice generated on a FVB/N background did not develop any signs of renal pathology[44],*Ctns*-/- mice on a pure C57BL/6 background showed defective proximal tubular reabsorption starting from 2 months of age corresponding to late adolescence in humans; however, evidence of decreased GFR was only detectable in adult mice at 10 months of age[10] and no podocyte damage was present[11]. This points to compensatory mechanisms in the FVB/N mice which are not present in C57BL/6 mouse, *Danio rerio* or in humans. A concise comparison of cystinosis in humans, mice and zebrafish is presented in Table 1.

In line with functional abnormalities, the morphological changes in the *ctns*-/- zebrafish strikingly resembled those described in human cystinotic kidneys. Similar to humans[39], pronephric podocytes showed partial foot process effacement and narrowed slit diaphragmatic spaces. Larval cystinotic PTECs showed lysosomal abundance and enlargement similar to human andmice cells[12,15]. We further elucidated the key mechanism behind the defective proximal tubular reabsorption in the mutant zebrafish larval model, which could be explained by the altered expression of the multi-ligand receptor, megalin at the proximal tubular brush border of *ctns*-/- zebrafish larvae. The mis-trafficking of intracytoplasmic megalin evidenced by the sub-apical punctate

and vacuolar megalin distribution, together with the resulting decrease in the receptor quantitative brush border expression will lead eventually to abnormal endocytosis and loss of various proteins, polypeptides and other compounds in urine[48]. In cystinotic mice, localized megalin expression in PTECs was apparently normal at 3 months of age but suffered a gradual and progressive descent over the course of the next 9 months[11]. Similarly, human PTECs also showed defective expression and function of megalin in manifesting cystinotic patients in both renal biopsies and isolated cells in culture[11,37].In our study the corresponding pathological process started at a much earlier phase in the zebrafish pronephros, which may signify the rapid development of the disease in zebrafish. Whether cystinosin dysfunction affects mammalian pronephros remains unknown, as this structure forms very early during embryonic development, and disappears by the 10th gestational day in mice and the25thgestational day in humans[49].

Although, the appearance of tissue cystine crystals is a hallmark of cystinosis, we couldn't observe any in the histopathological sections of the zebrafish larval model. It is perceivable that tissue cystine crystallization is a cumulative process and needs time to develop. For example, in human kidney tissues cystine crystals were not reported before six months of life[50]and in mice were not visualized before three months in the cornea and six months in the kidney proximal tubules[44,51].

Cysteamine, the only specific treatment for human cystinosis patients, is not the curative therapy as it mainly targets cystine accumulation. It is not effective in preventing the renal Fanconi syndrome or restoring other pathogenic mechanisms seen in cystinotic cells like enhanced autophagy[4,52], or altered vesicle trafficking[37]. Furthermore, it has many disadvantages such as the strict dose regimen, the bad breath and sweating odours[53], and the frequently severe gastrointestinal adverse effects[54]. These disadvantages greatly affect drug compliance especially in adolescents and young adults[55]. To avoid such adverse effects many drugs are being investigated to find an alternative therapeutic agent, especially among the structurally related cysteamine analogues and prodrugs[56,57]. On the other hand, substances targeting pathogenic mechanisms not related to cystine accumulation, such as autophagy and impaired endocytosis, are currently considered as an adjuvant therapy to cystine depletion[48,52]. The zebrafish model presented in our study is an excellent tool for *in vivo* testing as it presents many key features of the human renal disease and can be used for the high throughput screening or for a more profound functional drug testing.

In conclusion, the *ctns*-/- zebrafish mutant described here shows early phenotypic characteristics of the human disease including cystine accumulation, enhanced apoptosis, delayed development, increased glomerular permeability, decreased GFR and defective

proximal tubular reabsorption. Thus, it provides a robust and versatile model that can be used for the study of the pathophysiological aspects of cystinosis and for the *in vivo* screening of novel therapeutic agents.

Materials and methods

Fish maintenance and breeding

The animal care and experimental procedures were carried out in accordance with the ethical committee guidelines for laboratory animal experimentation at KU Leuven and the reference European directive: DIRECTIVE 2010/63/EU on the protection of animals used for scientific purposes. Zebrafish *(Danio rerio)* used in the current study were AB strain wild-type and *ctns*−/− mutant initially purchased as heterozygous (*ctns*−/+) from the European Zebrafish Resource Centre (EZRC), Karlsruhe, Germany. Cystinotic and wt adult fish were raised at 28.5°C, on a 14/10 hour light/dark cycle under standard aquaculture conditions[58]. By the 3rd generation in our facility, we could isolate sufficient numbers of mutant homozygous male and female zebrafish and mating was performed only between homozygous adult fish (*ctns*−/−). A mating setting always included four females and two males. After mating, every 50-60 fertilized embryos were transferred into a fresh 10 cm petri dish which was approximately ¾ filled with clean egg water (Instant Ocean Sea Salts, 60 µg/ml) and methylene blue (0.3 ppm). Embryos were sorted out for debris and unfertilized eggs and incubated at 28.5°C. Every day the medium was refreshed, the debris was removed and dead embryos were sorted out. All experiments were performed between 3rd and 6th days post fertilization.

Zebrafish genotyping

For determining the genotype of adult zebrafish, we extracted DNA from the tail (caudal) fin of live adult fish. DNA was separated by the Wizard SV genomic DNA purification system for animal tissues (Promega, Madison, WI, USA) according to manufacturer's protocol. Exon 8 PCR of zebrafish *ctns* gene was performed using: 5′-AGTACAGCGATTACTTAACAGGT-3′ and 5′-GACACCCAGTTTAATGTAGGA-3′ as forward and reverse primers, respectively. PCR products were prepared for sequencing through the Big Dye Terminator technology and sequenced on ABI 3100 sequence analyser (Applied Biosystems, Carlsbad, CA, USA). Data were analysed using SEQUENCE Pilot (JSI Medical Systems, Kippenheim, Germany).

Morpholino

Fluorescein tagged antisense morpholino oligonucleotides targeting the 5' UTR of zebrafish *ctns* mRNA and a control morpholino were obtained from GeneTools

(Philomath, OR, USA). The sequences for the *ctns* and control morpholinos were ATTGTTCTGTCGTTCAGCTTAACGC and GGATTAAAATCCGCTACTCACATCC, respectively. 0.2 mM of either *ctns* or control morpholino with 0.1 mM p53 morpholino (GCGCCATTGCTTTGCAAGAATTG) to minimize apoptosis, were injected into the yolk sac of one cell stage embryos in a total volume of 1 nl, as previously described[59]. Success of injection was checked immediately under fluorescent microscopy. Evaluation of morphological changes was performed at 4 dpf, while homogenization for cystine assay was performed at 6 dpf.

Cystine measurement

Cystine content in homogenates of zebrafish larvae (6 dpf) or organs of adult zebrafish (8 months) of each genotype was evaluated using high performance liquid chromatography(HPLC)[60]. *ctns*-/- larvae were either free of treatment (N=133) or subjected to 0.1 or 1.0 mM of cysteamine in the swimming water (N=111 and 121 larvae, respectively). The swimming water was refreshed with the specified concentrations of cysteamine starting from 3 hpf and every 24 hours. Cystine levels were compared with wt embryos (N=191) in two independent experiments. Groups of 20-40 embryos of each treatment condition and each genotype were homogenized together by sonication in 200 μl of 5mM N-ethylmaleimide (NEM) (Sigma, St Louis, MO, USA) in 0.1 M PBS. 100 μl of 12% sulfosalicylic acid (SSA) were added to each homogenate and samples were centrifuged at 12,000 g for 10min. Supernatants containing stabilized cystine were removed completely and preserved at −80°C until time of analysis, while pellets were dissolved overnight at 4°C in 300 μl of 0.1M NaOH then kept at −80°C until protein is measured. Adult organs of 8 months *ctns*-/- or wt zebrafish (N=3 each), were dissected then homogenized in a similar way to larval samples.

Glutathione measurement

Oxidized glutathione (GSSG) was measured in homogenates of 6 dpf wt and *ctns*-/- larvae with NEM similar to cystine, while total glutathione (GSH) and free cysteine were measured in larval homogenates without the addition of NEM (wt =158 larvae, untreated *ctns*-/- =80 larvae, 0.1mM cysteamine treated *ctns*-/- =108 larvae and 1.0mM cysteamine treated *ctns*-/- =104 larvae). Immediately after preparation of 3-5homogenates of each condition, 12% SSA was added to prevent protein binding of glutathione. The homogenates were centrifuged at 12,000 g for 10 min at 4°C. The supernatants of corresponding samples were used for measurements of GSSG or GSH by HPLC[60].All results were referred to protein measurements in pellets.

Evaluation of development

The developmental stages for both *ctns*-/- and wt zebrafish were monitored over the first three days of maturation at predetermined time points (3h, 6h, 24h, 48h and 72h post fertilization) according to the staging system by Kimmel et al,. 1995[61]. The outcomes of four independent crossings involving 16 females and eight males from each genotype were used (363 *ctns*-/- and 322 wt embryos). Percentages of different developmental stages were calculated per total number of living embryos for each genotype at each time point and compared by Chi-square test.

Evaluation of apoptosis

Acridine orange (AO):Morphologically sound 5dpf zebrafish wt and*ctns*-/- larvae were washed with egg water three times and immersed in5µg/ml of the fluorescent DNA binding dye AO (Sigma) for 1 hour. Cystinotic larvae were either untreated or treated with 0.1 mM of cysteamine starting at 2 hpf (N= 10 for each group). After incubation larvae were washed 3 times for 5 min each in egg water to remove residual dye. Larvae were anesthetized with 80 µg/ml tricaine methanesulfonate, then fluorescent images were obtained with the Zeiss inverted fluorescence microscope (Discovery.V8) using the AxioVision release 4.7.2 software (Zeiss, Jena, Germany). Three high magnification images were obtained for each larva (head, trunk and tail), and abnormal fluorescent spots corresponding to apoptotic areas were delineated manually and quantified using the ImageJ software (http://imagej.nih.gov/ij/).

Caspase-3 immunohistochemistry: Five dpf *ctns*-/- larvae were fixed in 4% PF, transferred to 70% ethanol and embedded in paraffin. Sections were deparaffinised, and antigen retrieval was performed. Sections were incubated with an anti–cleaved caspase-3 (Asp175) rabbit antibody (1:300; Cell Signaling, Danvers, MA, USA) overnight at room temperature. Binding of the primary antibody was visualized with labelled anti-rabbit envision antibody (DAKO, Glostrup, Denmark) and diaminobenzidine as a chromogen.

Caspase-3/7 enzyme assay: Five dpf wt and *ctns*-/- larvae were homogenized in RIPA buffer with aprotinin, sodium orthovanadate and PMSF. On average 20 larvae were homogenized per 300µl of the buffer and 3 replicates were performed for each genotype. After centrifugation supernatants were preserved at –20°C till day of analysis. Caspase-3/7 enzyme activity were assayed in 1/100 dilution of each homogenate in duplicate using a commercial luciferase based assay (Promega, Madison, WI, USA) according to manufacturer's protocol. Enzyme activities were expressed in luminescence units (RLU)/ µg protein of each sample.

Evaluation of locomotor activity

Fivedpf *ctns*−/− and wt zebrafish larvae were preincubated in 100 µl of 0.3× Danieau's solution (1.5 mM HEPES, pH 7.6, 17.4 mM NaCl, 0.21 mM KCl, 0.12 mM MgSO4, and 0.18 mM $CaNO3_2$) in individual wells of a 96-well plate at 28.5°C (N=56 and 52, respectively). Larvae were allowed to habituate for 10 min in the light in a chamber of an automated tracking device (ZebraBox™; Viewpoint, Lyon, France) followed by 1h tracking in the light, then 10 min habituation in the dark followed by 1h tracking in the dark. Locomotor activities of two independent experiments were quantified using ZebraLab™ software (Viewpoint, Lyon, France). Total movement or activity was expressed in "actinteg" units reported every 5 min of the tracking period[62]. The actinteg value of the ZebraLab™ software is defined as the sum of all image pixel changes detected for each larva during the reporting time period.

Microscopy

Light microscopy: whole zebrafish larvae at 3 and 6 dpf were prepared for light microscopy. They were fixed in 4% PFA for 24 hours, transferred to 70% ethanol and embedded in paraffin. After transversal sectioning (3 µm), the samples were deparaffinised and stained with haematoxylin and eosin.

Block face scanning electron microscopy: Samples were prepared and imaged with the help of the EM Facility at the Faculty of Life Sciences, University of Manchester, UK, as previously described[38]. Four dpf wt and *ctns*−/− larvae were fixed in 2.5% glutaraldehyde/4% formaldehyde in 0.1 HEPES, pH 7.2, before high density staining for serial block face imaging. Briefly, samples were washed in ddH2O and incubated in 1% osmium tetroxide/1.5% potassium ferrocyanide in 0.1M cacodylate buffer for 1 hour at RT and washed again. Specimens were then incubated for 1 hr at RT in 1% aqueous thiocarbohydrazide, then 1 hr incubation in 1% aqueous osmium tetroxide followed by 1 hr incubation in 1% aqueous uranyl acetate. Samples were then incubated at 60°C for 30 mins in Walton's lead aspartate solution, followed by dehydration in a graded ethanol series and acetone. Samples were embedded in TAAB 812 Hard and trimmed to locate the pronephros. Serial block face scanning EM was carried out using a Gatan 3View microtome within an FEI Quanta 250 FEG scanning electron microscope. Large images were acquired following ten 100 nm cuts of pronephros (54.4 µm x 54.4 µm) with a pixel resolution ~10 nm and 10 µs dwell time. Image analysis for lysosomal number and surface area was performed using ImageJ software.

Transmission electron microscopy: wt and *ctns*−/− larvae at 6 dpf were fixed with 1.5% glutaraldehyde in 0.1 M sodium cacodylate buffer (pH 7.4) for 24 hours, rinsed twice with 0.1 M sodium cacodylate, incubated for 1 hour in 1% osmium tetroxide in 0.1 M sodium

cacodylate buffer, dehydrated sequentially in 70%, 80%, 90%, and 100% ethanol, and then immersed in 1:1 propylene oxide: epon LX-112 solution for 1 hour. After washing, infiltration with pure epon for 2 hours, and embedding in epon LX-112, samples were polymerized at 60°C for 2 days. Ultrathin (100 nm) sections were cut using a Leica EM UC6 ultramicrotome, collected on a slot grid, post-stained with 7% uranyl acetate for 20 minutes followed by Reynolds' lead citrate for 10 minutes, and examined at 120 kV in a JEOL JEM-1011 electron microscope equipped with a MegaView III digital camera (JEOL, Inc., Peabody, MA, USA).

Evaluation of glomerular and tubular proteinuria

Evaluation of proteinuria was performed by injecting dextran tracers intravenously and assessing both loss of fluorescence in the retinal vascular bed and resorption droplets. The different assessment models were implemented in different groups of zebrafish in separate experiments. *ctns*−/− and wt zebrafish larvae (72 hpf) were anesthetized with 80 μg/ml tricaine methanesulfonate, then injected sequentially into the cardiac venous sinus (sinus venosus) with 2 nl of 50 mg/ml 70-kDa rhodamine B isothiocyanate-Dextran or 4.4-kDa tetramethyl rhodamine isothiocyanate-Dextran (Sigma). Injections were performed using FemtoJet micro-injector (Eppendorf, Hamburg, Germany). Success of injection was evaluated directly after injection with the Zeiss inverted fluorescence microscope. in the retinal bed was evaluated in *ctns*−/− and wt zebrafish larvae injected with the 70-kDa tracer (n=20 for each genotype) by taking images after injection and 24h post injection. The peak fluorescence intensities in zebrafish retinal vascular bed were evaluated using fixed diameter circles by the ImageJ software[16].

Assessment of glomerular permeability and tubular reabsorption capacity were performed in separate groups of zebrafish injected with the 70-kDa or 4-kDa dextran tracers, respectively (n=10 in each group). Successfully injected larvae were fixed in 4% PFA at 60min post-injection traced separately for each larva. After 24h of fixation, they were transferred to 70% ethanol and kept at 4°C till processing. Larvae were washed with demineralized water, packed in groups of five using Shandon' Cytoblock' cell block preparation system, embedded in paraffin for oriented sectioning (3 μm). Sections containing PTECs were investigated by fluorescence microscope. Fluorescent droplets in the proximal tubules were counted, representing endosomes of dextran that have passed the glomerular filtration barrier and were subsequently reabsorbed by PTECs.

Evaluation of glomerular filtration rate

We evaluated GFR in zebrafish larvae using the fluorescein isothiocyanate (FITC)-inulin injection method as previously described[36]. Five percent (w/v) FITC-inulin (5-kDa)

were dissolved in physiological saline. *ctns*-/- and wt zebrafish larvae (N=43 and 45, respectively) were anesthetized using 80 μg/ml tricaine methanesulfonate, injected with 2 nl of the 5% FITC-inulin in the sinus venosus at 96 hpf using the FemtoJet microinjector. Images were taken immediately after injection using the fluorescent microscope Leica MZ10F (Leica Microsystems, Wetzlar, Germany) and then larvae were transferred to 70 μl of water and incubated in the dark. Exactly after 4 hours tracked separately for each larva a second image was obtained by the fluorescent microscope using the exact same setting as the first image. Larvae not showing clear fluorescence in the vascular system immediately after injection were discarded. The fluorescence intensities over the caudal artery were evaluated using ImageJ software. Three mean intensity values for each larva were obtained over the somites 14, 15 and 16 at zero and four hours. The percentage of fluorescence intensity decline after 4 hours was evaluated for each somite and the average was taken for each larva. Two independent experiments were performed.

RNA isolation and quantitative real-time PCR

ctns-/- and wt zebrafish larvae were homogenized at 3 dpf and 6 dpf. Total RNA was isolated from 30-80 whole larvae of each genotype at each time point using the TRIzol® reagent (Invitrogen, Waltham, MA, USA). Total RNA was eluted in 30-80 μl of nuclease-free water and stored at −80°C until further use. cDNA was synthesized from 1 μg of total RNA with the SuperScript® III RT kit (Invitrogen). qPCR reactions were carried out for zebrafish *lrp2a* gene (transcript ENSDART00000167243, Fw: GAACACACCAAATGCCAGTC, Rv: GAGAGGTACAGGTAATGGGC) using SYBR green with ROX in the StepOnePlus RT-PCR system (Applied Biosystems). Gene expression levels were normalized to the reference zebrafish gene *eef1a1l1* (eukaryotic translation elongation factor 1 alpha 1, like 1, transcript: ENSDART00000023156, Fw: CTTCTCAGGCTGACTGTGC, Rv: CCGCTAGCATTACCCTCC), and then compared with wt larvae. Results were derived from at least 5 individually obtained RNA extracts for each genotype and presented as mean fold expression ± SD.

Megalin staining

Five dpf *ctns*-/- and wt zebrafish larvae were fixed using 4% PFA overnight at 4°C, then washed with PBS 3x5 min before incubation with absolute methanol at -20°C for 20 min. Larvae were then mounted in cryosectioning moulds (4 larvae per each block), frozen on dried ice and sectioned using a Leica CM3050 S cryotome. Slides were stained for rabbit anti-megalin antibody (1:100, kindly provided by Michele Marino, University of Pisa, Italy) overnight at 4°C then for 3 hours at room temperature with Alexa-488

(1:200, Thermo Fisher Scientific, Waltham, MA USA). Megalin fluorescence intensity measurements were performed using ImageJ software. The region of interest was selected outlining the periphery of the kidney tubule, and background fluorescence was set at the same intensity as the internal lumen, and subtracted from the total fluorescence intensity[38].

Statistical analysis

Statistical analysis was performed using WINPEPI statistical software, version 11.43[63]. Unless otherwise specified, results were expressed as mean ± standard deviation and differences were tested using the student's unpaired *t* test for numerical data and by Chi-squared test for categorical data. Two-tailed P values <0.05 were considered significant.

Acknowledgments

M.A.E is supported by ERA-Net, E-Rare2-JTC2014: Novel therapies for cystinosis. E.L is supported by the Research Foundation - Flanders (F.W.O. Vlaanderen), grant 1801110N and the Cystinosis Research Network (CRN). We gratefully acknowledge Francesco Emma (Bambino Gesù Children's Hospital, IRCCS, Rome) for valuable discussions and scientific assistance and Pieter Baatsen (VIB BIO Imaging Core, KU Leuven) and Tobias Starborg (University of Manchester FMBH EM Facility) for help with the development of EM images. We sincerely thank Marina G. Mori da Cunha, Ekaterina A. Ivanova, Inge Bongaers, Daniëlle Copmans and Jan Maes (KU Leuven) for valuable assistance.

Author contributions

M.A.E, LV and E.L designed the experiments. M.A.E, R.K, L.K, L.K, F.A.O, J.M, A.P, P.T, A.N, P.A.D, M.L, H.J.B, L.V and E.L performed the experiments and/or analyzed the results and interpreted the data. M.A.E and R.K drafted the manuscript and all authors critically revised the manuscript for intellectual content.

Competing financial interests

The authors declare no competing financial interests.

References

1. Town, M. *et al*. A novel gene encoding an integral membrane protein is mutated in nephropathic cystinosis. *Nat. Genet.*18, 319–324 (1998).
2. Gahl, W. A., Thoene, J. G.&Schneider, J. A. Cystinosis. *N. Engl. J. Med.*347, 111–121 (2002).
3. Greco, M., Brugnara, M., Zaffanello, M., Taranta, A., Pastore, A.&Emma, F. Long-term outcome of nephropathic cystinosis: a 20-year single-center experience. *Pediatr. Nephrol.*25, 2459–2467 (2010).
4. vanova, E. A. *et al*. Altered mTOR signalling in nephropathic cystinosis. *J. Inherit. Metab. Dis.*39,457–464 (2016).
5. Sansanwal, P.&Sarwal, M. M. Abnormal mitochondrial autophagy in nephropathic cystinosis. *Autophagy.*6, 971–973 (2010).
6. Galarreta, C. I.*et al.*The swan-neck lesion: proximal tubular adaptation to oxidative stress in nephropathic cystinosis. *Am. J. Physiol. Renal. Physiol.***308,** F1155–1166 (2015).
7. Sumayao, R., McEvoy, B., Newsholme, P.&McMorrow, T. Lysosomal cystine accumulation promotes mitochondrial depolarization and induction of redox-sensitive genes in human kidney proximal tubular cells. *J. Physiol.*594, 3353–3370 (2016).
8. Elmonem, M. A. *et al*.Clinical utility of chitotriosidase enzyme activity in nephropathic cystinosis. *Orphanet. J. Rare. Dis.*9, 155 (2014).
9. Prencipe, G.*et al*. Inflammasome activation by cystine crystals: implications for the pathogenesis of cystinosis. *J. Am. Soc. Nephrol.*25, 1163–1169 (2014).
10. Nevo, N.*et al*.Renal phenotype of the cystinosis mouse model is dependent upon genetic background. *Nephrol. Dial. Transplant.* 25, 1059–1066 (2010).
11. Gaide Chevronnay, H. P.*et al*.Time course of pathogenic and adaptation mechanisms in cystinotic mouse kidneys. *J. Am. Soc. Nephrol.*25, 1256–1269 (2014).
12. Gaide Chevronnay, H. P.*et al*. A mouse model suggests two mechanisms for thyroid alterations in infantile cystinosis: decreased thyroglobulin synthesis due to endoplasmic reticulum stress/unfolded protein response and impaired lysosomal processing. *Endocrinology*156, 2349–2364 (2015).
13. Johnson, J. L., Napolitano, G., Monfregola, J., Rocca, C. J, Cherqui, S.&Catz, S. D.Upregulation of the Rab27a-dependent trafficking and secretory mechanisms improves lysosomal transport, alleviates endoplasmic reticulum stress, and reduces lysosome overload in cystinosis. *Mol. Cell. Biol.* 33, 2950–2962 (2013).
14. Napolitano, G.*et al*. Impairment of chaperone-mediated autophagy leads to selective lysosomal degradation defects in the lysosomal storage disease cystinosis. *EMBO. Mol. Med.*7, 158–174 (2015).
15. Raggi, C., Luciani, A., Nevo, N., Antignac, C., Terryn, S.&Devuyst, O.Dedifferentiation and aberrations of the endolysosomal compartment characterize the early stage of nephropathic cystinosis. *Hum. Mol. Genet.*23, 2266–2278 (2014).
16. Hanke, N.*et al*."Zebrafishing" for novel genes relevant to the glomerular filtration barrier. *Biomed. Res. Int.*2013, 658270 (2013).
17. Ivanova, E. A.*et al.* Cystinosin deficiency causes podocyte damage and loss associated with increased cell motility. *Kidney. Int.***89,**1037–1048.(2016).
18. Dina, C.*et al*.Genetic association analyses highlight biological pathways underlying mitral valve prolapse. *Nat. Genet.*47, 1206–1211(2015).
19. Gonzaga-Jauregui, C.*et al*.Exome sequence analysis suggests that genetic burden contributes to phenotypic variability and complex neuropathy. *Cell. Rep.*12, 1169–1183 (2015).
20. Neumann, J. C., Dovey, J. S., Chandler, G. L., Carbajal, L.&Amatruda, J. F. Identification of a heritable model of testicular germ cell tumor in the zebrafish. *Zebrafish.* 6, 319–327 (2009).

21. Poureetezadi, S. J.&Wingert, R. A.Little fish, big catch: zebrafish as a model for kidney disease. *Kidney. Int.*89,1204–1210 (2016).
22. Raghupathy, R. K., McCulloch, D. L., Akhtar, S., Al-mubrad, T. M.&Shu, X.Zebrafish model for the genetic basis of X-linked retinitis pigmentosa. Zebrafish. 10, 62–69 (2013).
23. Tietz Bogert, P. S.*et al*.The zebrafish as a model to study polycystic liver disease. *Zebrafish.*10, 211–217 (2013).
24. Schlegel, A.&Gut, P. Metabolic insights from zebrafish genetics, physiology, and chemical biology. *Cell. Mol. Life. Sci.*72, 2249–2260 (2015).
25. Drummond, I. A. Kidney development and disease in the zebrafish. *J. Am. Soc. Nephrol.*16, 299–304 (2005).
26. McCampbell, K. K., Springer, K. N.&Wingert, R. A.Atlas of cellular dynamics during zebrafish adult kidney regeneration. *Stem. Cells. Int.*2015, 547636 (2015).
27. Drummond, I. A.*et al*. Early development of the zebrafish pronephros and analysis of mutations affecting pronephric function. *Development.*125, 4655–4667 (1998).
28. Cheng, C. N.&Wingert, R. A.Nephron proximal tubule patterning and corpuscles of Stannius formation are regulated by the sim1a transcription factor and retinoic acid in zebrafish. *Dev. Biol.* 399, 100–116 (2015).
29. Ebarasi, L., Oddsson, A., Hultenby, K., Betsholtz, C.&Tryggvason, K. Zebrafish: a model system for the study of vertebrate renal development, function, and pathophysiology. *Curr. Opin. Nephrol. Hypertens.* 20, 416–424 (2011).
30. McKee, R. A.&Wingert, R. A. Zebrafish Renal Pathology: Emerging Models of Acute Kidney Injury. *Curr. Pathobiol. Rep.*3, 171–181 (2015).
31. Gerlach, G. F.&Wingert, R. A. Zebrafish pronephros tubulogenesis and epithelial identity maintenance are reliant on the polarity proteins Prkc iota and zeta. *Dev. Biol.*396, 183–200 (2015).
32. McKee, R., Gerlach, G. F., Jou, J., Cheng, C. N.&Wingert, R. A.Temporal and spatial expression of tight junction genes during zebrafish pronephros development. *Gene. Expr. Patterns.* 16, 104–113 (2014).
33. MacRae, C. A.&Peterson, R. T.Zebrafish as tools for drug discovery. *Nat. Rev. Drug. Discov.*14, 721–731 (2015).
34. Attard, M.*et al*. Severity of phenotype in cystinosis varies with mutations in the CTNS gene: predicted effect on the model of cystinosin. Hum. Mol. Genet.8, 2507–2514 (1999).
35. Huh, W.*et al*.Expression of nephrin in acquired human glomerular disease. *Nephrol. Dial. Transplant.* 17, 478–484 (2002).
36. Rider, S. A. *et al*.Techniques for the in vivo assessment of cardio-renal function in zebrafish (Danio rerio) larvae. *J. Physiol.*590, 1803–1809 (2012).
37. Ivanova, E. A. *et al*. Endo-lysosomal dysfunction in human proximal tubular epithelial cells deficient for lysosomal cystine transporter cystinosin. *PLoS One.*10,e0120998 (2015).
38. Oltrabella, F. *et al.* The Lowe syndrome protein OCRL1 is required for endocytosis in the zebrafish pronephric tubule. *PLoS. Genet.*11, e1005058 (2015).
39. Wilmer, M. J., Christensen, E. I., van den Heuvel, L. P., Monnens, L. A. &Levtchenko, E. N. Urinary protein excretion pattern and renal expression of megalin and cubilin in nephropathic cystinosis. *Am. J. Kidney. Dis.* 51, 893–903 (2008).
40. Ali, S., Champagne, D. L., Spaink H. P.& Richardson, M. K.Zebrafish embryos and larvae: A new generation of disease models and drug screens. *Birth. Defects. Res. C. Embryo. Today.*93, 115–133 (2011).
41. Howe, K.*et al*.The zebrafish reference genome sequence and its relationship to the human genome. *Nature.*496, 498–503 (2013).
42. Bedell, V. M., Westcot, S. E. &Ekker, S. C.Lessons from morpholino-based screening in zebrafish. *Brief. Funct. Genomics.*10, 181–188 (2011).

43. Taranta, A. *et al.*Distribution of cystinosin-LKG in human tissues. *Histochem. Cell. Biol.*138, 351–363 (2012).
44. Cherqui, S.*et al.*Intralysosomal cystine accumulation in mice lacking cystinosin, the protein defective in cystinosis. *Mol. Cell. Biol.* 22, 7622–7632 (2002).
45. Wilmer, M. J. *et al.* Cysteamine restores glutathione redox status in cultured cystinotic proximal tubular epithelial cells. *Biochim. Biophys. Acta.*1812, 643-651.
46. Park, M. A., Pejovic, V., Kerisit, K. G., Junius, S. &Thoene, J. G. Increased Apoptosis in Cystinotic Fibroblasts and Renal Proximal Tubule Epithelial Cells Results from Cysteinylation of Protein Kinase Cδ. *J. Am. Soc. Nephrol.*17, 3167–3175 (2006).
47. Huang, J. *et al.* A zebrafish model of conditional targeted podocyte ablation and regeneration. *Kidney. Int.*83,1193-1200 (2013).
48. Marzolo, M. P. &Farfán, P. New insights into the roles of megalin/LRP2 and the regulation of its functional expression. *Biol. Res.*44, 89-105 (2011).
49. Woolf, A. S., Winyard, P. J. D., Hermanns, M. H. & Welham, S. J. M. Maldevelopment of the human kidney and lower urinary tract. An overview. in: *Kidney From Normal Development to Congenital Disease*, (eds. Vize, P. D., Woolf, A. S. & Bard, J. B. L.) 377–393, (Elsevier Inc., 2003).
50. Mahoney, C. P&Striker, G. E. Early development of the renal lesions in infantile cystinosis. *Pediatr. Nephrol.*15, 50-56 (2000).
51. Simpson, J.*et al.* Quantitative in vivo and ex vivo confocal microscopy analysis of corneal cystine crystals in the Ctns knockout mouse. *Mol. Vis.*17,2212-2220 (2011).
52. Rega, L. R.*et al.*Activation of the transcription factor EB rescues lysosomal abnormalities in cystinotic kidney cells. *Kidney. Int.*89, 862–873 (2016).
53. Besouw, M., Blom, H., Tangerman, A., de Graaf-Hess, A.&Levtchenko, E.The origin of halitosis in cystinotic patients due to cysteamine treatment. *Mol. Genet. Metab.*91, 228–233 (2007).
54. 54. Dohil, R.*et al.* Understanding intestinal cysteamine bitartrate absorption. *J. Pediatr.***148,** 764–769 (2006).
55. Ariceta, G.*et al.*Cysteamine (Cystagon®) adherence in patients with cystinosis in Spain: successful in children and a challenge in adolescents and adults. *Nephrol. Dial. Transplant.*30, 475–480 (2015).
56. Frost, L., Suryadevara, P., Cannell, S. J., Groundwater, P. W., Hambleton, P. A. &Anderson, R. J.Synthesis of diacylated γ-glutamyl-cysteamine prodrugs, and in vitro evaluation of their cytotoxicity and intracellular delivery of cysteamine. *Eur. J. Med. Chem.*109, 206–215 (2016).
57. Omran, Z., Moloney, K. A., Benylles, A., Kay, G., Knott, R. M.&Cairns, D.Synthesis and in vitro evaluation of novel pro-drugs for the treatment of nephropathic cystinosis. *Bioorg. Med. Chem.*19, 3492–3496 (2011).
58. Harper, C. & Lawrence, C. The Laboratory Zebrafish (Laboratory Animal Pocket Reference). Eugene, OR: CRC Press (2010).
59. Verleyen, D., Luyten, F. P.&Tylzanowski, P.Orphan G-protein coupled receptor 22 (Gpr22) regulates cilia length and structure in the zebrafish Kupffer's vesicle. *PLoS One.*9, e110484 (2014).
60. de Graaf-Hess, A., Trijbels, F.&Blom, H. New method for determining cystine in leukocytes and fibroblasts. *Clin. Chem.*45, 2224–2228 (1999).
61. Kimmel, C. B., Ballard, W. W., Kimmel, S. R., Ullmann, B.&Schilling, T. F.Stages of embryonic development of the zebrafish. *Dev. Dyn.*203, 253–310 (1995).
62. Orellana-Paucar, A. M.*et al.*Anticonvulsant activity of bisabolene sesquiterpenoids of Curcuma longa in zebrafish and mouse seizure models. *Epilepsy. behav.*24, 14–22 (2012).
63. Abramson, J. H. WINPEPI updated: computer programs for epidemiologists, and their teaching potential. *Epidemiol. Perspect. Innov.*8, 1 (2011).

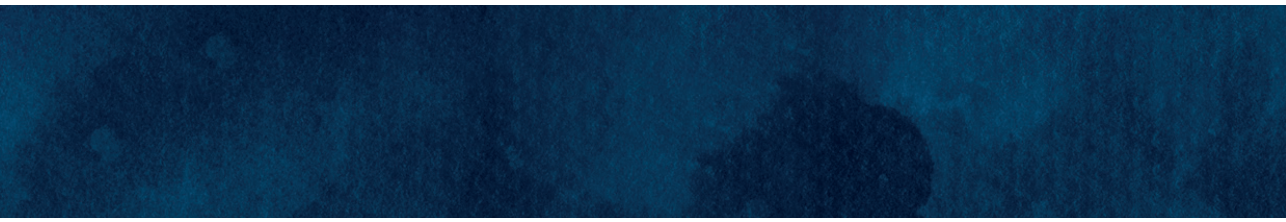

CHAPTER 3

Glomerular permeability is not affected by heparan sulfate glycosaminoglycan deficiency in zebrafish embryos

American Journal of Physiology-Renal Physiology. 2019, 317:5, F1211-F1216

Ramzi Khalil[1], Reshma A. Lalai[1], Malgorzata I. Wiweger[2], Cristina M. Avramut[3], Abraham J. Koster[3], Herman P. Spaink[4], Jan A. Bruijn[1], Pancras C.W. Hogendoorn[1], Hans J. Baelde[1]

[1]Department of Pathology, Leiden University Medical Center, Leiden, The Netherlands;
[2]International Institute of Molecular and Cell Biology in Warsaw, Warsaw, Poland
[3]Department of Cell and Chemical Biology, Leiden University Medical Center, Leiden, The Netherlands;
[4]Institute of Biology Leiden, Leiden University, Leiden, The Netherlands

Abstract

Proteinuria develops when specific components in the glomerular filtration barrier have impaired function. Although the precise components involved in maintaining this barrier have not been fully identified, heparan sulfate proteoglycans are believed to play an essential role in maintaining glomerular filtration. Although *in situ* studies showed that a loss of heparan sulfate glycosaminoglycans increases the permeability of the glomerular filtration barrier, recent studies using experimental models showed that podocyte-specific deletion of heparan sulfate glycosaminoglycan assembly does not lead to proteinuria. However, tubular reabsorption of leaked proteins might have masked an increase in glomerular permeability in these models. Furthermore, not only podocytes, but also glomerular endothelial cells are involved in heparan sulfate synthesis in the glomerular filtration barrier. Therefore, we investigated the effect of a global heparan sulfate glycosaminoglycan deficiency on glomerular permeability.

We used a zebrafish embryo model carrying a homozygous germline mutation in the *ext2* gene. Glomerular permeability was assessed with a quantitative dextran tracer injection method. In this model, we accounted for tubular reabsorption. Loss of anionic sites in the glomerular basement membrane was measured using polyethyleneimine (PEI) staining.

Although mutant animals had significantly fewer negatively charged areas in the glomerular basement membrane, glomerular permeability was unaffected. Moreover, heparan sulfate glycosaminoglycan–deficient embryos had morphologically intact podocyte foot processes.

Glomerular filtration remains fully functional despite a global reduction of heparan sulfate.

Keywords: glomerular basement membrane, glomerular filtration barrier, heparan sulfate, zebrafish, proteinuria

Introduction

Proteinuria is associated with a wide variety of renal diseases. Proteinuria is an independent risk factor for loss of renal function, renal failure, and cardiovascular mortality.(1, 18) Proteinuria occurs when proteins pass the glomerular filtration barrier (GFB) and are not fully reabsorbed by tubular epithelial cells; proteinuria can also develop when the reabsorption system is saturated. The GFB is comprised of fenestrated endothelial cells covered by a glycocalyx, the glomerular basement membrane (GBM), and podocyte foot processes.(19) The GFB filters molecules based on size and charge.(20)

The GFB's charge selectivity has long been attributed primarily to heparan sulfate proteoglycans (HSPGs) in the GBM.(8) HSPGs consist of a core protein to which heparan sulfate glycosaminoglycan (HS-GAG) chains are covalently attached. The HS-GAG chain is polymerized by enzymes encoded by the *EXT1* and *EXT2* genes. A defect in either is considered to be sufficient severely disrupt HS-GAG synthesis. Both during and after polymerization, the chain can be modified by several sulfotransferases and an epimerase, resulting in the addition of sulfate groups, which give the HS-GAGs and thus the whole HSPG a negative net charge.(9, 21)

HS-GAGs have been considered to be essential for GFB permeability as far back as 1980, when Kanwar *et al.* showed that enzymatic removal of HS-GAGs resulted in increased GBM permeability.(7, 8) These early results were supported by the finding that HSPG expression is reduced in several proteinuric renal diseases.(22) However, recent findings in various mouse models have challenged the notion that HS-GAGs are essential for maintaining GFB permeability; these models include podocyte-specific knockouts of perlecan and agrin (two specific types of HSPGs),(23, 24) *Ext1*,(25) *Extl3*,(26) and *Ndst1* (an enzyme involved in GAG sulfation).(27) . Although most of these models have a loss of anionic charge in the GBM, they do not develop significant proteinuria. However, HSPGs are also synthesized by mesangial cells and by glomerular endothelial cells.(28, 29) HSPGs produced by glomerular endothelial cells have been shown to be important for GFB function, as removal of HS-GAG from glomerular endothelial cells results in increased permeability to albumin in *in vitro* experiments.(29) The effects of an *in vivo* global HS-GAG deficiency on glomerular permeability remains unknown. Thus, the primary goal of this study was to investigate the effect of a global (in contrast to a podocyte-specific) HS-GAG deficiency on glomerular permeability. In addition, although various experimental models using podocyte-specific HS-GAG deletion do not develop proteinuria, they may have increased glomerular permeability. Indeed, Chen *et al.* hypothesized that a relatively moderate increase in tubular reabsorption may

prevent proteinuria despite reduced glomerular permeability.(25) To test this hypothesis, we performed quantitative analyses using a zebrafish embryo model in which we could account for tubular reabsorption capacity.

Materials and methods

Animals

Zebrafish (*Danio rerio H)* were maintained as described by Westfield (1995). Embryos were collected from natural crosses and kept at 28.5°C in E3 medium. Wild-type (WT) AB/TL strain zebrafish embryos and *dackel* mutant (*dak/ext2to273b*, referred to as "*dak/ext2*") zebrafish embryos were used for this study. Homozygous *dak/ext2* mutants contain a biallelic premature stop codon in the *ext2* gene. This mutation globally reduces zygotic *ext2* expression in homozygous *dak/ext2* mutants, resulting in impaired HS-GAG chain polymerization. Thus, HSPGs in homozygous mutants have truncated, functionally impaired HS-GAG side chains that are neither sulfated nor negatively charged.(9) This model has been characterized previously with respect to HSPG distribution.(21, 30-32) The total decrease of HS-GAGs in *dak/ext2* zebrafish embryos has previously been reported to be over 80%.(21, 30)

Homozygous *dak/ext2* mutants were sorted at 3 days post-fertilization (dpf) based on cranofacial, ear, and fin phenotypes as described previously.(33, 34) Embryos from separate crosses were used for each experiment.

All experiments were performed on embryos prior to the free-feeding stage and therefore did not fall under the animal experimentation law in accordance with to EU Animal Protection Directive 2010/63/EU.

Electron microscopy

WT and homozygous *dak/ext2* embryos at 3 and 5 dpf were anesthetized with 4% tricaine methanesulfonate (4 mg/ml), chemically fixed for one hour in 1.5% glutaraldehyde in 0.1 M sodium cacodylate buffer (pH 7.4), rinsed twice with 0.1 M sodium cacodylate, incubated for 1 hour in 1% osmium tetroxide in 0.1 M sodium cacodylate buffer, dehydrated sequentially in 70%, 80%, 90%, and 100% ethanol, and then immersed in 1:1 propylene oxide:epon LX-112 solution for 1 hour. The fish were then washed, infiltrated with pure epon for 2 hours, embedded in epon LX-112, and polymerized at 60°C for 2 days.

Ultrathin sections (100 nm) were mounted on copper slot grids (Storck Veco B.V., Eerbeek, The Netherlands), covered with formvar film and carbon layer, and then stained

with an aqueous solution of 7% uranyl acetate for 20 minutes, followed by Reynold's lead citrate for 10 minutes. Specimens were imaged at an acceleration voltage of 120 kV using a Tecnai 12 BioTWIN transmission electron microscope (FEI, Eindhoven, The Netherlands), equipped with a FEI 4k Eagle CCD camera. Virtual slides of zebrafish glomeruli were recorded at 18500x magnification, corresponding to a 1.2 nm pixel size at the specimen level, using automated data acquisition and stitching software.(35)

Loss of anionic sites in the GBM

The number of anionic sites in the GBM was measured using polyethylenimine (PEI) staining as described previously.(36, 37) Specifically, we measured the number of PEI particles per µm of GBM. PEI is a cationic polymer that binds to anionic sites. It was used a surrogate marker for HS-GAG, as HS-GAG are highly sulfated and therefore negatively charged. PEI is not specific to HS-GAG, as it binds to all anionic sites. Two samples each of homozygous *dak/ext2* and WT embryos were incubated in 1% PEI (PEI-600, Polysciences, Warrington, PA) in 0.1 M sodium cacodylate buffer (pH 7.4) for 6 hours with constant agitation. The samples were washed after incubation and subsequently fixed with 2% phosphotungstic acid and 1% glutaraldehyde. The samples were then stained with 1% osmium tetroxide and embedded in epon LX-112. A selection of representative images containing at least 13 µm of GBM was analyzed using transmission electron microscopy.

Foot process width

Foot process width was analyzed using a selection of representative EM images obtained from three different homozygous *dak/ext2* mutants and three different WT embryos. All images contained at least 9 µm of contiguous GBM. The formula $\frac{\pi}{4} * \frac{\Sigma \text{GBMlength}}{\Sigma \text{foot processes}}$ was used to calculate foot process width.(38)

Assessing glomerular permeability

The quantitative dextran tracer injection method (adapted from the qualitative method described by Ebarasi *et al.*(39)) was used to measure glomerular permeability. This method is not used for an assessment of charge- or size-selectivity, but for analyzing functionally significant alterations to the global permeability of the GFB. A total of 32 homozygous *dak/ext2* and 35 WT embryos were used for four experiments as follows: at 5 dpf, the zebrafish embryos were anesthetized with 4% tricaine methanesulfonate (4 mg/ml), injected intravenously with 1 nl of a mixture containing FITC-labeled lysine-fixable 70-kDa dextran (25 mg/ml; Invitrogen, Waltham, MA) and TRITC-labeled 3-kDa dextran (100 mg/ml; Invitrogen). As a positive control, WT zebrafish embryos

were also injected with puromycin aminonucleoside (PAN, Sigma-Aldrich, St. Louis, MO) at 4 dpf.(40) One hour after the dextrans were injected, the samples were fixed in 10% formalin for 24 hours and stored in 70% ethanol until further processing. The samples were then embedded in paraffin, sectioned at 4-μm thickness, and examined using immunofluorescence microscopy. The samples were analyzed in a blinded manner.

Under physiological conditions, 3-kDa dextran can readily pass the GFB, whereas 70-kDa dextran does not. If the integrity of the GFB is sufficiently compromised, the 70-kDa dextran can pass the GFB, after which it is reabsorbed by proximal tubule epithelial cells in endosomes. Therefore, we measured the number of 70-kDa dextran particles in the proximal tubule cells as a measure of glomerular permeability. To confirm functional tubular reabsorption, we also measured the number of 3-kDa dextran particles in the proximal tubule cells.

Statistical analyses

Statistical analyses were performed using SPSS version 20.0 (IBM Corp., Armonk, NY). The proportion of zebrafish embryos with pericardial edema was analyzed using Fisher's exact test. Dextran tracer measurements of glomerular permeability, foot process width, and the presence of anionic sites were analyzed using the Student's unpaired *t*-test. Differences with a p-value <0.05 were considered significant.

Results

The dackel mutant phenotype

Homozygous *dak/ext2to273b* (referred to hereafter as simply "*dak/ext2")* mutants develop a clear phenotype, as described before.[15] Consistent with previous reports, compared to wild-type (WT) embryos, mutant embryos lacked pectoral fins and had a protruding jaw, a non-inflated swim bladder, and a more concave body shape.(34, 36) In addition, homozygous *dak/ext2* mutants had a significantly higher prevalence of pericardial edema compared to WT embryos (31/34 versus 1/140, respectively; $p<0.0001$). An example of morphological changes and pericardial edema in a mutant embryo is shown in Figure 1.

Loss of anionic sites in the GBM

Because HS-GAGs are believed to be the primary contributor to the negative charge in the GBM(7), we expected that the loss of HS-GAGs in the homozygous *dak/ext2* mutants would result in reduced numbers of negatively charged sites in the GBM. We therefore tested this hypothesis using polyethylenimine (PEI) staining;(41) PEI molecules bind to

negatively charged sites and form electron-dense deposits. Consistent with our hypothesis, the mean number of electron-dense deposits per μm of GBM was significantly lower in homozygous *dak/ext2* mutants compared to WT embryos (0.80, SD 0.39, $n = 2$ versus 2.2, SD 0.72, $n = 2$, respectively; $p<0.05$) (Figure 2).

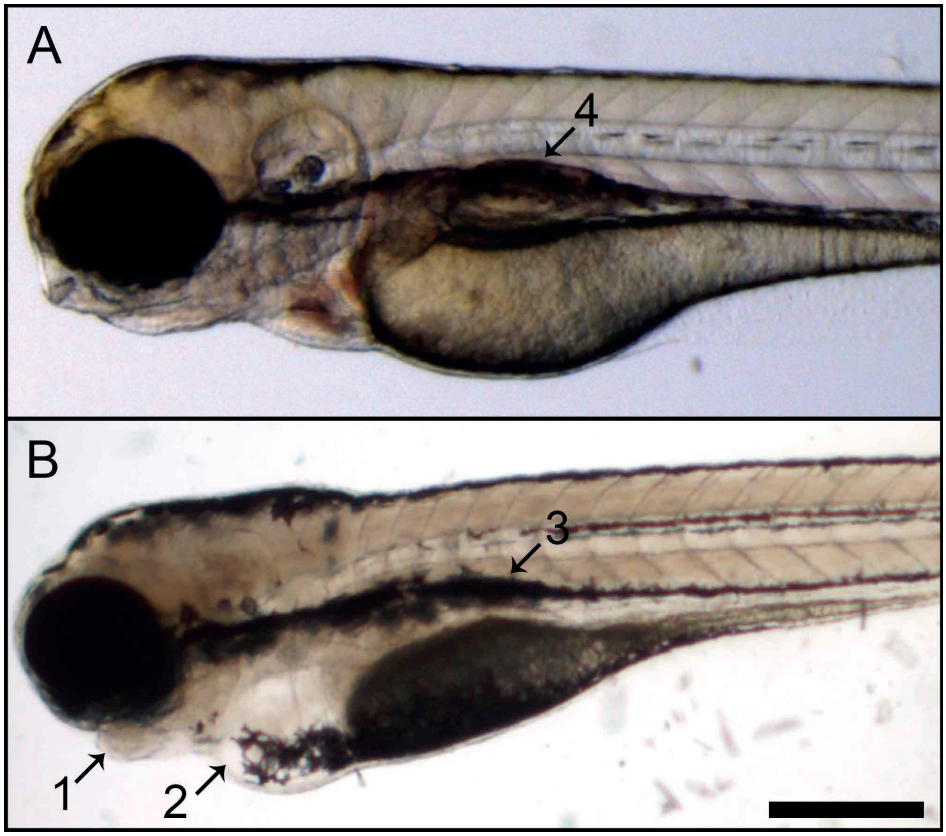

Figure 1. Homozygous dak/ext2 mutant zebrafish develop morphological changes
Shown are examples of a wild-type (A) and homozygous *dak/ext2* (B) embryo at 5 dpf, with several morphological changes in the mutant embryos. Arrows 1, 2, and 3 indicate a protruding jaw, pericardial edema, and a non-inflated swim bladder, respectively; arrow 4 shows a normally developed swim bladder in the WT embryo. Scale bar = 250 μm.

Foot process width

Ultrastructural analysis of the GFB using transmission electron microscopy revealed normal foot processes (Figure 2) in homozygous *dak/ext2* mutants. The mean width of foot process did not differ significantly between homozygous *dak/ext2* mutants and WT embryos (0.181. SD 0.025, $n = 3$ versus 0.176, SD 0.012, $n = 3$; $p=0.76$).

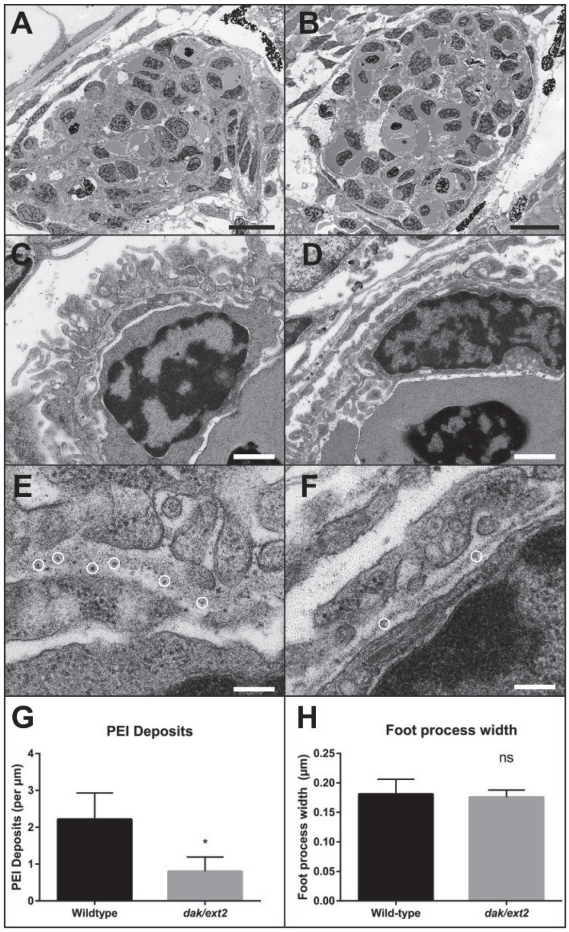

Figure 2. Homozygous dak/ext2 mutant zebrafish have significantly fewer electron dense-deposits in the GBM, but normal podocyte foot process width

Transmission electron micrographs of the glomerulus (A and B), a capillary loop (C and D) and representative sections of GBM (E and F) in a wild-type (A, C, and E) and homozygous *dak/ext2* mutant (B, D, and F) embryo. Sections were stained with PEI particles, which bind to negatively charged molecules in the GBM, forming electron-dense deposits (examples indicated by white circles in E and F). (G) Summary of the number of electron-dense PEI-containing deposits in the GBM; **p*<0.05. (H) Summary of the foot process width; ns, *p*>0.05. Scale bars = 10 µm (A and B), 1 µm (C and D) and 200 nm (E and F).

Glomerular permeability

Next, we analyzed the reabsorption of injected dextran particles (Figure 3). We found no significant difference between homozygous *dak/ext2* mutants and WT embryos with respect to the mean number of reabsorbed 3-kDa dextran droplets (22.69, SD 10.22, *n* = 32 versus 24.33 SD 12.51, *n* = 21; *p*=0.60). PAN-injected WT embryos, which were used as a positive control, had a similar number of 3-kDa dextran droplets (25.79, SD 13.33,

n = 14; *p*=0.75 versus WT and *p*=0.39 versus homozygous *dak/ext2*). As small particles can pass readily through the GFB, the similar number of 3-kDa dextran droplets indicates fully functional tubular reabsorption in all groups.

We also found no significant difference between homozygous *dak/ext2* mutants and WT embryos with respect to 70-kDa dextran particles (the mean number of droplets was 8.56, SD 5.33, *n* = 32 and 9.27, SD 3.72, *n* = 21 respectively; *p*=0.59) However, WT PAN-injected embryos had significantly more 70-kDa droplets (16.93, SD 5.41, *n* = 14) compared to both WT embryos (*p*<0.0001) and *dak/ext2* mutants (*p*<0.0001). Taken together, these data indicate that 70-kDa particles pass the GFB in similar quantities under physiological conditions and in an HS-GAG-free environment.

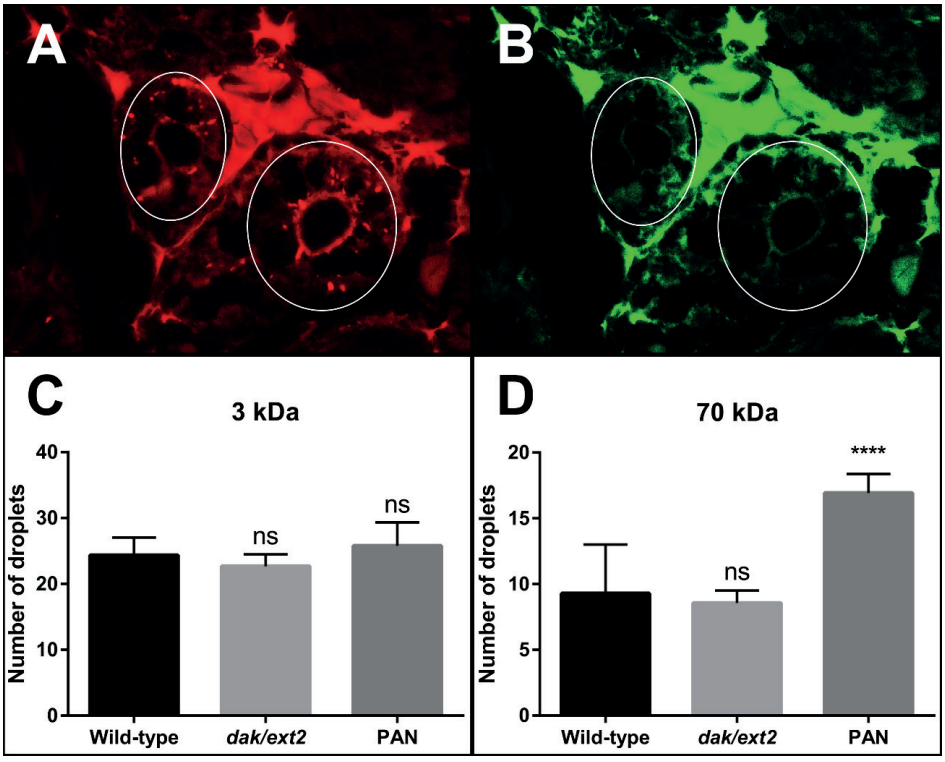

Figure 3. Homozygous dak/ext2 mutant zebrafish have normal glomerular permeability and tubular reabsorption capacity

Panels A and B show transverse sections through the proximal tubular epithelium of homozygous *dak/ext2* mutant embryos injected with red fluorescent 3-kDa dextran (A) and green fluorescent 70-kDa dextran (B). The white ellipse highlights the proximal tubule epithelial cells. The bright area between the circle reflects background fluorescence, partly due to auto-fluorescence. (C and D) Summary of the number of 3-kDa (C) and 70-kDa (D) dextran droplets in wild-type, homozygous *dak/ext2* mutant, and PAN-injected wild-type embryos. ns, *p*>0.05 versus wild-type; ****$p<0.0001$ versus wild-type. A digital high-pass filter has been placed over panels A and B to enhance the contrast between reabsorption droplets and the surrounding tissue. Scale bar = 5 μm.

Discussion

Here, we investigated whether HS-GAGs play an essential role in glomerular permeability using homozygous *dak/ext2* mutant zebrafish in which HS-GAGs are lacking in the entire embryo. We found that homozygous *dak/ext2* mutants develop an overall phenotype similar to previous reports.(34, 36) PEI staining of the GBM revealed significantly fewer anionic sites in homozygous mutants compared to WT embryos; however, despite having fewer negative sites in the GBM, homozygous *dak/ext2* mutants had normal glomerular permeability. Furthermore, our ultrastructural analysis revealed no difference between homozygous *dak/ext2* mutants and WT embryos with respect to podocyte foot width.

The classic paradigm based on the results of Kanwar *et al.*(8, 42) suggests that HS-GAGs are essential for normal glomerular filtration. In their study, the authors found that glomerular permeability increased after perfusing the kidney with heparinase III, an enzyme that cleaves HS-GAG chains. However, several other studies showed that podocyte-specific knockout of HS-GAGs did not result in proteinuria, suggesting that HS-GAGs may not necessarily be required for normal glomerular filtration.(23-27) Consistent with this notion, our results show that even when HS-GAGs are deleted in the entire embryo (and not specifically in podocytes), glomerular filtration is essentially intact. It remains possible that the size- and charge-selective properties of the GFB are altered in HS-GAG deficiency. However, overall glomerular permeability remains intact despite a severe and global loss of HS-GAG, as was hypothesized.

Previous *in vivo* models of HS-GAG deficiency used proteinuria as a readout of glomerular permeability; thus, albumin retrieval by proximal tubule epithelial cells may have masked changes in glomerular permeability, as suggested by Chen *et al.*(25) Therefore, we used tubular reabsorption of 70-kDa dextran particles as our readout of glomerular permeability; this method has previously been reported as providing a reliable measure of overall glomerular permeability.(40, 43) Although dextrans are known to move through a network as chains rather than as hydrodynamic spheres, dextrans have been validated as a sensitive marker for loss of glomerular permeability in various zebrafish models.(40, 43-46) Tubular reabsorption mechanisms were found to be fully functional in homozygous *dak/ext2* mutants, as a similar number of 3-kDa dextran droplets, which readily pass the GFB, was found between mutant and wild-type embryos.

Pericardial edema has previously been used as an indicator of renal damage in zebrafish.(43) Interestingly, although homozygous *dak/ext2* mutants lack HS-GAGs throughout the entire body and develop pericardial edema, they have essentially normal glomerular permeability. We therefore speculate that the pericardial edema observed in homozygous

dak/ext2 mutants is not caused by renal damage. For example, HS-GAG deficiency may have had an effect on the permeability of systemic capillaries because of an altered glycocalyx composition. Such a correlation between the endothelial glycocalyx of systemic capillaries and vascular permeability has been reported previously.(47)

An important difference between Kanwar *et al.*'s study and our approach using a germline mutation is that Kanwar *et al.* investigated the acute loss of HS-GAG by enzymatic activity, whereas our approach deleted HS-GAGs for an extended period. This difference may account for the difference in results between the two studies. For example, with a germline mutation, the effects will be present throughout the animal's life; therefore, other GAGs may have functionally replaced the deleted HS-GAGs. In the *in situ* set-up used by Kanwar *et al.,* loss of HS-GAG is acute and there is not enough time for such a compensatory mechanism to take place. Another possible explanation for the different results is that the enzymes used by Kanwar *et al.* may have caused collateral damage to other components of the GFB, which could have led to their observed increase in glomerular permeability.

The charge-selective nature of the GBM has long been attributed to the presence of HS-GAG.(7) In contrast, Miner proposed that charge selectivity is not an essential factor in glomerular permeability, as several studies found that a decreased number of anionic sites does not necessarily coincide with proteinuria.(48) Consistent with this notion, we found that glomerular permeability was not affected in homozygous *dak/ext2* mutants, despite the fact that these animals had significantly fewer PEI particles in the GBM. It is important to note that although negatively charged sites were significantly reduced in the GBM of homozygous *dak/ext2* mutants, these sites were not completely absent. Thus, these residual anionic sites could reflect negatively charged particles other than HS-GAGs. For example, type IV collagen, which is one of the primary constituents of the GBM, contains negatively charged sialic acid residues.(49) Therefore, we cannot exclude the possibility that the residual negatively charged sites in the GBM are sufficient for conferring charge selectivity.

Our ultrastructural analysis of the glomeruli in zebrafish embryos revealed that homozygous *dak/ext2* mutants have normal podocyte foot processes. Although similar results were reported in podocyte-specific agrin-deficient and perlecan-deficient mice, podocyte-specific *Ext1* knockout mice have foot process effacement.(23-25) The difference between our global *ext2* deficient zebrafish model and the podocyte-specific *Ext1* knockout mice may be due to differential effects of Ext1 and Ext2 on podocyte cytoskeletal organization. Both EXT1 and EXT2 have been reported to influence cytoskeletal organization in

chondrocytes obtained from patients with EXT1 or EXT2 mutations,(50) in which the specific mutation seemed to determine the effect on cytoskeletal organization. Whether EXT1 and/or EXT2 directly affect cytoskeletal organization in podocytes, independently of HS-GAG side chains, remains an open question.

This study has several limitations. First, a direct local decrease in HS-GAGs could not be shown by immunohistochemistry. However, *dak/ext2* mutants had significantly less anionic sites in the GBM than WT animals in our PEI labelling experiment. This is indirect proof of a decrease in HS-GAGs. Thus, the degree of HS-GAG deficiency in the glomerulus is at least 63%, as this is the relative difference in PEI particles. These particles could reflect HS-GAGs, other sulfated GAGs or other negatively charged areas. Also, the total decrease of HS-GAGs in *dak/ext2* zebrafish embryos has previously been reported to be over 80%.(21, 30) Although a relative and significant decrease in PEI-particles was observed, the absolute extent of PEI-labeling is less than in mammalian systems. A possible explanation is that this is due to a methodological difference, as we did not perform an *in vivo* labelling.(25) Also, it could be a reflection of interspecies variation in anionic site distribution in the GBM.

Furthermore, the *dak/ext2* model does not have a complete loss of HS-GAG. Theoretically, a double knock out of ext1 and ext2 would result in even more pronounced loss of HS-GAG. As zebrafish have three ext1 genes (ext1a, ext1b and ext1c) and up to date, characterized mutants lines are not available for any of these semi-orthologues, this could not be confirmed experimentally. To the best of our knowledge, this is the first study to examine the effect of a global HS-GAG deficiency on glomerular permeability. Globally deleting HS-GAGs in most vertebrates causes extremely early lethality;(51) Thus, the homozygous *dak/ext2* mutant zebrafish is currently the only viable model for global loss of HS-GAGs that survives gastrulation when both copies of the ext2 gene are impaired and that gives unique opportunity to study glomerular filtration that cannot be rescued by HS-GAGs produced by other type of cells. Although homozygous *dak/ext2* mutants do not survive to adulthood, Lee *et al.* hypothesized that these mutants survive the first part of the embryonic phase due to the maternal contribution of Ext2;(30) by 5 dpf, maternal contribution of Ext2 decreases to non-detectable levels.(30)

In conclusion, we provide the first report that glomerular permeability is not affected by a global HS-GAG deficiency. These results support the growing body of evidence that HS-GAGs do not play an essential role in mediating glomerular permeability.

Acknowledgements

The authors would like to thank Peter Neeskens and Brendy van den Akker for assistance with EM experiments.

Grants

This work was supported by the Dutch National Kidney Foundation (IP 11.57).

Disclosures

The authors declare no competing interests.

Author's contributions

All authors contributed to conception or design, or analysis and interpretation of data, provided intellectual content of article drafting or revision and have provided final approval of the version to be published.

RK designed and performed experiments, analyzed data, and wrote the paper. RAL performed experiments and analyzed data, MIW and CMA designed and performed experiments, AJK, HPS, JAB, and PCW designed experiments and provided conceptual advice. HJB designed experiments, provided technical support and conceptual advice.

References

1. Aoki S, Saito-Hakoda A, Yoshikawa T, Shimizu K, Kisu K, Suzuki S, Takagi K, Mizumoto S, Yamada S, van Kuppevelt TH, Yokoyama A, Matsusaka T, Sato H, Ito S, and Sugawara A. The reduction of heparan sulphate in the glomerular basement membrane does not augment urinary albumin excretion. *Nephrology, dialysis, transplantation : official publication of the European Dialysis and Transplant Association - European Renal Association* 33: 26-33, 2018.
2. Bernard MA, Hogue DA, Cole WG, Sanford T, Snuggs MB, Montufar-Solis D, Duke PJ, Carson DD, Scott A, Van Winkle WB, and Hecht JT. Cytoskeletal abnormalities in chondrocytes with EXT1 and EXT2 mutations. *J Bone Miner Res* 15: 442-450, 2000.
3. Brenner BM, Hostetter TH, and Humes HD. Molecular basis of proteinuria of glomerular origin. *N Engl J Med* 298: 826-833, 1978.
4. Chen S, Wassenhove-McCarthy DJ, Yamaguchi Y, Holzman LB, van Kuppevelt TH, Jenniskens GJ, Wijnhoven TJ, Woods AC, and McCarthy KJ. Loss of heparan sulfate glycosaminoglycan assembly in podocytes does not lead to proteinuria. *Kidney international* 74: 289-299, 2008.
5. Clement A, Wiweger M, von der HS, Rusch MA, Selleck SB, Chien CB, and Roehl HH. Regulation of zebrafish skeletogenesis by ext2/dackel and papst1/pinscher. *PLoS Genet* 4: e1000136, 2008.
6. de Andrea CE, Prins FA, Wiweger MI, and Hogendoorn PC. Growth plate regulation and osteochondroma formation: insights from tracing proteoglycans in zebrafish models and human cartilage. *The Journal of pathology* 224: 160-168, 2011.
7. Ebarasi L, He L, Hultenby K, Takemoto M, Betsholtz C, Tryggvason K, and Majumdar A. A reverse genetic screen in the zebrafish identifies crb2b as a regulator of the glomerular filtration barrier. *Developmental biology* 334: 1-9, 2009.
8. Esko JD, and Selleck SB. Order out of chaos: assembly of ligand binding sites in heparan sulfate. *Annual review of biochemistry* 71: 435-471, 2002.
9. Faas FG, Avramut MC, van den Berg BM, Mommaas AM, Koster AJ, and Ravelli RB. Virtual nanoscopy: generation of ultra-large high resolution electron microscopy maps. *The Journal of cell biology* 198: 457-469, 2012.
10. Goldberg S, Harvey SJ, Cunningham J, Tryggvason K, and Miner JH. Glomerular filtration is normal in the absence of both agrin and perlecan-heparan sulfate from the glomerular basement membrane. *Nephrology, dialysis, transplantation : official publication of the European Dialysis and Transplant Association - European Renal Association* 24: 2044-2051, 2009.
11. Gundersen HJ, Seefeldt T, and Osterby R. Glomerular epithelial foot processes in normal man and rats. Distribution of true width and its intra- and inter-individual variation. *Cell Tissue Res* 205: 147-155, 1980.
12. Hanke N, King BL, Vaske B, Haller H, and Schiffer M. A Fluorescence-Based Assay for Proteinuria Screening in Larval Zebrafish (Danio rerio). *Zebrafish* 12: 372-376, 2015.
13. Hanke N, Staggs L, Schroder P, Litteral J, Fleig S, Kaufeld J, Pauli C, Haller H, and Schiffer M. "Zebrafishing" for novel genes relevant to the glomerular filtration barrier. *BioMed research international* 2013: 658270, 2013.
14. Harvey SJ, Jarad G, Cunningham J, Rops AL, van d, V, Berden JH, Moeller MJ, Holzman LB, Burgess RW, and Miner JH. Disruption of glomerular basement membrane charge through podocyte-specific mutation of agrin does not alter glomerular permselectivity. *Am J Pathol* 171: 139-152, 2007.
15. Hentschel DM, Mengel M, Boehme L, Liebsch F, Albertin C, Bonventre JV, Haller H, and Schiffer M. Rapid screening of glomerular slit diaphragm integrity in larval zebrafish. *American journal of physiology Renal physiology* 293: F1746-1750, 2007.
16. Hogendoorn PC, de Heer E, Weening JJ, Daha MR, Hoedemaeker PJ, and Fleuren GJ. Glomerular capillary wall charge and antibody binding in passive Heymann nephritis. *J Lab Clin Med* 111: 150-157, 1988.

17. Holmborn K, Habicher J, Kasza Z, Eriksson AS, Filipek-Gorniok B, Gopal S, Couchman JR, Ahlberg PE, Wiweger M, Spillmann D, Kreuger J, and Ledin J. On the roles and regulation of chondroitin sulfate and heparan sulfate in zebrafish pharyngeal cartilage morphogenesis. *The Journal of biological chemistry* 287: 33905-33916, 2012.
18. Jeansson M, and Haraldsson B. Morphological and functional evidence for an important role of the endothelial cell glycocalyx in the glomerular barrier. *Am J Physiol Renal Physiol* 290: F111-F116, 2006.
19. Jungers P, Hannedouche T, Itakura Y, Albouze G, Descamps-Latscha B, and Man NK. Progression rate to end-stage renal failure in non-diabetic kidney diseases: a multivariate analysis of determinant factors. *Nephrol Dial Transplant* 10: 1353-1360, 1995.
20. Kanwar YS, and Farquhar MG. Presence of heparan sulfate in the glomerular basement membrane. *Proceedings of the National Academy of Sciences of the United States of America* 76: 1303-1307, 1979.
21. Kanwar YS, Linker A, and Farquhar MG. Increased permeability of the glomerular basement membrane to ferritin after removal of glycosaminoglycans (heparan sulfate) by enzyme digestion. *The Journal of cell biology* 86: 688-693, 1980.
22. Laurent TC, Sundelof LO, Wik KO, and Warmegard B. Diffusion of dextran in concentrated solutions. *Eur J Biochem* 68: 95-102, 1976.
23. Lee JS, von der Hardt S, Rusch MA, Stringer SE, Stickney HL, Talbot WS, Geisler R, Nusslein-Volhard C, Selleck SB, Chien CB, and Roehl H. Axon sorting in the optic tract requires HSPG synthesis by ext2 (dackel) and extl3 (boxer). *Neuron* 44: 947-960, 2004.
24. Lin X, Wei G, Shi Z, Dryer L, Esko JD, Wells DE, and Matzuk MM. Disruption of gastrulation and heparan sulfate biosynthesis in EXT1-deficient mice. *Developmental biology* 224: 299-311, 2000.
25. Matsushita K, van d, V, Astor BC, Woodward M, Levey AS, de Jong PE, Coresh J, and Gansevoort RT. Association of estimated glomerular filtration rate and albuminuria with all-cause and cardiovascular mortality in general population cohorts: a collaborative meta-analysis. *Lancet* 375: 2073-2081, 2010.
26. Miner JH. Glomerular filtration: the charge debate charges ahead. *Kidney international* 74: 259-261, 2008.
27. Nayak BR, and Spiro RG. Localization and structure of the asparagine-linked oligosaccharides of type IV collagen from glomerular basement membrane and lens capsule. *J Biol Chem* 266: 13978-13987, 1991.
28. Rider SA, Bruton FA, Collins RG, Conway BR, and Mullins JJ. The Efficacy of Puromycin and Adriamycin for Induction of Glomerular Failure in Larval Zebrafish Validated by an Assay of Glomerular Permeability Dynamics. *Zebrafish* 15: 234-242, 2018.
29. Rosenzweig LJ, and Kanwar YS. Removal of sulfated (heparan sulfate) or nonsulfated (hyaluronic acid) glycosaminoglycans results in increased permeability of the glomerular basement membrane to 125I-bovine serum albumin. *Lab Invest* 47: 177-184, 1982.
30. Salmon AH, and Satchell SC. Endothelial glycocalyx dysfunction in disease: albuminuria and increased microvascular permeability. *The Journal of pathology* 226: 562-574, 2012.
31. Schurer JW, Hoedemaeker J, and Molenaar I. Polyethyleneimine as tracer particle for (immuno) electron microscopy. *J Histochem Cytochem* 25: 384-387, 1977.
32. Singh A, Satchell SC, Neal CR, McKenzie EA, Tooke JE, and Mathieson PW. Glomerular endothelial glycocalyx constitutes a barrier to protein permeability. *Journal of the American Society of Nephrology : JASN* 18: 2885-2893, 2007.
33. Sugar T, Wassenhove-McCarthy DJ, Esko JD, van Kuppevelt TH, Holzman L, and McCarthy KJ. Podocyte-specific deletion of NDST1, a key enzyme in the sulfation of heparan sulfate glycosaminoglycans, leads to abnormalities in podocyte organization in vivo. *Kidney international* 85: 307-318, 2014.

34. van den Born J, van den Heuvel LP, Bakker MA, Veerkamp JH, Assmann KJ, Weening JJ, and Berden JH. Distribution of GBM heparan sulfate proteoglycan core protein and side chains in human glomerular diseases. *Kidney international* 43: 454-463, 1993.
35. van Det NF, van den Born J, Tamsma JT, Verhagen NA, Berden JH, Bruijn JA, Daha MR, and van der Woude FJ. Effects of high glucose on the production of heparan sulfate proteoglycan by mesangial and epithelial cells. *Kidney international* 49: 1079-1089, 1996.
36. van Eeden FJ, Granato M, Schach U, Brand M, Furutani-Seiki M, Haffter P, Hammerschmidt M, Heisenberg CP, Jiang YJ, Kane DA, Kelsh RN, Mullins MC, Odenthal J, Warga RM, and Nusslein-Volhard C. Genetic analysis of fin formation in the zebrafish, Danio rerio. *Development* 123: 255-262, 1996.
37. Wiweger MI, Avramut CM, de Andrea CE, Prins FA, Koster AJ, Ravelli RB, and Hogendoorn PC. Cartilage ultrastructure in proteoglycan-deficient zebrafish mutants brings to light new candidate genes for human skeletal disorders. *The Journal of pathology* 223: 531-542, 2011.
38. Wiweger MI, Zhao Z, van Merkesteyn RJ, Roehl HH, and Hogendoorn PC. HSPG-deficient zebrafish uncovers dental aspect of multiple osteochondromas. *PloS one* 7: e29734, 2012.

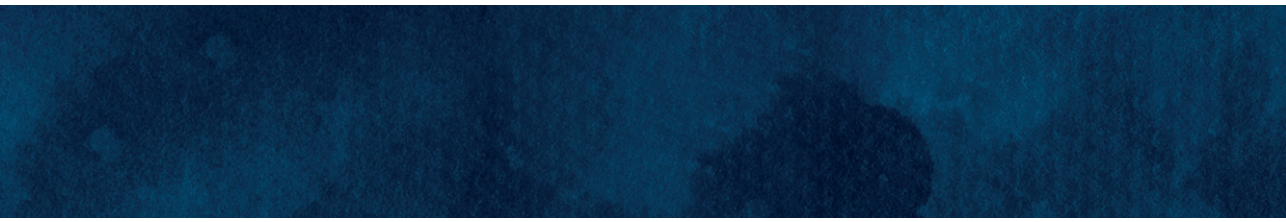

CHAPTER 4

Mutations in the heparan sulfate backbone elongating enzymes EXT1 and EXT2 have no major effect on endothelial glycocalyx and the glomerular filtration barrier

Molecular Genetics and Genomics 2022, 297, 397–405

Ramzi Khalil[1], Margien G.S. Boels[2], PALGA Group[3], Bernard M. van den Berg[2], Jan A. Bruijn[1], Ton J. Rabelink[2], Pancras C.W. Hogendoorn[1], Hans J. Baelde[1]

[1] *Department of Pathology, Leiden University Medical Center, Leiden, The Netherlands*
[2] *The Einthoven Laboratory for Vascular and Regenerative Medicine, Department of Internal Medicine, Division of Nephrology, Leiden University Medical Center, Leiden, The Netherlands,*
[3] *PALGA Group*

Abstract

In this study, the effect of heterozygous germline mutations in the heparan sulfate (HS) glycosaminoglycan chain co-polymerases EXT1 and EXT2 on glomerular barrier function and the endothelial glycocalyx in humans is investigated.

Heparan sulfate (HS) glycosaminoglycans are deemed essential to the glomerular filtration barrier, including the glomerular endothelial glycocalyx. Animal studies have shown that loss of HS results in a thinner glycocalyx. Also, decreased glomerular HS expression is observed in various proteinuric renal disease in humans. A case report of a patient with an *EXT1* mutation indicated that this could result in a specific renal phenotype. This patient suffered from multiple osteochondromas, an autosomal dominant disease caused by mono-allelic germline mutations in the *EXT1* or *EXT2* gene. These studies imply that HS is indeed essential to the glomerular filtration barrier. However, loss of HS did not lead to proteinuria in various animal models.

We demonstrate that multiple osteochondroma patients do not have more microalbuminuria or altered glycocalyx properties compared to age-matched controls (n = 19). A search for all Dutch patients registered with both osteochondroma and kidney biopsy (n = 39), showed that an *EXT1* or *EXT2* mutation does not necessarily lead to specific glomerular morphological phenotypic changes.

In conclusion, this study shows that a heterozygous mutation in the HS backbone elongating enzymes EXT1 and EXT2 in humans does not result in (micro)albuminuria, a specific renal phenotype or changes to the endothelial glycocalyx, adding to the growing knowledge on the role of EXT1 and EXT2 genes in pathophysiology.

Background

The effect of heterozygous germline mutations in *EXT1* or *EXT2* on the glomerular filtration barrier, with special attention to the endothelial glycocalyx, is investigated in this study. We hypothesized that patients with a mutation in *EXT1* or *EXT2* have a perturbed endothelial glycocalyx and glomerular basement membrane that results in changes in renal morphology and altered glomerular permeability. Therefore, we performed a cross-sectional observational study in a cohort of patients with *EXT1* and *EXT2* mutations to investigate endothelial glycocalyx health and the glomerular barrier function in humans. In addition, we identified a historic cohort of renal biopsy or autopsy tissue from patients with osteochondromas in which we examined whether a specific renal morphological phenotype is present. HS is made up of repeating disaccharide units of *N*-acetyl glucosamine and glucuronic acid, covalently attached to a core protein, such as syndecans and glypicans.(9) Biosynthesis of HS comprises three steps: chain initiation, chain elongation, (requiring the EXT1 and EXT2 co-polymerase)and chain modification. Depending on the modification state of HS, various sulfate groups are attached to the chain and thus infer negative charge, anti-coagulatory properties, and the capability to bind various cytokines and chemokines (52).

HS has been studied extensively in the glomerular filtration barrier (GFB).(7, 8) The GFB consists of fenestrated endothelial cells covered by glycocalyx, the glomerular basement membrane, and specialized visceral epithelial cells (podocytes) with interdigitating foot processes. There has a been a longstanding discussion on whether HS is essential to glomerular permeability (53). Glomeruli of patients with lupus nephritis, membranous glomerulonephritis, minimal change disease, and diabetic nephropathy showed a decreased staining of heparan sulfate.(22) Degradation of HS in the glycocalyx by heparanase increases glomerular permeability to albumin, results in increased accessibility to autoantibodies, and loss of HS was observed in various proteinuric renal diseases (22, 29, 37). On the other hand, a genetic HS deficiency has been shown not to result in significant proteinuria in various experimental animal models. (23, 25, 27, 54, 55)

Gleadle *et al.* reported on a patient with a monoallelic germline mutation in an HS polymerizing gene, *EXT1*, that presented with a nephrotic syndrome. Histology from a renal biopsy of this patient showed specific changes on EM of fibrillar deposition in the GBM and mesangium (56). Based on this case, the renal disease 'glomerulopathy of hereditary multiple exostoses' is recognised as a separate disease entity (57). *EXT1* or *EXT2* loss of function mutations result in the autosomal dominant disease multiple

osteochondromas (MO, OMIM no. 133700 and 133701), previously also known as hereditary multiple exostoses (HME) and multiple hereditary multiple exostoses (MHE) (58). MO is defined as a disease 'characterized by development of two or more cartilage capped bony outgrowths (osteochondromas) of the long bones.' (59, 60). More than 85% of MO patients have a germline mutation in the *EXT1* or *EXT2* gene.(59) The *EXT1* and *EXT2* gene products form a co-polymerase that initiates chain elongation in heparan sulfate glycosaminoglycan synthesis.(9) Existence of another exostosin gene, *EXT3,* has been suggested but not proven.(61) However, as stated above, the diagnosis is often based on radiological and clinical assessment. Therefore, in many patients, genetic testing is regarded as optional in establishing the diagnosis.(62)

In MO patients, a decrease in HS levels has been described in the circulatory system and in exostosis growth plates (63, 64). However, the effect of heterozygous *EXT1* and *EXT2* mutations on the endothelial glycocalyx have not yet been described. Moreover, it is currently unknown whether a loss of HS as a result of perturbed HS assembly results in an increase in glomerular permeability in humans.

HS is also a major structural component of the glycocalyx, a coat of sugars, proteins, and lipids, lining the luminal side of the endothelium (65). Endothelial dysfunction is an important process in both cardiovascular and renal disease (66, 67). Recent technological advances have now made it possible to assess the red blood cell (RBC) count accessibility to the endothelial surface glycocalyx, in which a healthy glycocalyx is reflected by a low perfused boundary region (PBR) and a glycocalyx at risk is reflected by a high PBR (5, 68).

Methods

Ethics

Ethical approval for this study was obtained through the LUMC Medical Ethical Committee under registration number P15.106. Anonymized patient material from the PALGA search was handled in accordance with institutional guidelines, Good Research Practice, and the Code of conduct for responsible use.

MO patient study population

Patients were approached through the Dutch HME-MO Association (www.hme-mo.nl). Controls were obtained from the general population and matched for age and gender. All participants were required to be capacitated and over 18 years of age. After obtaining informed consent, participants were handed a digital questionnaire. Data on mutation status, use of medication, smoking, hypertension, and relevant medical history was

collected. Participants were asked to perform one site visit, during which a glycocalyx measurement was performed and urine samples were collected.

Glycocalyx measurements

Sublingual microvasculature was visualised non-invasively using a sidestream–darkfield MicroScan Video Microscope (MicroVision Medical, Inc., Wallingford, PA), connected to Glycocheck™ acquisition and analysis software (Microvascular Health Solutions Inc., Salt Lake City, UT, USA) to automatically acquire microvascular video recordings after predefined image quality criteria (motion, intensity, and focus) are fulfilled. Each complete measurement consists of at least ten 2-second videos (40 frames/video), containing a total of about 3000 vascular segments of 10μm length each. During the measurement, the camera is moved to different positions under the tongue to obtain different sublingual microvascular sites. The vascular segments are automatically subjected to a quality check by the GlycoCheck™ software, discarding invalid segments. Next, the software obtains up to 840 radial intensity profiles for each valid vascular segment and, based on the RBC column width (RBCW) it automatically groups vessels from 4 to 25 μm diameter in 22 separate diameter classes (1μm each). Data from two complete measurements were extracted, analyzed and averaged offline to avoid sampling error and to counterbalance spatial-temporal heterogeneity of the sublingual microcirculation. These analyses resulted in the following parameters: perfused capillary density; capillary blood volume; dynamic perfused boundary region (PBR). PBR is a measure for glycocalyx quality by measuring dynamic lateral RBC movement into the glycocalyx: a larger PBR reflects a disturbance of the glycocalyx (5, 68).

Detailed information about the video acquisition and software used is described elsewhere (68).

Urinary albumin / protein excretion

Spot urine samples were collected during the site visit and analysed for albumin, total protein, and creatinine at the LUMC department of Clinical Chemistry. Albumin-creatinin ratio (ACR) and protein-creatinin ratio (PCR) were used to identify the presence of (micro)albuminuria and (micro)proteinuria according to the KDIGO CKD guideline (2).

Historic PALGA cohort selection

The Dutch pathology national automated archive (PALGA) was searched for cases containing both the search terms 'kidney and biopsy' and 'osteochondroma and multiple osteochondromas', to identify potential MO patients who have undergone a renal biopsy

or autopsy in which renal tissue was collected between 1978 and 2014. The slides and EM material of the identified cases were requested from the corresponding hospitals. Sections were assessed for specific light microscopic changes and, if available, irregularities on EM.

Statistical analyses

Baseline characteristics are expressed as mean (± standard deviation [SD]), or as percentage. Groups were matched for age and gender. Difference between groups in sublingual measures and albuminuria was determined using unpaired t-tests. ANOVA was used for side-by-side comparison of PBR in various vessel sizes. Pearson's correlation coefficient was calculated to assess correlations. Graphpad Prism (version 8.4.2 (GraphPad Software, San Diego, California USA) was used for statistical analyses. $p < 0.05$ was considered statistically significant.

Results

Patient Characteristics

20 MO patients responded to the call for our study. 1 patient retracted from the study before performing the site visit. Of the 19 remaining patients, 6 had a confirmed *EXT1* (4) or *EXT2* (2) mutation and 13 had a clinical diagnosis of MO without mutational confirmation. (62) 27 Controls, of which 19 are age and sex matched, were selected from the general population. No differences were observed in gender, age or body mass index (Table 1).

Table 1. Patient characteristics

	MO patients	**Healthy controls**
Subjects	19	19
Age, mean (SD), y	45 (±15.6)	45 (±16.0)
Men, n (%)	2 (10.5)	2 (10.5)
BMI (SD)	26,0 (± 6.5)	23,4 (± 2.8)
Smoking, n (%)	1 (5.3)	1 (5.3)
Hypertension, n (%)	4 (21.1)	0
ACE inhibitor, n (%)	2 (10.5)	0
ARB, n (%)	0	0
NSAID use, n (&)	7 (33.3)	3 (14.3)
Diabetes, n (%)	2 (10.5)	0
Type 1, n (%)	0	0
Type 2 n (%)	2 (10.5)	0
EXT1 mutation, n (%)	4 (21.1)	N/A
EXT2 mutation, n (%)	2 (10.5)	N/A
Mutation unknown, n (%)	13 (68.4)	N/A

BMI: Body Mass Index, ACE: angiotensin converting enzyme, ARB: angiotensin 2 receptor blocker, NSAID: non-steroidal anti inflammatory drugs, EXT: exostosin

EXT1/EXT2 mutations do not result in changed microvascular endothelial glycocalyx properties

Since mutations in one of the HS elongation enzymes *EXT1* and *EXT2* could result in compositional changes of the endothelial glycocalyx we investigated possible perturbations in glycocalyx properties. Sublingual measurements of the microcirculation of control and MO patients did not reveal a difference in perfused vascular density (352.69±102.16 vs. 322.25±68.17 μm/mm^2, respectively; p>0.99, Figure 1A) nor in changes in the perfused boundary regions (2.05±0.29 vs. 2.15±0.21 μm, respectively; p>0.99, Figure 1B). Subanalysis of PBR in vessels 5 to 9 μm, 10 to 19 μm, and 20 to 25 μm also showed no difference between MO patients and controls (p>0.99 in all instances Figure 1C through E). No correlation was found between increasing age and any of the used outcome parameters, which were density, PBR 5-25, PBR 5-9, PBR 10-19, and PBR 20-25. This was the case in the overall group (r = 0.20, 0.21, -0.13, 0.20, and 0.24 with p = 0.19, 0.18, 0.42, 0,21, and 0,13 respectively) as well as when analysing the MO patient (r = 0.28, -0.12, -0.08, -0.25, and 0.06 with p = 0.27, 0.66, 0.77, 0.34, and 0.82 respectively) and control group (r = 0.18, 0.35, -0.17, 0.38, and 0.33 with p = 0.37, 0.08, 0.43, 0.06, and 0.11 respectively) separately.

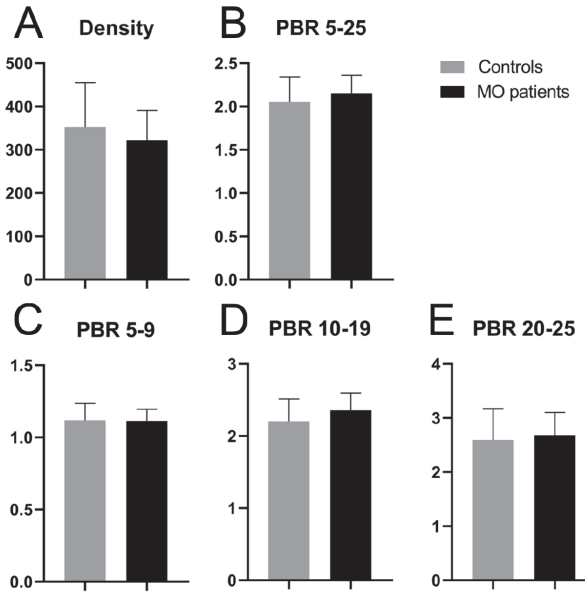

Figure 1. MO patients have normal vascular density and perfused boundary region
(**A** through **E**) Summary of vascular density (**A**) and perfused boundary region (**B** through **E**). No difference is seen in both vascular density and PBR between controls and MO patients. Subanalysis of PBR in vessels of 5 to 9 μm (**C**), 10 to 19 μm (**D**), and 20 to 25 μm (**E**) also shows no difference between controls and MO patients. *: p > 0.99

EXT1/EXT2 mutations do not directly induce proteinuria

Analysis of the collected urine samples was performed by matching MO patients to controls based on age and gender. Analysis revealed no difference in ACR nor PCR of patients compared to controls (p=0.13, Figure 2). All MO patients in this study were found to be normoalbuminuric. Five control cases were microalbuminuric and one control case was albuminuric according to the KDIGO CKD guideline (2). No correlation was found between age and ACR or PCR in both patients (r = -0.09 and 0.10 with p = 0.72 and 0.69*)* and controls (r = -0.24 and -0.19 with p = 0.33 and 0.43 respectively).

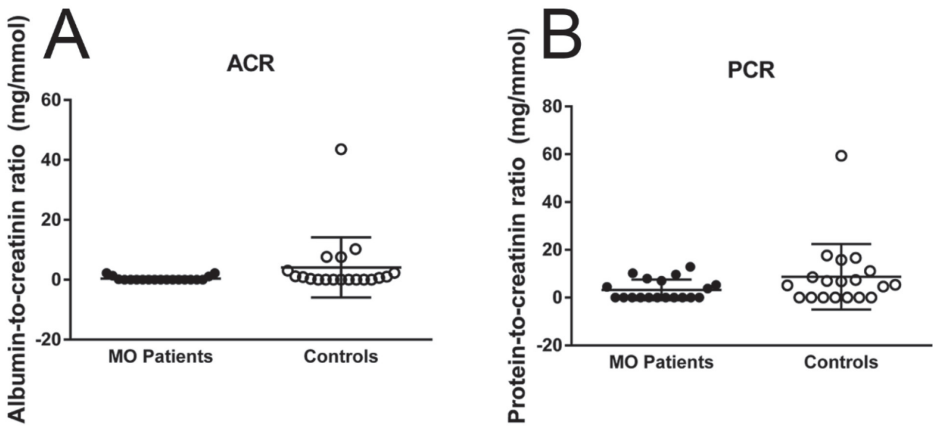

Figure 2. MO patients are normoalbuminuric
(**A** and **B**) MO patients do not have a higher albumin-to-creatinin (**A**) nor a higher protein-to-creatinin ratio (B). p = 0.1251 and p = 0.1282 respectively.

Renal morphological change in patients with osteochondromas

Searching the Dutch pathological anatomy national automated archive (PALGA) for cases in which both 'osteochondroma' and 'kidney' are mentioned, resulted in 178 reports from 63 patients. After excluding cases in which no renal tissue was present, slides and EM material from 77 reports out of 39 cases were requested from the corresponding hospitals. We received material from 24 cases. Out of these cases, at least 4 can be classified as having MO based on clinical criteria available in the pathology reports. Genetic data of this cohort is unknown.

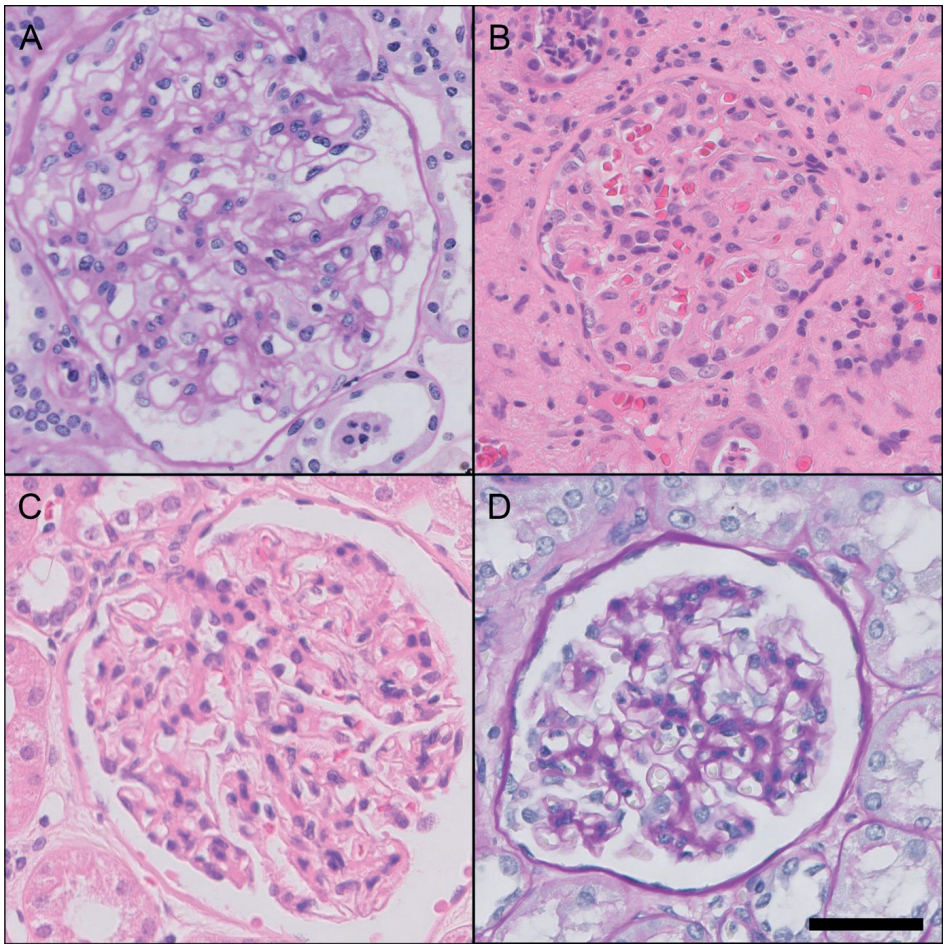

Figure 3. Light microscopy of glomeruli from MO patients shows relatively normal morphology
Snapshots of glomeruli from MO patients are shown. No specific lesions other than those related to the primary disease were observed. The examples are derived from patients with IgA nephropathy (**A**, PAS), glomerulonephritis after transplantation (**B**, H&E), and neoplastic diseases (**C**, H&E and D, PASD). Original magnification 40x. Scale bar = 50 µm

Evaluation of the renal sections by light microscopy did not reveal notable changes that could be specific for MO (56). A selection of representative images is shown in figure 3. However, EM analysis revealed a highly aberrant phenotype in one case with a noteworthy clinical history. This patient had received a kidney transplantation after suffering from a renal insufficiency. The primary disease was noted to have 'membrane anomalies reminiscent of a hereditary nephritis. We re-examined the EM grids of this patient, and found segmental fibrillar deposition that seemed similar to that reported by Roberts *et al.*

(56). Cross-striated fibrils with a diameter of 140 nm and regular periodicity were found in the mesangial area and the laminae rarae of the glomerular basement membrane of the native kidney (Figure 4). This was the only patient in the cohort for whom EM data was available. Genetic data of this patient was not available.

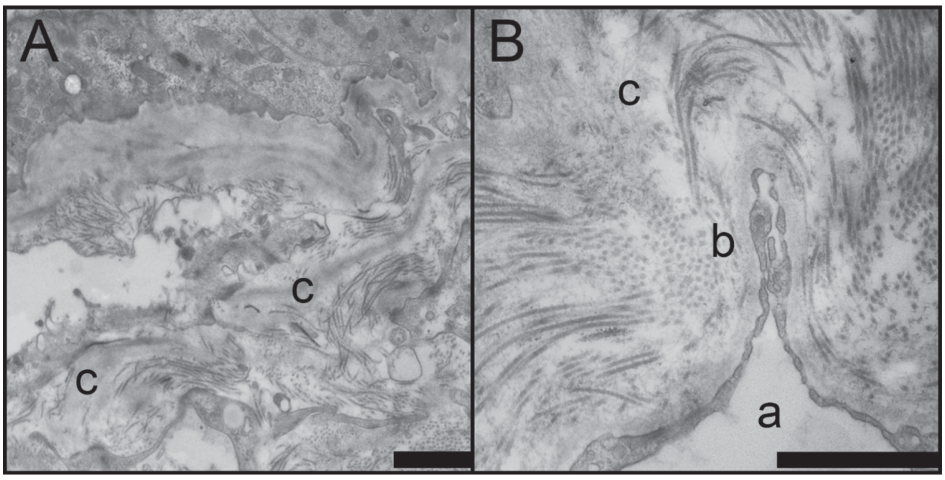

Figure 4. Glomerular fibril deposition HME-MO glomerulopathy
(**A** and **B**) Deposition of large fibrils with a diameter of 140 nm was seen in the glomerulus of an MO patient. The fibril depositions are seen in the laminae rarae of the GBM and in the mesangium. (c) General morphology is disrupted due to the fibril deposition. In figure B, endothelial lumen (a) and fenestrated endothelial cells can be seen (b). The fibrils in the GBM appear to be collagenous in nature. (c) Scale bar = 5 μm.

Discussion

In this study, we investigated the effect of heterozygous *EXT1* or *EXT2* germline mutations on glomerular permeability, glomerular morphology, and the endothelial glycocalyx. No (micro)albuminuria was observed in these patients, despite also having a higher prevalence of other risk factors for developing proteinuria with more hypertension, diabetes and NSAID use, as shown in Table 1. Furthermore, no specific glomerular morphological changes were observed in biopsies from a historic cohort of MO patients without clinical symptoms of renal damage. However, one of MO patient with renal pathology showed a glomerular phenotype resembling MO glomerulopathy. No significant difference was found in PBR thickness or vascular density between MO patients and controls.

This study shows that heterozygous *EXT1* or *EXT2* germline mutations do not significantly influence glomerular permeability or the endothelial glycocalyx. Glomerular permeability was not affected by these mutations, as no difference was found in albuminuria between

patients and controls. We found no difference in PBR and vascular density between patients with an *EXT1* or *EXT2* mutation and controls, indicating that these mutations do not significantly alter the endothelial glycocalyx. Also, we found no specific glomerular phenotype in patients with osteochondromas. These results contribute to the widely discussed topic of the role of HS in the GFB.(25, 55)

Interestingly, one patient in this group showed a complicated medical history with an unexplained renal insufficiency that resulted in renal replacement therapy. Our EM analysis of this patient showed glomerular deposition of large collagen fibrils in the mesangium and GBM, similar to those found by Roberts *et al.* (56).

Previously, circulating HS derived from MO patients was found to be structurally normal, but quantitatively diminished compared to healthy controls (63). Whether MO patients have structurally aberrant HS in the GFB and glycocalyx is currently unknown. Our results could imply that the mono-allelic germline mutation in *EXT1* or *EXT2* in MO does not lead to these structural changes. Potentially, one functional allele is sufficient to prevent a phenotype from developing. Because most MO patients showed a normal glomerular morphology, we hypothesize that a second trigger is required to develop glomerular pathology specific to the *EXT1* or *EXT2* gene defect. In MO pathogenesis, germline heterozygous mutations in EXT1 or EXT2 are not sufficient to cause osteochondroma formation. Loss of heterozygosity is needed for osteochondroma to develop.(69, 70) Analogous to this tenet, our data supports the notion that a germline heterozygous mutation in the EXT1 or EXT2 gene alone is not enough to cause a pathologic phenotype in the glomerulus or endothelial glycocalyx. Cases such as those described by Roberts *et al.* and here, are likely to have a distinct, local loss of heterozygosity and as such, loss of HS, leading to a specific phenotype. Potentially, factors other than HS could also play a role in these rare cases. Our group has previously shown that a bi-allelic germline mutation of EXT in zebrafish also does not lead to a renal phenotype, although it does result in a specific cartilaginous and dental phenotype.(31, 33, 55, 71) Overall, based on the results from the current study and others, MO patients do not seem to have an increased risk of developing clinically significant microvascular complications. However, rare pathology exists in this disease and the current study might be underpowered to fully assess that risk.

A limitation of this study is that both glycocalyx measurements and urine samples were not collected multiple times. Glycocalyx measurements are of a dynamic nature with a small variability, and multiple measurements, as we have performed, increase reproducibility.(72)

Although multiple urine samples over a period of time would result in a more representative result of a patient's typical albumin excretion, the absence of proteinuria, especially in the MO patient group, strongly suggests that indeed, no clinically significant pathology is present.

In this study, 6 out of 19 patients had a confirmed *EXT1* or *EXT2* mutation status. As stated in the introduction, the clinical diagnosis of the autosomal dominant disease of MO is often made without genetic testing, as in previous studies, a germline mutation in the *EXT1* or *EXT2* gene was found in almost 90% of cases.(59, 62) All MO patients in this study were included through the Dutch Multiple Hereditary Exostoses/Multiple Osteochondromas Association. In this study, outcome parameters were similar in subjects with and without a confirmed genetically confirmed diagnosis.

Most patients from the historic PALGA cohort did not have a confirmed *EXT1* or *EXT2* mutation. At least four patients from this cohort can be classified as having MO based on clinical criteria. The only clinical data we had available on these patients, were the pathology reports. So this is most likely an underestimation of the total amount of MO patients within this cohort. We deduce that if a specific morphological phenotype with pathophysiological consequences would exist due to these mutations, our method results in an adequate appreciation of this topic. Besides the single patient described, the fact that no changes were found implies that *EXT1* or *EXT2* mutations do not necessarily cause changes to glomerular morphology. However, these results could be misinterpreted due to a lack of power.

In conclusion, this study shows that in humans, mono-allelic germline *EXT1* and *EXT2* mutations do not result in proteinuria or significant changes to the endothelial glycocalyx. Loss of heterozygosity could be an explanation for the very rare case of MO glomerulopathy described previously.(56) Based on the current study, MO patients do not appear to be at an increased risk for clinically significant pathology of the glycocalyx or glomerular filtration barrier. Future studies might further elucidate the loss of heterozygosity theory and potentially identify other factors that might lead to the rare specific renal phenotype seen in only a very small subset of MO patients. This could assist in understanding not only the MO phenotype, but the pathophysiology of the glomerular filtration barrier and endothelial glycocalyx.

List of abbreviations

GAG: glycosaminoglycan
GBM: glomerular basement membrane
GFB: glomerular filtration barrier
HME: hereditary multiple exostoses
HS: Heparan sulfate
MO: multiple osteochondromas
PBR: perfused boundary region
RBC(w): red blood cell (width)

Ethics approval and consent to participate

Ethical approval for this study was obtained through the LUMC Medical Ethical Committee under registration number P15.106. Patient material from the PALGA search was handled in accordance with institutional guidelines, Good Research Practice, and the Code of conduct for responsible use.

Consent for publication

Not applicable

Competing interests

No potential conflicts of interest relevant to this article were reported.

Funding

No external funding was used in this study.

Authors' contributions

RK designed and performed experiments, analyzed and interpreted data, and wrote the paper. MGSB designed and performed experiments, and analyzed and interpreted data. PALGA group, consisting of those mentioned in the acknowledgements section, provided clinical data and material from the Dutch pathological anatomy national automated archive. JAB and TJR made substantial contributions to the conception and design of the work. BB, PCWH, and HJB made substantial contributions to the conception and design of the work, interpretation of data, and revisions of the manuscript. All authors read and approved the final manuscript.

Acknowledgements

The authors extend their gratitude to the Dutch Multiple Hereditary Exostoses/Multiple Osteochondromas Association for their involvement in this project.

We thank Hans Vink (Glycocheck) for the use of the Glycocheck software.

We also thank the PALGA foundation and all participating laboratories and researchers: A. Bezuijen, J.E. Boers, P.C. de Bruin, M.A.A.M. van Dijk, P. Drillenburg, A.F. Hamel, H.M. Hazelbag, G.N. Jonges, R.E. Kibbelaar, K.H. Lam, H. van der Linden, J. van Marsdijk, C. Meijer, I.D. Nagtegaal, J.J. Oudejans, J.J.T.H. Roelofs, L. Rozendaal, S.H. Sastrowijoto, M.M. Smits, J. Stavast

References

1. Deanfield JE, Halcox JP, Rabelink TJ: Endothelial function and dysfunction: testing and clinical relevance. *Circulation* 2007, 115(10):1285-1295.
2. Stam F, van Guldener C, Becker A, Dekker JM, Heine RJ, Bouter LM, Stehouwer CD: Endothelial dysfunction contributes to renal function-associated cardiovascular mortality in a population with mild renal insufficiency: the Hoorn study. *Journal of the American Society of Nephrology : JASN* 2006, 17(2):537-545.
3. Reitsma S, Slaaf DW, Vink H, van Zandvoort MA, oude Egbrink MG: The endothelial glycocalyx: composition, functions, and visualization. *Pflugers Archiv : European journal of physiology* 2007, 454(3):345-359.
4. Esko JD, Selleck SB: Order out of chaos: assembly of ligand binding sites in heparan sulfate. *Annual review of biochemistry* 2002, 71:435-471.
5. Xu D, Esko JD: Demystifying heparan sulfate-protein interactions. *Annual review of biochemistry* 2014, 83:129-157.
6. Kanwar YS, Farquhar MG: Presence of heparan sulfate in the glomerular basement membrane. *Proceedings of the National Academy of Sciences of the United States of America* 1979, 76(3):1303-1307.
7. Kanwar YS, Linker A, Farquhar MG: Increased permeability of the glomerular basement membrane to ferritin after removal of glycosaminoglycans (heparan sulfate) by enzyme digestion. *The Journal of cell biology* 1980, 86(2):688-693.
8. Garsen M, Rops AL, Rabelink TJ, Berden JH, van der Vlag J: The role of heparanase and the endothelial glycocalyx in the development of proteinuria. *Nephrol Dial Transplant* 2014, 29(1):49-55.
9. van den Born J, van den Heuvel LP, Bakker MA, Veerkamp JH, Assmann KJ, Weening JJ, Berden JH: Distribution of GBM heparan sulfate proteoglycan core protein and side chains in human glomerular diseases. *Kidney Int* 1993, 43(2):454-463.
10. Singh A, Satchell SC, Neal CR, McKenzie EA, Tooke JE, Mathieson PW: Glomerular endothelial glycocalyx constitutes a barrier to protein permeability. *Journal of the American Society of Nephrology : JASN* 2007, 18(11):2885-2893.
11. Hogendoorn PC, de Heer E, Weening JJ, Daha MR, Hoedemaeker PJ, Fleuren GJ: Glomerular capillary wall charge and antibody binding in passive Heymann nephritis. *The Journal of laboratory and clinical medicine* 1988, 111(2):150-157.
12. Chen S, Wassenhove-McCarthy DJ, Yamaguchi Y, Holzman LB, van Kuppevelt TH, Jenniskens GJ, Wijnhoven TJ, Woods AC, McCarthy KJ: Loss of heparan sulfate glycosaminoglycan assembly in podocytes does not lead to proteinuria. *Kidney Int* 2008, 74(3):289-299.
13. Harvey SJ, Jarad G, Cunningham J, Rops AL, van der Vlag J, Berden JH, Moeller MJ, Holzman LB, Burgess RW, Miner JH: Disruption of glomerular basement membrane charge through podocyte-specific mutation of agrin does not alter glomerular permselectivity. *Am J Pathol* 2007, 171(1):139-152.
14. Goldberg S, Harvey SJ, Cunningham J, Tryggvason K, Miner JH: Glomerular filtration is normal in the absence of both agrin and perlecan-heparan sulfate from the glomerular basement membrane. *Nephrol Dial Transplant* 2009, 24(7):2044-2051.
15. Sugar T, Wassenhove-McCarthy DJ, Esko JD, van Kuppevelt TH, Holzman L, McCarthy KJ: Podocyte-specific deletion of NDST1, a key enzyme in the sulfation of heparan sulfate glycosaminoglycans, leads to abnormalities in podocyte organization in vivo. *Kidney Int* 2014, 85(2):307-318.
16. Khalil R, Lalai RA, Wiweger MI, Avramut CM, Koster AJ, Spaink HP, Bruijn JA, Hogendoorn PCW, Baelde HJ: Glomerular permeability is not affected by heparan sulfate glycosaminoglycan deficiency in zebrafish embryos. *American journal of physiology Renal physiology* 2019, 317(5):F1211-F1216.

17. Roberts IS, Gleadle JM: Familial nephropathy and multiple exostoses with exostosin-1 (EXT1) gene mutation. *Journal of the American Society of Nephrology : JASN* 2008, 19(3):450-453.
18. Colvin RB, Chang A: Diagnostic Pathology: Kidney Diseases: Elsevier Health Sciences; 2015.
19. Wuyts W, Van Hul W: Molecular basis of multiple exostoses: mutations in the EXT1 and EXT2 genes. *Human mutation* 2000, 15(3):220-227.
20. Bovee JV: Multiple osteochondromas. *Orphanet journal of rare diseases* 2008, 3:3.
21. Bovee JV, Hogendoorn PC: Multiple osteochondromas. In: *World Health Organization classification of tumours : pathology and genetics tumours of soft tissue and bone.* edn. Edited by Fletcher CDM, Unni KK, Mertens F. Lyon: IARC Publications; 2002: 360–362.
22. Le Merrer M, Legeai-Mallet L, Jeannin PM, Horsthemke B, Schinzel A, Plauchu H, Toutain A, Achard F, Munnich A, Maroteaux P: A gene for hereditary multiple exostoses maps to chromosome 19p. *Human molecular genetics* 1994, 3(5):717-722.
23. Hameetman L, Bovee JV, Taminiau AH, Kroon HM, Hogendoorn PC: Multiple osteochondromas: clinicopathological and genetic spectrum and suggestions for clinical management. *Hereditary cancer in clinical practice* 2004, 2(4):161-173.
24. Anower EKMF, Matsumoto K, Habuchi H, Morita H, Yokochi T, Shimizu K, Kimata K: Glycosaminoglycans in the blood of hereditary multiple exostoses patients: Half reduction of heparan sulfate to chondroitin sulfate ratio and the possible diagnostic application. *Glycobiology* 2013, 23(7):865-876.
25. Hecht JT, Hall CR, Snuggs M, Hayes E, Haynes R, Cole WG: Heparan sulfate abnormalities in exostosis growth plates. *Bone* 2002, 31(1):199-204.
26. Dane MJ, Khairoun M, Lee DH, van den Berg BM, Eskens BJ, Boels MG, van Teeffelen JW, Rops AL, van der Vlag J, van Zonneveld AJ *et al*: Association of kidney function with changes in the endothelial surface layer. *Clinical journal of the American Society of Nephrology : CJASN* 2014, 9(4):698-704.
27. Lee DH, Dane MJ, van den Berg BM, Boels MG, van Teeffelen JW, de Mutsert R, den Heijer M, Rosendaal FR, van der Vlag J, van Zonneveld AJ *et al*: Deeper penetration of erythrocytes into the endothelial glycocalyx is associated with impaired microvascular perfusion. *PloS one* 2014, 9(5):e96477.
28. Group CW: KDIGO clinical practice guideline for the evaluation and management of chronic kidney disease. *Kidney Int Suppl* 2013.
29. Bovee JV, Cleton-Jansen AM, Wuyts W, Caethoven G, Taminiau AH, Bakker E, Van Hul W, Cornelisse CJ, Hogendoorn PC: EXT-mutation analysis and loss of heterozygosity in sporadic and hereditary osteochondromas and secondary chondrosarcomas. *American journal of human genetics* 1999, 65(3):689-698.
30. Reijnders CM, Waaijer CJ, Hamilton A, Buddingh EP, Dijkstra SP, Ham J, Bakker E, Szuhai K, Karperien M, Hogendoorn PC *et al*: No haploinsufficiency but loss of heterozygosity for EXT in multiple osteochondromas. *Am J Pathol* 2010, 177(4):1946-1957.
31. Wiweger MI, Zhao Z, van Merkesteyn RJ, Roehl HH, Hogendoorn PC: HSPG-deficient zebrafish uncovers dental aspect of multiple osteochondromas. *PloS one* 2012, 7(1):e29734.
32. Wiweger MI, de Andrea CE, Scheepstra KW, Zhao Z, Hogendoorn PC: Possible effects of EXT2 on mesenchymal differentiation--lessons from the zebrafish. *Orphanet J Rare Dis* 2014, 9:35.
33. Wiweger MI, Avramut CM, de Andrea CE, Prins FA, Koster AJ, Ravelli RB, Hogendoorn PC: Cartilage ultrastructure in proteoglycan-deficient zebrafish mutants brings to light new candidate genes for human skeletal disorders. *J Pathol* 2011, 223(4):531-542.
34. Eickhoff MK, Winther SA, Hansen TW, Diaz LJ, Persson F, Rossing P, Frimodt-Moller M: Assessment of the sublingual microcirculation with the GlycoCheck system: Reproducibility and examination conditions. *PloS one* 2020, 15(12):e0243737.

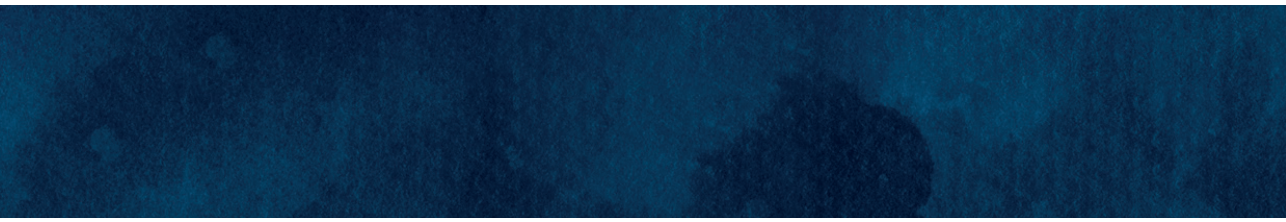

CHAPTER 5

Increased dynamin expression precedes proteinuria in glomerular disease

Journal of Pathology 2019, 247: 177-185.

Ramzi Khalil[1], Klaas Koop[1], Reinhold Kreutz[2], Herman P. Spaink[3], Pancras C.W. Hogendoorn[1], Jan A. Bruijn[1], Hans J. Baelde[1]

[1] *Department of Pathology, Leiden University Medical Center, Leiden, The Netherlands;*

[2] *Institute of Cligsenical Pharmacology and Toxicology, Charité – Universitätsmedizin Berlin, corporate member of Freie Universität Berlin, Humboldt-Universität zu Berlin, and Berlin Institute of Health Berlin, Germany;*

[3] *Institute of Biology Leiden, Leiden University, Leiden, The Netherlands*

Abstract

Dynamin plays an essential role in maintaining the structure and function of the glomerular filtration barrier. Specifically, dynamin regulates the actin cytoskeleton and the turnover of nephrin in podocytes, and knocking down dynamin expression causes proteinuria. Moreover, promoting dynamin oligomerization with Bis-T-23 restores podocyte function and reduces proteinuria in several animal models of chronic kidney disease. Thus, dynamin is a promising therapeutic target for treating chronic kidney disease. Here, we investigated the pathophysiological role of dynamin under proteinuric circumstances in a rat model and in humans. We found that glomerular *Dnm2* and *Dnm1* mRNA levels are increased prior to the onset of proteinuria in a rat model of spontaneous proteinuria. Also, in zebrafish embryos we confirm that knocking down dynamin translation results in proteinuria. Finally, we show that the glomerular expression of dynamin and cathepsin L protein is increased in several human proteinuric kidney diseases. We propose that the increased expression of glomerular dynamin reflects an exhausted attempt to maintain and/or restore integrity of the glomerular filtration barrier. These results confirm that dynamin plays an important role in maintaining the glomerular filtration barrier, and they support the notion that dynamin is a promising therapeutic target in proteinuric kidney disease.

Introduction

Chronic kidney disease (CKD) is a major health issue worldwide.(2) The progression of CKD is accompanied by a reduction in glomerular filtration rate and subsequent proteinuria. In order to develop new therapeutic strategies for CKD, it is important to understand the mechanisms and processes that underlie glomerular filtration. The glomerular filtration barrier (GFB) consists of several components, including the interdigitating foot processes of podocytes, the glomerular basement membrane, and a glycocalyx-covered fenestrated endothelium. Disrupting the GFB allows the passage of proteins into the urinary space. Under normal conditions, these proteins are then reabsorbed by proximal tubular epithelial cells; however, if the reabsorption mechanism is impaired or saturated, proteinuria can develop.

Dynamin is a recently identified protein that plays an important role in maintaining GFB integrity. This 96 kDa GTPase is expressed both in glomerular podocytes and in tubular epithelial cells.(13, 73) Within the GFB, dynamin has three identified functions: *i*) dynamin is involved in the turnover of nephrin (14); *ii*) dynamin interacts directly with actin and actin-regulatory proteins (12); and *iii*) dynamin is involved in the endocytosis of albumin by podocytes (74). Several groups have reported that loss of dynamin using a genetic knockdown model or via cleavage with the endopeptidase cathepsin L results in proteinuria.(13, 14, 75) Moreover, Schiffer *et al.* demonstrated that dynamin is a potential therapeutic target in CKD.(75) Specifically, the authors reported beneficial effects of treating several animal models of proteinuria with Bis-T-23, a small molecule compound that stimulates the oligomerization of dynamin to form a 72-subunit helical structure.(11) Importantly, Schiffer *et al.* found that administering Bis-T-23 restored the ultrastructure of podocyte foot processes, decreased proteinuria, lowered mesangial collagen IV deposition, reduced mesangial matrix expansion, and prolonged survival.(75) Ono *et al.* also showed that Bis-T-23 treatment prevented albuminuria and attenuated alterations in foot process formation in an experimental mouse model .(76)

Although these studies indicate that dynamin plays an important role in maintaining GFB structure and function, the majority of this research relied on the observation of morphological and/or functional changes in the kidney after genetic manipulation or other alterations in dynamin. Thus, intrinsic changes in dynamin expression under proteinuric conditions have not been investigated in animal models or patients.

Here, we report that dynamin expression is increased in proteinuric conditions. We show that glomerular *Dnm2* and *Dnm1* mRNA levels are increased in a rat model of spontaneous proteinuria prior to the onset of proteinuria. Also, we show that knocking

down dynamin translation in a zebrafish embryo model results in proteinuria. Lastly, we show that glomerular dynamin and cathepsin L protein levels are increased in human patients with proteinuric kidney disease.

Methods

Microarray analysis

We analyzed the microarray datasets of Dahl and SHR rats in order to identify differentially regulated cytoskeleton-related genes. The datasets were retrieved from the Gene Expression Omnibus of the NCBI, which is accessible using the GEO Series accession number GSE 13810. This analysis was performed using Affymetrix GeneChip Rat Genome 230 2.0 arrays. Pathway analysis was performed using the Gene Ontology Tree Machine and by global testing in the Kyoto Encyclopedia of Genes and Genomes in order to determine which differentially regulated genes are involved in cytoskeletal regulation.(77, 78) This microarray was performed on glomeruli obtained from animals at 4 and 6 weeks of age.

Animal studies: rats

Male spontaneously proteinuric Dahl salt-sensitive rats (Dahl) and non-proteinuric spontaneously hypertensive rats (SHR) were obtained from the Charite-University Medicine Berlin.(79) To prevent the early accelerated development of severe hypertension, the rats were fed a low-salt diet containing 0.2 % NaCl by weight content. Tissues were collected from animals at 2, 4, 6, 8, and 10 weeks of age. A total of 67 animals was used, with respectively 7, 7, 7, 8, and 8 Dahl rats per age group and 5, 4, 6, 7, and 8 SHR rats per age group. In each animal, the left kidney was used to isolate the glomeruli using magnetic retraction; these samples were used for mRNA analysis.(80) The right kidney of each animal was partially embedded in paraffin, snap-frozen, and stored at -80 °C.

RNA isolation and qPCR

RNA was isolated from rat glomeruli using TRIzol (Invitrogen, Waltham, MA). AMV reverse transcriptase (Roche Diagnostics) was used to reverse-transcribe the RNA into first-strand cDNA, which was then analyzed using qPCR with the primer pairs listed in Table 2. *HPRT* was used as an internal control. qPCR was performed on an iCycler real-time PCR machine with SYBR green supermix (Bio-Rad Laboratories, Hercules, CA), and iCycler IQ 3.1 software (Bio-Rad Laboratories) was used to analyze gene expression and to normalize the data. *Dnm1* and *Dnm2* mRNA levels are shown as relative to the average *Dnm1* or *Dnm2 mRNA* expression in SHR rats.

Animal studies: zebrafish

Wild-type (WT) AB/TL strain zebrafish (*Danio rerio H)* were maintained using previously defined standards.(81) Embryos were obtained through natural crossings and kept in E3 medium at 28.5 °C. In the 1-4-cell stage, the embryos were injected with 1 nl of a morpholino (Gene Tools, Philomath, OR) targeting the *dnm2* gene (to knockdown mRNA translation) or a scrambled control morpholino.(82)

Glomerular permeability and tubular reabsorption assay

A previously validated tubular dextran reabsorption model was used to assess glomerular permeability in zebrafish embryos.(40, 43) At 4 days post-fertilization (dpf), a group of wild-type embryos were injected with 3 nl puromycin aminonucleoside (PAN, 25 mg/ml, Sigma-Aldrich, St. Louis, MO) to induce kidney damage as a positive control for proteinuria.(40) At 5 dpf, all groups were injected with 3 nl of a mixture of TRITC-labeled 3 kDa (100 mg/ml; Invitrogen) and FITC-labeled 70-kDa (25 mg/ml; Invitrogen) dextran. One hour after injection, the animals were fixed in 10 % formalin for 24 hours. After subsequent storage in 70 % ethanol, the embryos were embedded in paraffin, sectioned at 3 μm thickness, and examined using fluorescence microscopy for the presence of reabsorption droplets in the proximal tubule epithelial cells by an investigator who was blinded with respect to the treatment conditions. The number of reabsorption droplets in the proximal tubule cells was counted and compared between groups. The 3 kDa dextran tracer freely passes the GFB and is subsequently reabsorbed by the proximal tubule epithelial cells. Therefore, reabsorption of this tracer is used as an indicator of sufficient tubular reabsorption function. In contrast, the 70 kDa tracer does not readily pass the GFB under normal conditions and is therefore used as an indicator of glomerular permeability.(43) The PAN and dextran injections were performed under anesthesia with 4 % tricaine methanesulfonate. All zebrafish experiments were performed prior to the free-feeding embryo stage and are therefore not considered animal experiments in accordance with the EU Animal Protection Directive 2010/63/EU.

Human materials

Biopsies from 26 patients with a variety of proteinuric kidney diseases were obtained from the LUMC tissue archive. Eight biopsies were from patients with minimal change disease, three were from patients with focal segmental glomerulosclerosis, three were from patients with IgA nephropathy, six were from patients with lupus nephritis, and six were from patients with diabetic nephropathy. In addition, 16 samples were used as a control group; these samples consisted of biopsy material obtained from patients with no evidence of glomerular pathology whose kidneys were unsuitable for transplantation due

to technical reasons, or from autopsy tissue. All tissue samples were obtained and handled in accordance with institutional guidelines and with the Code of Conduct regarding the responsible use of human tissues.(83) Patient characteristics are given in Table 3.

Immunohistochemistry

The mouse anti-dynamin antibody Hudy 1 (Upstate Biotechnology, catalog number 05-319, diluted 1:80) was used to detect dynamin. Hudy 1 is a monoclonal antibody that recognizes both dynamin 1 and dynamin 2. Hudy 1 recognizes the epitope of residues 822-838 within the proline-rich domain of dynamin. Anti-mouse Envision (Dako Cytomotion, Glostrup, Denmark) was used as a secondary antibody to detect the primary antibody. A rabbit anti-cathepsin L antibody (Abcam, ab203028, diluted 1:100) was used to detect cathepsin L. The results were analyzed by measuring the percent positive area in the glomeruli using the ImageJ digital image analysis program. No scarred glomeruli were included in these analyses.

Statistical analyses

Statistical analyses were performed using SPSS version 23.0 (IBM Corp., Armonk, NY). mRNA and protein levels were compared using one-way ANOVA (with Dunnett's post hoc analysis when more than 3 groups were compared). The Student's unpaired *t*-test was used when 2 or 3 groups were compared. Correlation analysis was performed using the Pearson correlation coefficient. Differences with a p-value < 0.05 were considered significant.

Results

Gene expression profiling between Dahl and SHR rats

First, we investigated differences in gene expression between Dahl rats and SHR rats using microarray analysis. With respect to cytoskeleton-related genes, we found 27 genes that were differentially regulated between Dahl rats and SHR rats (Table 1). Of these 27 genes, 25 were significantly upregulated (including *Dnm1*), and two genes (*Spna1* and *Pmfbp1*) were downregulated.

Table 1. Differential glomerular expression of cytoskeleton-related genes between 4-6-week-old Dahl rats and SHR rats

Gene name	Gene symbol	Chromosomal location	Fold difference in expression	Function
periplakin	*Ppl*	10q12	4.17	intermediate filament binding
moesin	*Msn*	Xq31	3.86	actin filament -- membrane cross-linking
dynamin 1	*Dnm1*	3p11	3.36	actin dynamics regulation
tropomyosin 4	*Tpm4*	16p14	2.73	actin binding
thymoma viral proto-oncogene 1	*Akt1*	6q32	2.71	cell projection organization and biogenesis
supervillin	*Svil*	17q12	2.62	actin binding
parvin, alpha	*Parva*	1q33	2.62	actin cytoskeleton organization and biogenesis
plastin 3 (T-isoform)	*Pls3*	Xq14	2.51	actin filament organization
tropomyosin 1, alpha	*Tpm1*	8q24	2.23	actin filament capping
microtubule-associated protein, RP/EB family, member 1	*Mapre1*	3q41	2.2	regulation of microtubule polymerization
Rho guanine nucleotide exchange factor (GEF) 17	*Arhgef17*	1q32	2.1	actin cytoskeleton organization and biogenesis
caldesmon 1	*Cald1*	4q22	2.1	actin binding
signal-regulatory protein alpha	*Sirpa*	3q36	2.04	actin filament organization
WD repeat domain 44	*Wdr44*	Xq12	2	vesicle recycling
myosin Ib	*Myo1b*	9q22	1.99	actin binding
echinoderm microtubule-associated protein like 4	*Eml4*	6q12	1.97	microtubule stabilization
actin-related protein 2/3 complex, subunit 1B	*Arpc1b*	12p11	1.89	cytoskeleton organization
filamin, beta	*Flnb*	15p14	1.87	actin binding
myosin IC	*Myo1c*	10q24	1.78	actin binding
mitogen-activated protein kinase 1	*Map3k1*	2q14	1.78	actin filament polymerization
CAP, adenylate cyclase-associated protein 1 (yeast)	*Cap1*	5q36	1.73	actin cytoskeleton organization and biogenesis
kinesin light chain 1	*Klc1*	6q32	1.59	microtubule motor activity
Src homology 2 domain-containing transforming protein C1	*Shc1*	2q34	1.57	actin cytoskeleton organization and biogenesis
ARP1 actin-related protein 1 homolog A (yeast)	*Actr1a*	1q54	1.55	cytoskeleton organization
actin, beta	*Actb*	12p11	1.54	cytoskeleton organization
A kinase (PRKA) anchor protein 2	*Akap2*	5q24	1.51	actin filament organization
spectrin alpha 1	*Spna1*	13q24	0.19	cytoskeleton organization
polyamine modulated factor 1 binding protein 1	*Pmfbp1*	19q12	0.14	cytoskeleton organization and biogenesis

Table 2. Primer sequences used for RT-PCR analysis

Name (species)	Gene symbol	mRNA accession number	Forward primer	Reverse primer
Dynamin 1 (rat)	*Dnm1*	NM_080689.4	TTGATGAGAAGGAACTGCGAAGG	AAGCGAGGTCAGGAGTGAAGAG
Dynamin 2 (rat)	*Dnm2*	NM_013199.1	TGAAATGCGTGGACCTGGTT	CAATGCGTTCGGTCTCCTCT
Cathepsin L (rat)	*Ctsl*	NM_013156.2	CAGTGGAAGTCCACACACAGA	GTGCTTCCCGTTGCTGTACT
Hypoxanthine phosphoribosyltransferase 1 (rat)	*Hprt1*	NM_012583.2	GGCTATAAGTTCTTTGCTGACCTG	AACTTTTATGTCCCCCGTTGA

Glomerular Dnm1 and Dnm2 mRNA—but not dynamin protein area expression—are increased in Dahl rats prior to the onset of proteinuria

Next, we measured glomerular dynamin expression in the Dahl salt-sensitive spontaneously proteinuric and hypertensive rat model (referred to here as simply Dahl rats) and the spontaneously hypertensive rat (SHR). Dahl rats under a low dietary salt intake developed significant proteinuria beginning at 6 weeks of age; in contrast, SHR rats did not develop proteinuria, even at 10 weeks of age (Figure 1A). Consistent with the spontaneous hypertension phenotype, both strains developed hypertension to a similar extent beginning at 8 weeks of age (Figure 1B).

As *Dnm2* is the ubiquitous and prevalent form of dynamin, we measured both glomerular *Dnm2* and *Dnm1* mRNA levels (Figures 1C and 1D respectively). When analysing only the Dahl group, no significant differences in glomerular *Dnm2* mRNA levels were seen between at weeks 2, 6, 8, and 10. However, these levels were higher at 4 weeks of age than in all other time points ($p < 0.0001$ compared to weeks 2, 6, 8, and 10, Figure 1C). In SHR rats, a significant difference in glomerular *Dnm2* levels was found between weeks 2 compared to weeks 8 and 10 ($p < 0.001$ and $p < 0.01$ respectively) and between weeks 4 and 8 ($p < 0.05$, Figure 1 C). A similar analysis of glomerular *Dnm1* mRNA levels in Dahl rats shows a gradual increase from weeks 2 to 6 after which the levels decrease. This difference is significant between weeks 6 and 10 ($p < 0.05$, Figure 1D). SHR rats show very low expression of glomerular *Dnm1* mRNA at week 2 which increases slightly, but not significantly up until 6 weeks (Figure 1D). None of the differences in mRNA levels at the different time points were significant in this group. When comparing dynamin mRNA levels between Dahl and SHR rats, the level of glomerular *Dnm2* mRNA was significantly increased in Dahl rats compared to SHR rats at 2 and 4 weeks of age (Figure 1C, $p < 0.05$ and $p < 0.0001$ respectively). Glomerular *Dnm1* mRNA was significantly higher in Dahl rats than in SHR rats at 2, 4, and 6 weeks of age (Figure 1D). Interestingly, the levels of both *Dnm1* and *Dnm2* mRNA at 2 weeks of age were higher in Dahl rats than in SHR rats, which is prior to the onset of proteinuria (i.e., at 6 weeks of age). Also when comparing the different age groups, animals that will become proteinuric (i.e., the Dahl rats) have an increase in glomerular *Dnm2* expression prior to onset of proteinuria. When comparing PCR C_t values, *Dnm2* mRNA levels were found to be over ten times higher than *Dnm1* levels. With respect to dynamin protein levels, immunohistochemistry revealed that the protein was present at the tubular brush border and in podocytes in both Dahl and SHR rats (Figure 2C and D) at similar levels at both 4 and 6 weeks of age (i.e., after Dahl rats develop proteinuria) ($p = 0.6$, Figure 2G).

Ctsl mRNA levels—but not dynamin protein area expression—are higher in Dahl rats compared to SHR rats

Cathepsin L, encoded by the *Ctsl* gene, is an enzyme that cleaves dynamin.(13) We therefore measured the expression of cathepsin L in the glomeruli of Dahl and SHR rats using RT-PCR (Figure 1I). We found that *Ctsl* mRNA levels were significantly higher in the glomeruli of Dahl rats compared to SHR, ranging from 1.3-fold to 1.7-fold higher, at all ages tested ($p < 0.01$). Immunohistochemistry revealed that there was no difference between Dahl and SHR rats in glomerular cathepsin L positive area. ($p = 0.11$ and $p = 0.70$ at 4 and 6 weeks of age respectively, Figure 1H)

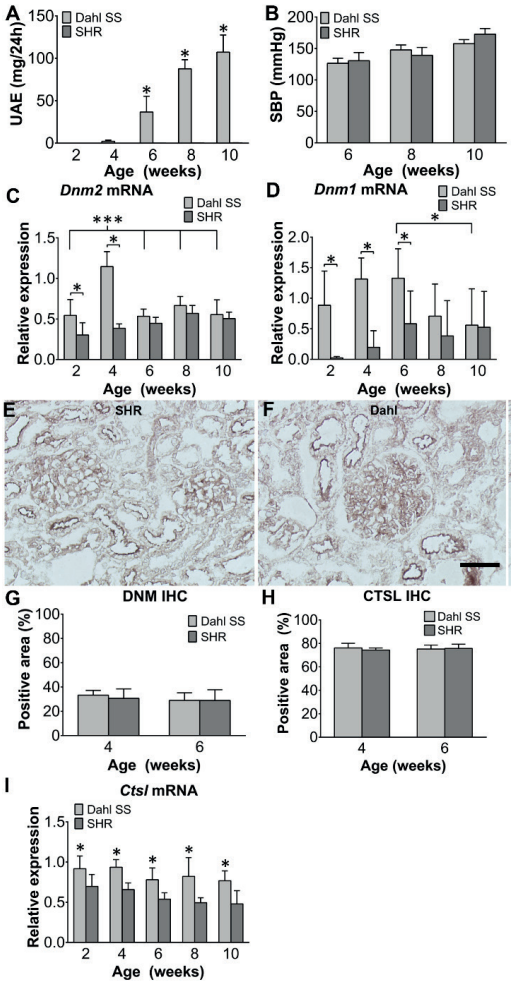

Figure 1. Glomerular Dnm2 and Dnm1 mRNA levels—but not dynamin protein levels—are increased in Dahl rats prior to the onset of proteinuria

Figure 1. Continued

(**A** and **B**) Summary of urinary albumin excretion (**A**) and systolic blood pressure (**B**). (**C** and **D**) Summary of glomerular *Dnm2* mRNA(**C**) and *Dnm1* mRNA (**D**). (**E** and **F**) Example images of glomeruli from an SHR rat (**E**) and Dahl rat (**F**) immunostained for dynamin. Similar to the pattern seen in human kidney sections, dynamin protein was present in podocytes and the tubular brush border. (**G – I**) Summary of the percent glomerular positive area for dynamin protein (**G**), the percent glomerular positive area for cathepsin L protein (**H**), and glomerular cathepsin L (*Ctsl*) mRNA (**I**) in Dahl and SHR rats at the indicated ages. No difference was seen in both dynamin and cathepsin L percent glomerular positive area. $*p < 0.05$ versus the SHR group. The images in E and F were taken at the same magnification; scale bar = 50 μm.

Knocking down dynamin translation causes proteinuria

Next, we knocked down dynamin expression in zebrafish embryos using morpholino injection followed by injection with a mixture of 3 kDa and 70 kDa dextran tracers (Figure 2A and B); as a positive control for inducing proteinuria, a separate group of embryos received an injection of puromycin aminonucleoside (PAN). We then quantified the reabsorption of dextran droplets. Our analysis revealed that the mean number of 3 kDa dextran droplets was similar between control zebrafish (which received an injection of a scrambled morpholino), dynamin-knockdown zebrafish, and PAN-injected zebrafish ($p = 0.96$, Figure 2C), indicating that a knockdown of dynamin in this model does not significantly affect tubular reabsorption. In contrast, the dynamin-knockdown zebrafish had significantly more reabsorption of 70 kDa droplets compared to control zebrafish ($p < 0.0001$, Figure 2D), indicating that loss of dynamin increases glomerular permeability, as also shown in the zebrafish model by Schiffer *et al.*(75)

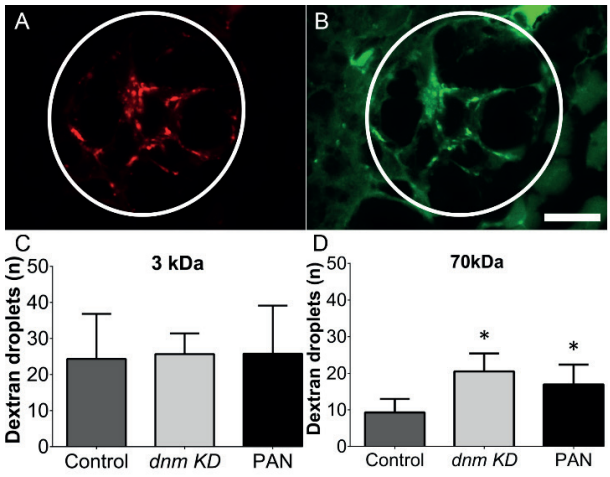

Figure 2. Blocking the translation of dnm mRNA in zebrafish embryos causes proteinuria

Wild-type zebrafish embryos were injected with an anti-*dnm* morpholino or a scrambled control morpholino, followed by a mixture of 3 kDa and 70 kDa dextran molecules. (**A** and **B**)

Figure 2. Continued

Representative fluorescence images of the proximal tubule epithelial cells (circled structure) in a dynamin-knockdown zebrafish embryo. (**C** and **D**) the number of fluorescent droplets below the luminal surface were counted in control embryos, dynamin-knockdown embryos, and wild-type embryos injected with puromycin aminonucleoside (PAN) as a positive control for increased glomerular permeability. *$p < 0.05$ versus control. A digital high-pass filter has been placed over figures A and B to enhance contrast between reabsorption droplets and the surrounding tissue. The images in A and B were taken at the same magnification; scale bar = 10 μm.

Dynamin protein levels are increased in the glomeruli of patients with proteinuria

Finally, we examined the expression of dynamin in the kidneys of patients with proteinuria (Figures 3A through D). Patient characteristics are given in Table 3. Biopsies were obtained from patients with proteinuric kidney disease and control subjects, and stained by immunohistochemistry for the presence of dynamin. Positive staining was found primarily in podocytes, at the tubular epithelial brush border, and in endothelial cells of larger vessels. When comparing individual disease groups to the controls, the glomeruli of patients with minimal change disease (MCD) and lupus nephritis (LN) had a significantly higher dynamin-positive area percentage. ($p = 0.03$ and $p = 0.04$, respectively, Figure 3I). No scarred glomeruli were included in these analyses. No correlation was found between proteinuria levels and dynamin expression levels.

Cathepsin L protein levels are also increased in the glomeruli of patients with proteinuria

The same cohort was also stained by immunohistochemistry for the presence of cathepsin L (Figures 3E through H). We found a significantly higher glomerular cathepsin L-positive area percentage in patients with minimal change disease (MCD), lupus nephritis (LN), and IgA nephropathy (IgAN, $p < 0.0001$ compared to controls in all three groups, Figure 3J). A positive correlation was found between the glomerular positive area percentages for dynamin and cathepsin L ($r = 0.928$, $p = 0.0075$).

Table 3. Patient characteristics

	Control	**DN**	**LN**	**MCD**	**FSGS**	**IgAN**
Number of patients (n)	15	6	6	8	5	4
Mean age, years (SD)	54,8 (16,11)	50,2 (19,11)	29,3 (12,15)	31,1 (20,88)	36,2 (7,19)	34,5
Mean serum creatinin, μmol/l (SD)	101,57 (37,95)	140,80 (76,30)	112,80 (39,51)	77,38 (27,77)	112,80 (60,24)	107,5 (34,09)
Proteinuria, g/24 h (SD)	0,14 (0,12)	1,15 (0,82)	2,50 (1,86)	3,56 (3,32)	5,08 (1,84)	4,40 (3,19)

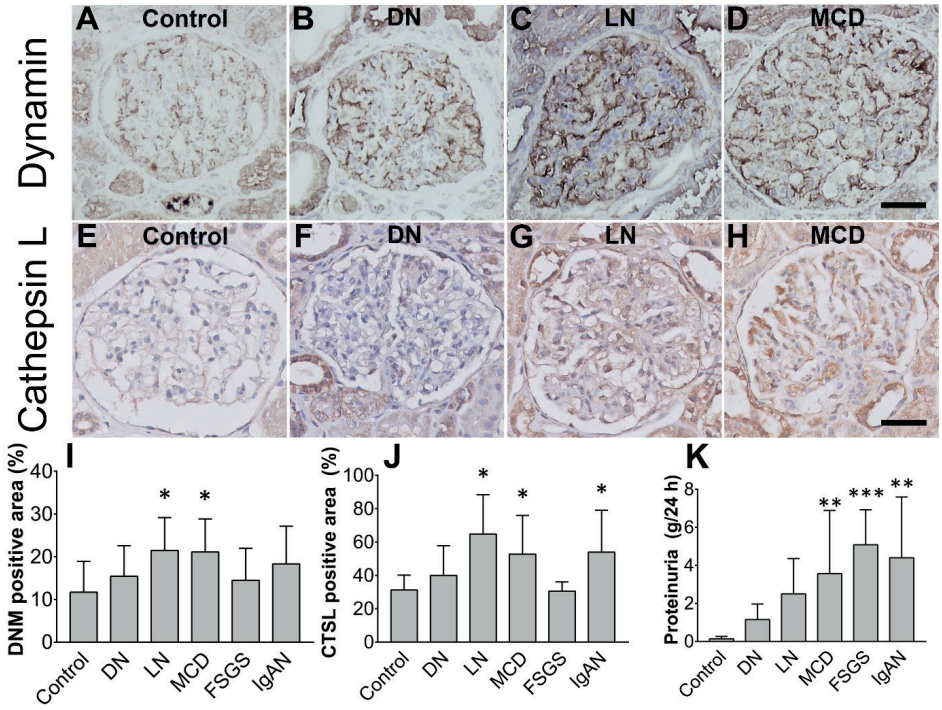

Figure 3. Glomerular dynamin protein levels are increased in human proteinuric kidneys

(**A** – **H**) Representative images of glomeruli immunostained for dynamin (**A** – **D**) or for cathepsin L (**E** – **H**) in a healthy control subject (**A** and **E**), a patient with diabetic nephropathy (**B** and **F**), a patient with lupus nephritis (**C** and **G**), and a patient with minimal change disease (**D** and **H**). (**I** and **J**) Summary of the percent glomerular positive area for dynamin (**I**) and cathepsin L (**J**) in patients with the indicated proteinuric kidney diseases. Dynamin protein expression is significantly higher in LN and MCD compared to control; $*p < 0.05$ versus control. Cathepsin L protein expression is significantly higher in LN, MCD and IgAN compared to control; $*p < 0.05$ versus control. (**K**) Summary of proteinuria data of the different patient groups. No correlation was found between the level of proteinuria and dynamin staining. Patients with MCD, FSGS and IgAN all had significantly more proteinuria than control patients; $**p < 0.01$, $***p < 0.001$, MCD, minimal change disease; FSGS, focal segmental glomerulosclerosis; IgAN, IgA nephropathy; LN, lupus nephritis; DN, diabetic nephropathy. All images were taken at the same magnification; scale bar = 50 µm.

Discussion

Here, we investigated dynamin expression under proteinuric conditions in both patients and rats. In addition, we examined whether dynamin is involved in glomerular proteinuria, tubular proteinuria, or both. We found a significant increase in glomerular levels of *Dnm2* and *Dnm1* mRNA in Dahl rats prior to the onset of albuminuria. Also, we show that knocking down dynamin translation results in proteinuria in a zebrafish embryo model. Lastly, we found that glomerular levels of dynamin and cathepsin L protein are significantly increased in patients with proteinuric kidney disease.

Our finding of increased dynamin protein and *Dnm1* and *Dnm2* mRNA levels in proteinuric disease, combined with the results of Soda *et al*. showing that dynamin knock out results in proteinuria, leads to the following two hypotheses on dynamin's role in GFB integrity. First, a minimum level of dynamin may be required for adequate GFB integrity; thus, if this level is not reached, GFB integrity is lost. Second, when the GFB is under stress, dynamin may be upregulated in an attempt to maintain or restore GFB integrity. We previously studied the expression of proteins required for proper GFB function in patients with acquired proteinuria and found changes that suggest a compensatory mechanism.(84) Thus, disease progression may occur when this compensatory mechanism becomes saturated or exhausted.

In Dahl rats, which spontaneously develop proteinuria, we found that the levels of *Dnm1* and *Dnm2* mRNA are increased prior to the onset of proteinuria, a symptom that manifests only when protein is present in excreted urine. Proteinuria occurs when proteins pass through the GFB and are not sufficiently reabsorbed by the tubular system either due to saturation or malfunction of the tubular reabsorption process. Thus, the increase in glomerular *Dnm1* and *Dnm2* mRNA levels prior to the onset of proteinuria might reflect a compensatory mechanism in response to an early, presymptomatic increase in GFB permeability that does not yet lead to actual proteinuria. However, as proteinuric disease progresses, this compensatory system can become exhausted, thereby failing to prevent the onset of proteinuria. This hypothetical process is depicted schematically in Figure 4.

Interestingly, we found that while animals that will become proteinuric (Dahl rats) express both more glomerular *Dnm2* and *Dnm1* mRNA before onset of proteinuria, this does not result in to an increase in dynamin protein. However, since dynamin is a regulatory GTPase, it is not necessary to have an increase in protein level to have an altered intracellular activity. Also, cathepsin L-mediated cleavage of dynamin may be increased and cause a decrease in dynamin protein staining.(13) In humans, we found that there is indeed an increase in glomerular cathepsin L protein which directly and strongly correlated with glomerular dynamin protein levels, as also observed by Sever *et al*.(13) Cleavage of dynamin by cytosolic L generates a 40 kDa N-terminal fragment of dynamin. As the used antibody recognizes an epitope of residues 822-838 of dynamin, these fragments were not identifiable in the immunohistochemistry experiments performed in this study. In our study, we found significantly higher levels of *Ctsl* mRNA in Dahl rats at all ages investigated, suggesting that in this rat model both the transcription and posttranslational cleavage of dynamin are increased.

Although the used Hudy 1 antibody does not discern between DNM1 and DNM2 protein, the higher *Dnm2* mRNA levels suggest that *Dnm2* is the more prevalent type of dynamin, as also reported by others.(14)

We found that the glomerular levels of dynamin protein were increased primarily in patients with minimal change disease (MCD) and lupus nephritis. Schiffer *et al.* recently proposed that dynamin's principal role in maintaining podocyte structure and preventing proteinuria is independent of the underlying disease pathogenesis.(75) Our results are consistent with this notion, given that lupus nephritis is considered to be immunological in origin, whereas MCD is not.(85, 86)

Sever *et al.* previously reported the levels of *CTSL* mRNA were increased in the glomeruli of patients with acquired proteinuric disease. (13) Notably, the levels of *CTSL* mRNA expression were increased in patients with focal segmental glomerulosclerosis (FSGS) and in patients with diabetic nephropathy, but not in patients with MCD. Interestingly, we found that dynamin expression was significantly increased in patients with MCD, but not in patients with FSGS or diabetic nephropathy; Sever *et al.* did not measure *CTSL* mRNA in patients with lupus nephritis. In our study, we found significantly more cathepsin L protein in glomeruli of patients with minimal change disease, lupus nephritis, and IgA nephropathy. Although we did see an increase in glomerular cathepsin L positive area percentage in DN patients, as also reported by Sever *et al.*, this increase was not statistically significant.

Thus, taken together, these results suggest that in human proteinuric disease, the interplay between cathepsin L and dynamin is part of a regulatory system influenced by proteinuria, as proposed previously.(13)

Dynamin's protective effect on the GFB could be effected through its role in nephrin turnover, as suggested by other groups.(14, 87-89) Nephrin (encoded in rats by the *Nphs1* gene) is a core component of the glomerular slit diaphragm.(16) In podocytes, nephrin is internalized by clathrin-mediated endocytosis and clathrin-independent raft-mediated endocytosis, both of which are dynamin-dependent processes.(88) We previously reported that *Nphs1* mRNA levels are increased significantly in Dahl rats by 10 weeks of age, although the pattern of nephrin protein is focal and segmental rather than linear, and effacement of the podocyte foot process occurs.(17) In this study, we found that the levels of *Dnm1* and *Dnm2* mRNA are significantly lower at 10 weeks of age compared to younger ages. These results suggest that the relative decrease in *Dnm1* and *Dnm2* mRNA in Dahl rats at later ages results in a loss of sufficient nephrin turnover, which then leads to reduced protection against podocyte pathology.

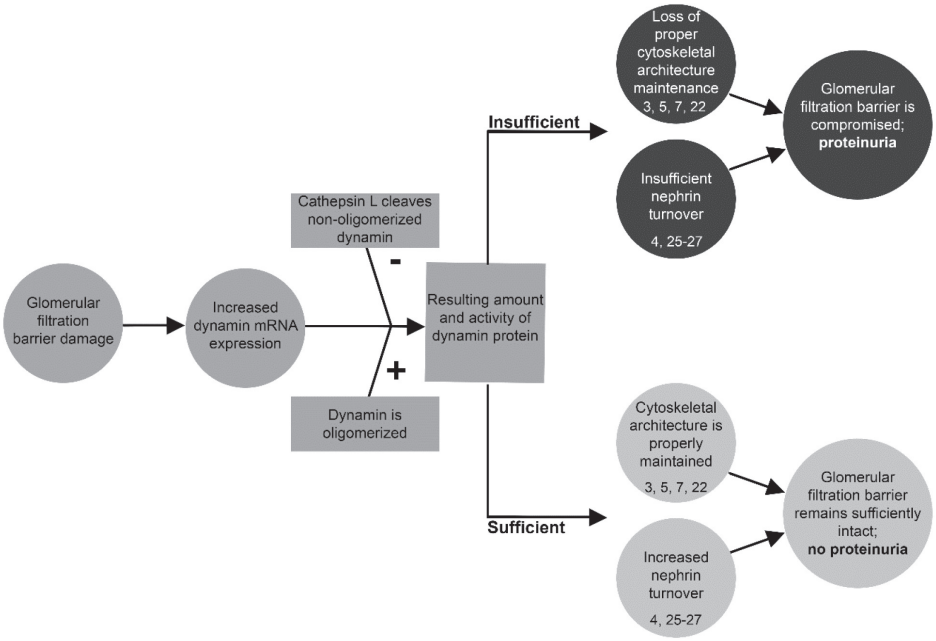

Figure 4. Increased dynamin expression precedes proteinuria

Flow chart illustrating the proposed compensatory mechanism in response to impaired integrity of the glomerular filtration barrier, in which increased dynamin expression precedes proteinuria. After damage to the glomerular filtration barrier, *DNM1* and *DNM2 are* upregulated, leading to increased levels of *DNM1* and *DNM2* mRNA. Whether this increase results in increased levels of dynamin protein depends upon the oligomerization status of dynamin and the activity of cathepsin L, which selectively cleaves non-oligomerized dynamin.(13) If the total amount of dynamin is sufficient, the glomerular filtration barrier remains intact, preventing the onset of proteinuria. However, if dynamin levels are insufficient—and/or if this compensatory response is exhausted—proteinuria develops. The suggested mechanisms of cytoskeletal architecture maintenance and nephrin turnover have been reported by others. (11-14, 75, 87-89)

Dynamin also directly interacts with the actin cytoskeleton, as shown by others.(11-13, 75) Consistent with this structural role, our microarray analysis revealed additional evidence that the cytoskeletal architecture is disrupted in Dahl rats, given the differential regulation of cytoskeleton-related genes. Further studies will likely provide new insight into how the actin cytoskeleton is regulated under proteinuric conditions.

In conclusion, our results provide evidence that dynamin expression is increased in human proteinuric disease. Moreover, we propose that a minimum level of dynamin is required for GFB integrity, and increases in *Dnm1* and *Dnm2* mRNA are part of a compensatory mechanism that support GFB integrity under stressful conditions. Given that this mechanism seems to play a role in patients with proteinuric kidney disease, dynamin may represent a promising target for therapeutic intervention.

Acknowledgments

This work was supported in part by the Dutch National Kidney Foundation (IP 11.57).

Statement of author contributions

RKh designed and performed experiments, analysed data and wrote the paper. KK designed and performed experiments. HPS, RKr, PCWH and JAB provided conceptual advice. HJB designed experiments and provided technical support and conceptual advice. All authors had final approval of the submitted and published versions.

References

1. Group CW. KDIGO clinical practice guideline for the evaluation and management of chronic kidney disease. *Kidney Int Suppl* 2013.
2. Raghavan V, Rbaibi Y, Pastor-Soler NM, *et al.* Shear stress-dependent regulation of apical endocytosis in renal proximal tubule cells mediated by primary cilia. *Proceedings of the National Academy of Sciences of the United States of America* 2014; 111: 8506-8511.
3. Sever S, Altintas MM, Nankoe SR, *et al.* Proteolytic processing of dynamin by cytoplasmic cathepsin L is a mechanism for proteinuric kidney disease. *The Journal of clinical investigation* 2007; 117: 2095-2104.
4. Soda K, Balkin DM, Ferguson SM, *et al.* Role of dynamin, synaptojanin, and endophilin in podocyte foot processes. *The Journal of clinical investigation* 2012; 122: 4401-4411.
5. Gu C, Yaddanapudi S, Weins A, *et al.* Direct dynamin-actin interactions regulate the actin cytoskeleton. *The EMBO journal* 2010; 29: 3593-3606.
6. Dobrinskikh E, Okamura K, Kopp JB, *et al.* Human podocytes perform polarized, caveolae-dependent albumin endocytosis. *American journal of physiology Renal physiology* 2014; 306: F941-951.
7. Schiffer M, Teng B, Gu C, *et al.* Pharmacological targeting of actin-dependent dynamin oligomerization ameliorates chronic kidney disease in diverse animal models. *Nature medicine* 2015; 21: 601-609.
8. Gu C, Chang J, Shchedrina VA, *et al.* Regulation of dynamin oligomerization in cells: the role of dynamin-actin interactions and its GTPase activity. *Traffic* 2014; 15: 819-838.
9. Ono S, Kume S, Yasuda-Yamahara M, *et al.* O-linked beta-N-acetylglucosamine modification of proteins is essential for foot process maturation and survival in podocytes. *Nephrology, dialysis, transplantation : official publication of the European Dialysis and Transplant Association - European Renal Association* 2017; 32: 1477-1487.
10. Wang J, Duncan D, Shi Z, *et al.* WEB-based GEne SeT AnaLysis Toolkit (WebGestalt): update 2013. *Nucleic acids research* 2013; 41: W77-83.
11. Kanehisa M, Goto S. KEGG: kyoto encyclopedia of genes and genomes. *Nucleic acids research* 2000; 28: 27-30.
12. Mehr AP, Siegel AK, Kossmehl P, *et al.* Early onset albuminuria in Dahl rats is a polygenetic trait that is independent from salt loading. *Physiol Genomics* 2003; 14: 209-216.
13. Baelde JJ, Bergijk EC, Hoedemaeker PJ, *et al.* Optimal method for RNA extraction from mouse glomeruli. *Nephrology Dialysis Transplant* 1995; 9: 304-308.
14. Westerfield M. The zebrafish book : a guide for the laboratory use of zebrafish (Danio rerio). ed). Institute of Neuroscience, University of Oregon: [Eugene, OR], 2007.
15. Kimmel CB, Ballard WW, Kimmel SR, *et al.* Stages of embryonic development of the zebrafish. *Dev Dyn* 1995; 203: 253-310.
16. Hanke N, Staggs L, Schroder P, *et al.* "Zebrafishing" for novel genes relevant to the glomerular filtration barrier. *BioMed research international* 2013; 2013: 658270.
17. Hentschel DM, Mengel M, Boehme L, *et al.* Rapid screening of glomerular slit diaphragm integrity in larval zebrafish. *American journal of physiology Renal physiology* 2007; 293: F1746-1750.
18. FEDERA. Human Tissue and Medical Research: Code of conduct for responsible use. ed). 2011.
19. Koop K, Eikmans M, Baelde HJ, *et al.* Expression of podocyte-associated molecules in acquired human kidney diseases. *Journal of the American Society of Nephrology : JASN* 2003; 14: 2063-2071.

20. Chugh SS, Clement LC, Mace C. New insights into human minimal change disease: lessons from animal models. *American journal of kidney diseases : the official journal of the National Kidney Foundation* 2012; 59: 284-292.
21. Davidson A. What is damaging the kidney in lupus nephritis? *Nature reviews Rheumatology* 2016; 12: 143-153.
22. Sampogna RV, Al-Awqati Q. Taking a bite: endocytosis in the maintenance of the slit diaphragm. *The Journal of clinical investigation* 2012; 122: 4330-4333.
23. Qin XS, Tsukaguchi H, Shono A*, et al.* Phosphorylation of nephrin triggers its internalization by raft-mediated endocytosis. *Journal of the American Society of Nephrology : JASN* 2009; 20: 2534-2545.
24. Waters AM, Wu MY, Huang YW*, et al.* Notch promotes dynamin-dependent endocytosis of nephrin. *Journal of the American Society of Nephrology : JASN* 2012; 23: 27-35.
25. Tryggvason K, Patrakka J, Wartiovaara J. Hereditary proteinuria syndromes and mechanisms of proteinuria. *The New England journal of medicine* 2006; 354: 1387-1401.
26. Koop K, Eikmans M, Wehland M*, et al.* Selective loss of podoplanin protein expression accompanies proteinuria and precedes alterations in podocyte morphology in a spontaneous proteinuric rat model. *The American journal of pathology* 2008; 173: 315-326.

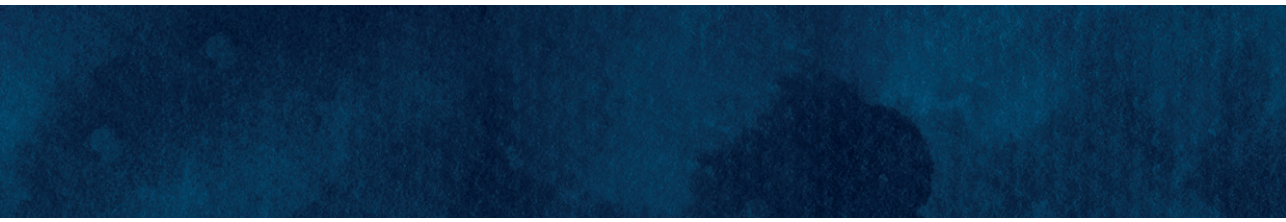

CHAPTER 6

Transmembrane Protein 14A protects glomerular filtration barrier integrity

Physiological Reports 2023, 11, e15847

Ramzi Khalil[1], Josephine Bonnemaijer[1], Reinhold Kreutz[2], Herman P. Spaink[3], Pancras C.W. Hogendoorn[1], Hans J. Baelde[1]

[1] *Department of Pathology, Leiden University Medical Center, Leiden, The Netherlands*
[2] *Institute of Clinical Pharmacology and Toxicology, Charité - University Medicine, Berlin, Germany*
[3] *Institute of Biology Leiden, Leiden University, Leiden, The Netherlands*

Abstract

Transmembrane protein 14A (TMEM14A) is a relatively unknown protein that is now identified to be required for maintaining the integrity of the glomerular filtration barrier. It is an integral transmembrane protein of 99 amino acids with 3 transmembrane domains. TMEM14A has been implied to suppress Bax mediated apoptosis in other studies. Other than that, little is currently known of its function. Here, we show that its expression is diminished before onset of proteinuria in a spontaneously proteinuric rat model. Knocking down *tmem14a* mRNA translation results in proteinuria in zebrafish embryos without affecting tubular reabsorption. Also, it is primarily expressed by podocytes. Lastly, an increase in glomerular *TMEM14A* expression is exhibited in various proteinuric renal diseases. Overall, these results suggest that TMEM14A is a novel factor in the protective mechanisms of the nephron to maintain glomerular filtration barrier integrity.

Introduction

Proteinuria is an important risk factor for progression of renal disease and cardiovascular mortality (2). Proteinuria occurs when glomerular filtration barrier (GFB) integrity is compromised. The GFB consists of fenestrated endothelial cells lined with glycocalyx, the glomerular basement membrane, and podocyte foot processes. Understanding the pathophysiology and mechanisms leading to proteinuria is essential in the quest to understanding nephron function and finding new potential therapeutic targets for proteinuric renal diseases.

To study the pathophysiology and underlying mechanisms of the development of proteinuria, we have further analyzed spontaneously proteinuric Dahl salt sensitive rats (Dahl) (79, 90-93). Analysis of differentially regulated glomerular mRNA yielded various genes potentially involved in the development of proteinuria.(17, 93) One of the noteworthy downregulated genes in the Dahl rat, was transmembrane protein 14A (Tmem14a).

TMEM14A is 99 amino acid integral membrane protein with three transmembrane domains. Its structure has been identified by nuclear magnetic resonance spectroscopy (94). Relatively little is known of its function. It has been described to be involved in preventing apoptosis by preventing loss of mitochondrial membrane potential through Bax suppression in an *in vitro* study (95). However, its function in maintenance of GFB integrity has not yet been described. Interestingly, Apoptosis of podocytes has been described as a pathophysiological process in proteinuric renal disease, especially diabetic nephropathy, in various experimental models (96-100). Moreover, podocyte detachment and loss has been suggested to been dependent on apoptotic caspases in an experimental animal model.(101)

As *Tmem14a* was found to be downregulated in rats with a proteinuric phenotype in the Dahl array, we hypothesize that it is required for maintaining GFB integrity and that is also differentially expressed in human proteinuric disease.

Materials and Methods

Microarray

Microarray data containing information on differentially regulated genes in glomeruli obtained from spontaneously proteinuric Dahl salt sensitive (Dahl) male rats strain and non-proteinuric spontaneous hypertensive (SHR) male rats at 4 and 6 weeks of age was used to identify genes potentially involved in the development of proteinuria. The

dataset with GEO Series accession number GSE 13810 was accessed through the Gene Expression Omnibus of the NCBI. As described previously, this analysis was performed with Affymetrix GeneChip Rat Genome 230 2.0 arrays (93).

Animal studies: rats

Animal studies in rats were performed with the same animal material as previously described and in accordance with institutional guidelines (17, 93). Rat experiments were approved by the respective Institutional Animal Care and Use Committee. Dahl and SHR male rats were obtained from Freie Universität Berlin (79). They were fed a low salt diet containing 0.2 percent NaCl by weight to prevent early development of hypertension. To investigate the time relation between Tmem14a expression and the development of proteinuria, groups of rats were studied at 2, 4, 6, 8, and 10 weeks of age. mRNA expression was investigated in a total of 67 animals. For the respective ages stated above the respective number of investigated animals per age group were 7, 7, 7, 8, and 8 for the Dahl rats and a number of 5, 4, 6, 7, and 8 for the SHR group. For protein expression, 2 rats were investigated per age and group.

Animal studies: zebrafish

Wild-type (WT) AB/TL strain zebrafish (*Danio rerio H)* were injected with 1 nL of a morpholino (Gene Tools, Philomath, OR) blocking the mRNA translation of the zebrafish *tmem14a* homologue, zgc:163080, or a scrambled control morpholino during the 1-to-4 cell stage of embryonic development (82). Experiments were performed concurrently with previously described studies (55, 93)

All zebrafish experiments were performed prior to the free-feeding stage of embryos and therefore are not considered animal experiments in accordance with EU Animal Protection Directive 2010/63/EU.

Glomerular permeability and tubular reabsorption assay

A tubular reabsorption assay was performed as described previously (55, 93, 102). This method was adapted from Hentschel *et al.* and has been previously validated to reliably assess glomerular permeability and tubular reabsorption function (40, 43). In short, a 1 nl mixture of 3 kDa TRITC labelled dextran (100 mg/ml; Invitrogen) and 70 kDa FITC labelled dextran (25 mg/ml; Invitrogen) was injected intravenously at 5 days post fertilization (dpf), fixed one hour after injection in 10% formalin for 24 hours, stored in ethanol 70%, embedded in paraffin, sectioned and examined by fluorescence microscopy.

The number of proximal tubule reabsorption droplets were quantified manually in a blinded fashion. As a positive control, a section of control zebrafish embryos was injected with puromycin aminonucleoside (PAN, Sigma-Aldrich, St. Louis, MO) at 4 dpf (40). Under physiological conditions, the 3 kDa tracer freely passes the GFB and the 70 kDa does not. After passing the GFB, these tracers are absorbed by proximal tubule cells in endosomes, appearing as small droplets. Hence, observing 70 kDa reabsorption droplets in proximal tubule cells indicates loss of GFB integrity. Reabsorption droplets of the 3-kDa tracer were used to assess the correct location of the proximal tubule cells and whether tubular reabsorption mechanisms are sufficiently intact.

Although injecting dextrans of sizes larger than 70 kDa could theoretically provide additional information on the severity of loss of GFB integrity, previous pilot experiments (data not shown) have shown 70 kDa to produce the most consistent and reliable results when fixing the samples 1 hour after injection. We were not able to reliably differentiate between the 70 kDa and larger tracers when maintaining this timeframe. Therefore, in this study, only the validated 3- and 70 kDa tracers were used.

Cell culture

Immortalized podocytes (Moin Saleem, Bristol, UK, human), embryonic kidney (HEK) 293 cells (ATCC), and human umbilical vein endothelial cells (Huvec) (Lonza, Allendale, NJ, USA) ATCC were used to measure mRNA expression for *TMEM14A*. Podocytes were also used for localization of TMEM14A protein expression by immunohistochemistry as described below. Immortalized podocytes were cultured in RPMI 1640 Medium with added Penicillin, Streptomycin, Insulin, Transferrin, Selenite (Sigma Chemicals, Dorset, UK) and 10% Fetal Bovine Serum at 33 °C (in 5% CO_2) for proliferation and at 37 °C (in 5% CO_2) for differentiation.

RNA isolation, reverse transcription and qPCR

RNA isolation, reverse transcription and qPCR were performed as described previously (93). To quantify gene expression of *TMEM14A* in different cell lines, RNA from podocytes, HEK, and Huvec cells, and RNA from purified glomeruli and whole kidney tissue was isolated using TRIzol (Invitrogen, Waltham, MA). AMV reverse transcriptase (Roche Diagnostics) was used for reverse transcription into cDNA. Primer sequences are listed in Table 1. GAPDH was used as a housekeeping gene for cell culture experiments. For purified rat glomeruli experiments, *Hprt1* was used as internal control. mRNA expression values are given as relative to *Hprt1* expression. Quantitative real-time PCR

(qPCR) was performed on an iCycler real-time PCR machine with SYBR green supermix. (Bio-Rad Laboratories, Hercules, CA), and Bio-Rad CFX Maestro software was used for normalised gene expression calculations. (Bio-Rad Laboratories).

Table 1. Primer sequences

Name	Symbol	mRNA sequence	Forward primer Reverse primer
Transmembrane protein 14A (human)	TMEM14A	NM_014051.3	TTTGGTTATGCAGCCCTCGT ATAGCCGGCCAAACATCCAA
Glyceraldehyde-3-phosphate dehydrogenase (human)	GAPDH	NM_002046	TGGTCACCAGGGCTGCTT AGCTTCCCGTTCTCAGCCTT
Hypoxanthine-guanine phosphoribosyltransferase 1 (human)	HPRT1	NM_000194.2	TGACACTGGCAAAACAATGCA GGTCCTTTTCACCAGCAAGCT
Transmembrane protein 14A (rat)	*Tmem14a*	NM_014051.4	GGCCACCATAATGGGTGTGA CAGCAGCAGGACAAGTCTCA
Hypoxanthine-guanine phosphoribosyltransferase 1 (rat)	*Hprt1*	NM_012583.2	GGCTATAAGTTCTTTGCTGACCTG AACTTTTATGTCCCCCGTTGA

Human material

Anonymised tissue from renal biopsies from patients with various proteinuric renal diseases was collected from a previously described archive, including 20 patients with IgA nephropathy, 20 patients with lupus nephritis class III or IV, 10 patients with minimal change disease (MCD), and 13 patients with diabetes nephropathy (DN) at the department of pathology, Leiden University Medical Center.(93) Tissue of 10 kidneys that were unsuitable for transplantation and tumor-free renal resection material of 10 patients with a tumor elsewhere in the material were collected and used as a control group. All material was obtained, anonymised and handled according to institutional guidelines, Good Research Practice, and the Code of conduct for responsible use.

Immunohistochemistry

A commercially available polyclonal goat anti-TMEM14A antibody (Santa Cruz Biotech, sc-248899, Dallas, TX) was used for immunohistochemical staining of TMEM14A on human and rat material. In zebrafish material, the quality of staining was insufficient for reliable assessment.

Immortalized podocytes that were confluent for 2 weeks were transferred to small glasses in a 24 wells plate. After 24 hours incubation immunohistochemistry was performed. Podocytes were washed in PBS and fixated using – 20 °C methanol. The glasses were then

washed in PBS and blocked with 5% Normal Rabbit Serum (NRS) for 1 hour. 5% NRS was aspirated, and the glasses were incubated with primary antibody diluted in 1% BSA in PBS (polyclonal goat anti-TMEM14A) at 4°C overnight.

For rat and human kidney tissue, after sectioning at 4 μm, the slides were deparaffinized, dehydrated, and boiled in Tris/EDTA buffer for antigen retrieval for 10 minutes. The slides were washed in PBS and incubated with the primary antibody diluted in 1% BSA in PBS (polyclonal goat anti-TMEM14A 1:200 for rat tissue, 1:150 for human tissue) at 4°C overnight.

For all mentioned materials, after incubation of the primary antibody the samples were washed in PBS and incubated for 30 minutes with the secondary antibody ((Polyclonal Rabbit Anti-Goat Immunoglobulins/horse radish peroxidase, Cat no: P0160, AgilentDako, CA, United States). The material was then washed in PBS again and immunoreactivity was detected with diaminobenzidine. After counterstaining with haematoxylin, the material was dehydrated and mounted.

For quantification of stained slides in both rat and human material, we used a semi-quantitative approach. TMEM14A staining was evaluated on a semi-quantitative scale with a score of 0 to 4 in a blinded manner, subdivided in respectively no podocyte staining (0), 0-10% of the podocytes (1), 10-30% of the podocytes (2), 30-60% of the podocytes (3) more than 60% of the podocytes (4).

Statistical analyses

Statistical analyses were performed using Graphpad Prism 9.4.1 (GraphPad Software, San Diego, California). Student's unpaired t-testing was used for comparisons between 2 or 3 groups. When more than 3 groups were compared, one-way ANOVA with Tukey's post hoc analysis was used. A *p*-value below 0.05 was considered significant.

Results

Glomerular gene expression pattern of proteinuric rats

Tmem14a was identified as potentially involved in the development of proteinuria through analysis of a previously published microarray dataset comparing Dahl andSHR rats. The top 5 downregulated genes are shown in Table 2. These genes are found in both SHR and Dahl rats. *Tmem14a* was selected for further analysis based on this differential expression and the availability of a zebrafish homologue to perform experimental *in vivo* analysis of development of proteinuria, as performed later in this study.

Table 2. Glomerular gene expression in Dahl rats compared to SHR

Gene name	Symbol	Region of rat chromosome	Fold change
Aldo-keto reductase family 1, member B8	Akr1b8	4q22	-4.5
Similar to interferon regulatory factor 10	RGD1562711	3q41	-3.9
Acyl-Coenzyme A oxidase 2, branched chain	Acox2	15p14	-3.7
Similar to RIKEN cDNA 4921520P21; DMRTC1	LOC363483	Xq31	-3.4
Transmembrane protein 14A	Tmem14a	9q13	-3.0

Glomerular Tmem14a mRNA and protein expression is diminished in spontaneously proteinuric rats before onset of proteinuria

Glomerular mRNA and protein expression of Tmem14a were investigated in Dahl rats and compared to spontaneously hypertensive rats at 2, 4, 6, 8, and 10 weeks of age. Of note, Dahl rats develop significant proteinuria from 6 weeks of age. (Figure 1A) When comparing the two groups at each time point, glomerular *Tmem14a* mRNA expression is consistently significantly lower in the Dahl rats ($p < 0.0001$ at every time point, Figure 1A). Looking at the difference in expression between the different time points in only the Dahl rats, expression starts high and decreases quickly; at 2 weeks of age expression is significantly higher than at all other time points ($p < 0.0001$), but no significant difference was seen between the other time points. Doing the same in the spontaneously hypertensive control, glomerular *Tmem14a* mRNA expression was significantly higher at a younger age at weeks 2, 4, and 6 compared to week 10 ($p < 0.01$, $p < 0.05$, and $p < 0.0001$ respectively). At weeks 2, 4, and 6, expression was significantly higher than at 8 weeks of age ($p < 0.05$, $p < 0.05$, and $p < 0.001$ respectively).

After 2 weeks of age Tmem14a protein expression was lower in Dahl rats than in SHR at all time points. This was significantly so at 4 and 8 weeks of age ($p < 0.001$). At later timepoints, no significant differences in glomerular Tmem14a protein expression were seen. So, in Dahl rats, glomerular Tmem14a mRNA and protein expression is diminished before onset of proteinuria.

Knocking down tmem14a mRNA translation results in proteinuria in zebrafish embryos

The functional role of TMEM14A in the development of proteinuria was further investigated using a zebrafish embryo model. First, the zebrafish homologue of TMEM14A, zgc:163080, was knocked down by blocking its mRNA translation through morpholino injection. Then, a mixture of 3 and 70 kDa dextran tracers was injected. Puromycin aminonucleoside (PAN) injected zebrafish were used as a positive control for inducing proteinuria. PAN is a validated method to induce proteinuria in this zebrafish embryo model (40, 43). If the injected dextran tracers pass the GFB, they are subsequently reabsorbed by proximal tubular epithelial cells.

These cells reabsorb the dextran tracers in endosomes. Through immunofluorescence microscopy, these endosomes appear as small fluorescent droplets in the proximal tubule cells. The number of these proximal tubule reabsorption droplets were counted in a blinded fashion. (Figures 2A through F) No difference was found in the mean number of 3 kDa reabsorption droplets, indicating that tubular reabsorption mechanisms remained intact in all three groups (Figure 2G). A significantly higher number of 70 kDa reabsorption droplets was measured in both zebrafish embryos with a *tmem14a* knockdown and in the positive control group, indicating loss of GFB integrity (Figure 2H, $p < 0.05$). The effectivity of *tmem14a* knockdown in zebrafish was primarily assessed by quantifying its effect on glomerular permeability.

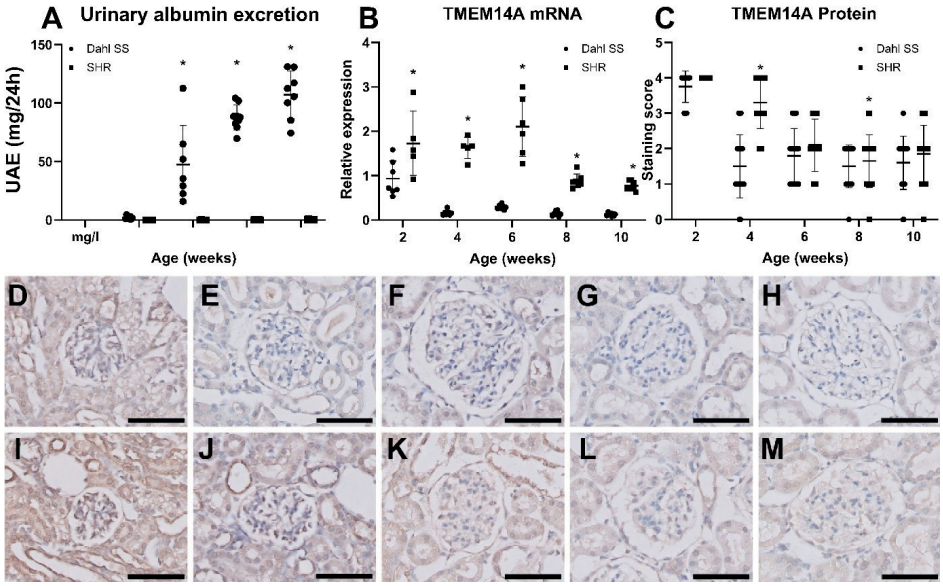

Figure 1. Glomerular TMEM14A expression is diminished before onset of proteinuria

(A) Urinary albumin excretion is significantly higher in Dahl rats compared to SHR from 6 weeks of age. Y-axis shows urinary albumin excretion in mg/24h, and the X-axis shows animal age in weeks.

(B) Glomerular TMEM14A mRNA expression in Dahl rats is significantly lower than in SHR controls at all time points. The Y-axis shows mRNA expression as relative expression compared to *Hprt1,* and the X-axis shows animal age in weeks. No correlation was observed between TMEM14A expression and urinary albumin excretion in both SHR (r = - 0.80, CI -0.98 – 0.27) and Dahl (r = -0.60, CI -0.97 to 0.60) using Pearson's correlation coefficient.

(C) Glomerular staining for Tmem14a protein is lower in Dahl rats than in SHR after 2 weeks. This difference is significant at weeks 4 and 8 of age. The columns represent mean semi-quantitative score

Dahl rats develop proteinuria at 6 weeks of age. Thus, both mRNA and protein expression levels drop before onset of proteinuria. ANOVA with Tukey's post hoc analysis was used.

(**D - M**) Representative images of glomeruli of spontaneously proteinuric Dahl (**D** – **H**) and SHR (**I** – **M**) rats at respectively 2 (**D** and **I**), 4 (**E** and **J**), 6 (**F** and **K**), 8 (**G** and **L**), and 10 (**H** and **M**) weeks of age. (**A – C**) Horizontal lines indicate mean with SD.

Scalebar = 50 μm *$p < 0.001$

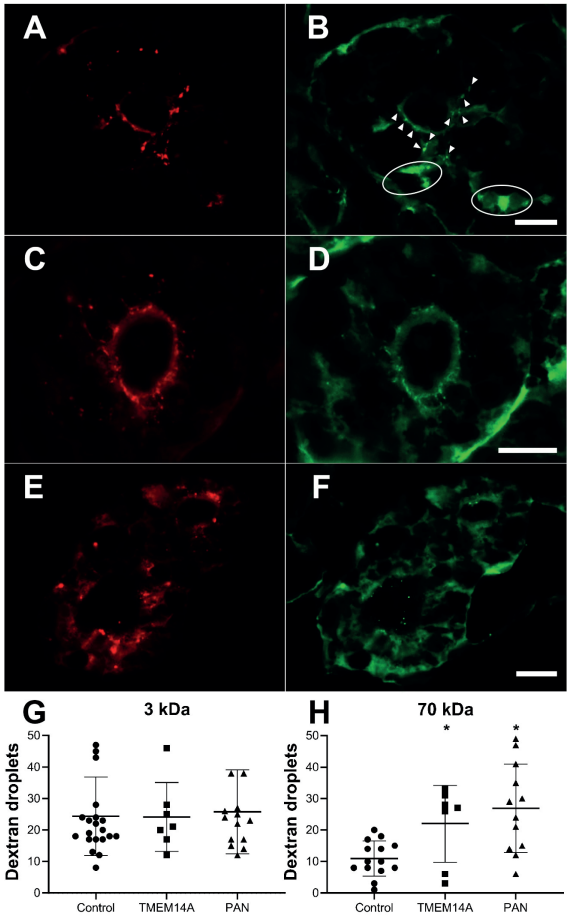

Figure 2. Knocking down TMEM14A mRNA translation causes proteinuria

Knocking down mRNA translation of the zebrafish homologue of TMEM14A through morpholino injection results in proteinuria.

(A - F) Representative immunofluorescence images of transversal sections of zebrafish proximal tubule cells after injection of a mixture of red labeled 3 kDa dextran tracer **(A, C, and E)** and green labeled 70 kDa dextran tracer **(B, D, and F)** in controls (**A** and **B**), TMEM14A knockdowns (**C** and **D**), and PAN injected positive controls (**E** and **F**)**.** Dextran tracers that passed the GFB are reabsorbed by proximal tubule epithelial cells in endosomes. Thus, reabsorbed dextran tracer appears as fluorescent droplets. The number of proximal tubule reabsorption droplets was counted in a blinded manner in sections as those shown here. The arrowheads in B point out examples of counted droplets. The circled areas show high fluorescence due to dextran present in the peritubular capillaries. These areas are not counted as reabsorption droplets. The sharpness of the images in panels A through F has been enhanced by overlaying them with a digital high pass filter.

(G and **H)** Uptake of the red 3 kDa marker **(G)** was used to assess tubular reabsorption function, which was intact in both TMEM14A knockdown animals and controls. In the knockdown model, significantly more 70 kDa droplets (**H**) have passed the GFB and were subsequently reabsorbed. Puromycin aminonucleoside (PAN) injected zebrafish were used as positive controls. Students *t*-test was used.

(**G and H**) Horizontal lines indicate mean with SD. Scalebar = 20 μm

* = $p < 0.05$

TMEM14A is primarily expressed by podocytes in the kidney

TMEM14A mRNA expression was investigated - in both whole kidney tissue and purified glomeruli and compared to immortalized podocytes, HEK, and HUVEK cells. It revealed that *TMEM14A* is expressed by podocytes and endothelial cells. Moreover, its expression is higher in purified glomeruli than in whole kidney. mRNA expression was highest in differentiated podocytes (Figure 3A). Immunohistochemistry results from the previous experiments show that TMEM14A is also expressed in distal tubular cells (images 1C – K).

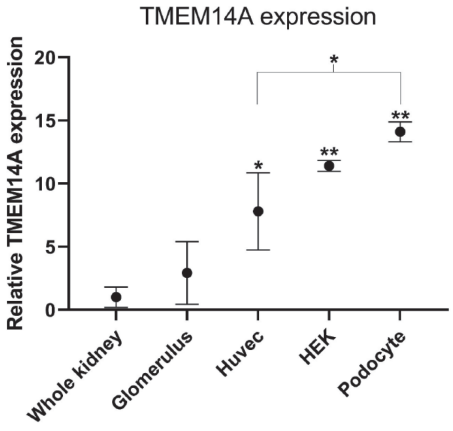

Figure 3. TMEM14A is primarily expressed by podocytes
In vitro experiments of relative TMEM14A mRNA expression show expression relative to GAPDH expression when comparing mRNA extracts from whole kidney, purified glomeruli, human umbilical vein endothelial cells (Huvec), human embryonic kidney (HEK), and finally podocytes. Expression in podocytes, HEK and Huvec was significantly higher than in whole kidney ($p < 0.001$ for all groups) and then purified glomeruli ($p < 0.001$ for podocytes and HEK, $p < 0.05$ for Huvec). Podocyte expression was highest of all cells and significantly so compared to Huvec ($p < 0.05$). Mean and SD shown. ANOVA with Tukey's post hoc analysis was used.

Glomerular TMEM14A protein expression is increased in proteinuric disease

To establish whether TMEM14A also plays a role in the development of proteinuria in human disease, glomerular TMEM14A protein expression was examined in human kidney biopsies from patients with IgA nephropathy (IgAN), lupus nephritis (LN), minimal change disease (MCD), or diabetic nephropathy (DN). Here, we found that TMEM14A protein expression is significantly increased in IgAN, LN and MCD ($p < 0.0001$) but not in DN (Figure 4). No correlation was found between the level of proteinuria and the score in TMEM14A positivity ($r = 0.09$).

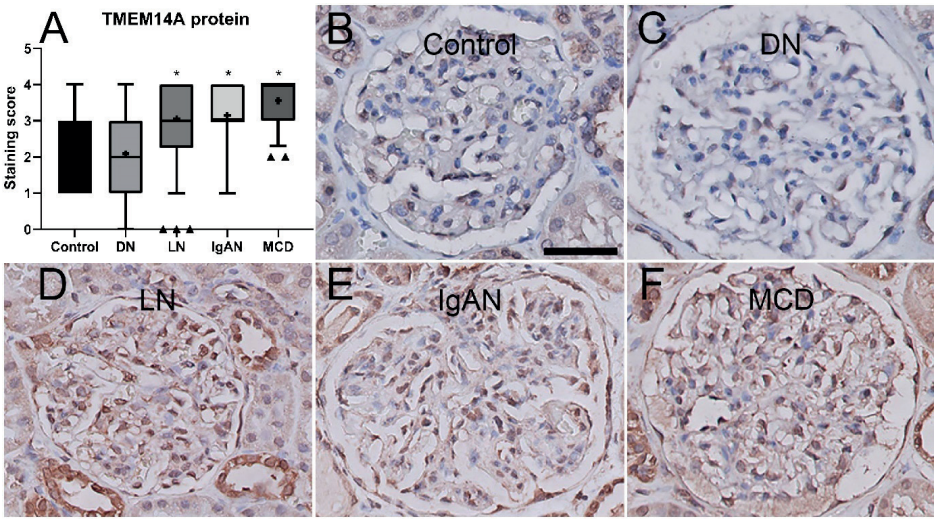

Figure 4. Glomerular TMEM14A expression is increased in human proteinuric renal diseases

(A) Glomerular TMEM14A protein expression was examined in human kidney biopsies from patients with diabetic nephropathy (DN), lupus nephritis (LN), IgA nephropathy (IgAN), minimal change disease (MCD), and healthy controls. Compared to controls, TMEM14A protein expression is significantly more extensive in IgAN, LN, and MCD, but not in DN. **(B – F)** Representative images of glomeruli stained for TMEM14A in healthy controls **(B)**, diabetic nephropathy **(C)**, lupus nephritis **(D)**, IgA nephropathy **(E)**, and minimal change disease **(F)**. Slides were stained with goat anti-TMEM14A antibody and immunoreactivity was assessed by diaminobenzidine. This results in a brown colour which then indicates TMEM14A localization. Counterstaining with haematoxylin results in blue-purple colouring of cell nuclei. Boxes in A show the range of values between the lower and upper quartile, the whiskers show 5th to 95th percentile, triangles show values lying outside the 5th to 95th percentile, the line in the box shows the median, and '+' indicates the mean. The scale bar in B applies to B through F and indicates 50μm. * = $p < 0.001$. ANOVA with Tukey's post hoc analysis was used.

Discussion

TMEM14A is a relatively unknown protein that is identified to be essential in maintaining GFB integrity. In spontaneously proteinuric rats, we show that glomerular Tmem14a mRNA and protein expression is relatively diminished, especially before onset of proteinuria. Also, knocking down *tmem14a* mRNA translation in zebrafish results in proteinuria. *In vitro* experiments reveal that *TMEM14A* is primarily expressed by podocytes. Lastly, we show that glomerular TMEM14A protein expression is increased in various proteinuric renal diseases, but not in diabetic nephropathy.

Overall, these results imply that TMEM14A is an important factor in the development of proteinuria. Based on the results in this study, we postulate that its role in GFB integrity appears to be a protective one. First, a lack of sufficient *Tmem14a* expression in spontaneously proteinuric rats before onset of proteinuria supports this notion. Furthermore, direct inhibition of *tmem14a* mRNA translation resulted in proteinuria in the zebrafish model.

The specific function of the TMEM14A protein is not yet fully understood. As stated before, it has been associated with preventing Bax-mediated apoptosis (95). Apoptosis was previously deemed to not be a significant cause of podocyte loss in most proteinuric diseases (103). However, recent experiments by Yamamoto *et al.* show that loss of podocytes seems to be initiated by the start of the apoptotic process by caspase 3 (101). Apoptosis pathways have previously been implicated as one of the pathophysiological mechanisms in the development of diabetic nephropathy and can be attenuated by ACE or ARBII inhibition (96, 99). As no increase in glomerular TMEM14A protein expressing surface area was seen in diabetic nephropathy glomeruli, insufficient prevention of apoptosis due to a pre-existent relative lack or impairment of TMEM14A might be a factor in the development of proteinuria in these patients. This would be in line with recent results from other studies suggesting that induction of apoptosis causes podocyte detachment (101). Interestingly, previous studies show that Dahl rats indeed have a lower number of podocytes compared to SHR (17). The difference in TMEM14A expression between DN and other investigated proteinuric renal disease warrants further exploration, specifically into TMEM14A and apoptosis in diabetic nephropathy models.

The main limitation of this study is that is largely descriptive in nature, where the exact function of TMEM14A is not yet known. Additionally, external factors influencing its potential expression, degradation and activation are not yet known and as such not yet investigated.

Also, although the use of various experimental models and species in this study is one of its strengths, it also provides a potential limitation due to interspecies variability, which might lead to an incomplete or incorrect analysis and extrapolation of results. As TMEM14A has strong homology across species, it could very well be an evolutionary well-conserved gene that is part of a biological mechanism with broader involvement than the nephron alone.

Future studies are needed to further elucidate the exact role and surrounding mechanisms of TMEM14A in nephron function. In particular, interactions with other proteins involved in maintaining GFB integrity are yet to be unravelled. Moreover, the effect of knocking down TMEM14A through morpholino injection could be due to off-target effect of morpholino injection.(104) The used anti-TMEM14A antibody did not provide reliable assessment of TMEM14A expression in zebrafish and as such, it is possible that the observed proteinuria is an off-target effect. It has been suggested in literature to validate observed morpholino induced phenotypes in embryos bearing mutations in the respective gene. The generation of a TMEM14A mutant would not only establish whether

its role is indeed essential in the development of proteinuria, but also allow for additional mechanistic studies to its function.

Data availability

Micro array data analyzed in this study is deposited and accessible at the Gene Expression Omnibus of the NCBI, which is accessible using the GEO Series accession number GSE 13810

Grants

This work was supported in part by the Dutch National Kidney Foundation (IP 11.57).

Disclosures

The authors declare that the research was conducted in the absence of any commercial or financial relationships that could be construed as a potential conflict of interest.

Author contributions

RKh conceived and designed research, performed experiments, analyzed data, interpreted results of experiments, prepared figures, drafted, edited, and revised the manuscript. JB performed experiments, analyzed data, interpreted results of experiments, prepared figures, and approved final version of manuscript. RKr and HS conceived and designed research, interpreted results of experiments and approved final version of the manuscript. PH conceived and designed research, interpreted results of experiments, edited and revised manuscript. and approved final version of the manuscript. HB conceived and designed research, performed experiments, analyzed data, interpreted results of experiments, edited and revised manuscript. and approved final version of the manuscript.

References

1. Group CW. KDIGO clinical practice guideline for the evaluation and management of chronic kidney disease. Kidney Int Suppl. 2013.
2. Garrett MR, Dene H, Rapp JP. Time-course genetic analysis of albuminuria in Dahl salt-sensitive rats on low-salt diet. J Am Soc Nephrol. 2003;14(5):1175-87.
3. Garrett MR, Joe B, Yerga-Woolwine S. Genetic linkage of urinary albumin excretion in Dahl salt-sensitive rats: influence of dietary salt and confirmation using congenic strains. Physiological Genomics. 2006;25(1):39-49.
4. Mehr AP, Siegel AK, Kossmehl P, Schulz A, Plehm R, de Bruijn JA, et al. Early onset albuminuria in Dahl rats is a polygenetic trait that is independent from salt loading. Physiological Genomics. 2003;14(3):209-16.
5. Siegel AK, Kossmehl P, Planert M, Schulz A, Wehland M, Stoll M, et al. Genetic linkage of albuminuria and renal injury in Dahl salt-sensitive rats on a high-salt diet: comparison with spontaneously hypertensive rats. Physiol Genomics. 2004;18(2):218-25.
6. Khalil R, Koop K, Kreutz R, Spaink HP, Hogendoorn PC, Bruijn JA, et al. Increased dynamin expression precedes proteinuria in glomerular disease. J Pathol. 2019;247(2):177-85.
7. Koop K, Eikmans M, Wehland M, Baelde H, Ijpelaar D, Kreutz R, et al. Selective loss of podoplanin protein expression accompanies proteinuria and precedes alterations in podocyte morphology in a spontaneous proteinuric rat model. Am J Pathol. 2008;173(2):315-26.
8. Klammt C, Maslennikov I, Bayrhuber M, Eichmann C, Vajpai N, Chiu EJ, et al. Facile backbone structure determination of human membrane proteins by NMR spectroscopy. Nat Methods. 2012;9(8):834-9.
9. Woo IS, Jin H, Kang ES, Kim HJ, Lee JH, Chang KC, et al. TMEM14A inhibits N-(4-hydroxyphenyl)retinamide-induced apoptosis through the stabilization of mitochondrial membrane potential. Cancer Lett. 2011;309(2):190-8.
10. Lee SH, Yoo TH, Nam BY, Kim DK, Li JJ, Jung DS, et al. Activation of local aldosterone system within podocytes is involved in apoptosis under diabetic conditions. Am J Physiol Renal Physiol. 2009;297(5):F1381-90.
11. Zhou LL, Cao W, Xie C, Tian J, Zhou Z, Zhou Q, et al. The receptor of advanced glycation end products plays a central role in advanced oxidation protein products-induced podocyte apoptosis. Kidney Int. 2012;82(7):759-70.
12. Zhou LL, Hou FF, Wang GB, Yang F, Xie D, Wang YP, et al. Accumulation of advanced oxidation protein products induces podocyte apoptosis and deletion through NADPH-dependent mechanisms. Kidney Int. 2009;76(11):1148-60.
13. Cardoso VG, Goncalves GL, Costa-Pessoa JM, Thieme K, Lins BB, Casare FAM, et al. Angiotensin II-induced podocyte apoptosis is mediated by endoplasmic reticulum stress/PKC-delta/p38 MAPK pathway activation and trough increased Na(+)/H(+) exchanger isoform 1 activity. BMC Nephrol. 2018;19(1):179.
14. Tao Y, Yazdizadeh Shotorbani P, Inman D, Das-Earl P, Ma R. Store-operated Ca(2+) entry inhibition ameliorates high glucose and Ang' induced podocyte apoptosis and mitochondria damage. Am J Physiol Renal Physiol. 2023.
15. Yamamoto K, Okabe M, Tanaka K, Yokoo T, Pastan I, Araoka T, et al. Podocytes are lost from glomeruli before completing apoptosis. Am J Physiol Renal Physiol. 2022;323(5):F515-F26.
16. Kimmel CB, Ballard WW, Kimmel SR, Ullmann B, Schilling TF. Stages of embryonic development of the zebrafish. Dev Dyn. 1995;203(3):253-310.
17. Khalil R, Lalai RA, Wiweger MI, Avramut CM, Koster AJ, Spaink HP, et al. Glomerular permeability is not affected by heparan sulfate glycosaminoglycan deficiency in zebrafish embryos. Am J Physiol Renal Physiol. 2019;317(5):F1211-F6.

18. Elmonem MA, Khalil R, Khodaparast L, Khodaparast L, Arcolino FO, Morgan J, et al. Cystinosis (ctns) zebrafish mutant shows pronephric glomerular and tubular dysfunction. Sci Rep. 2017;7:42583.
19. Hentschel DM, Mengel M, Boehme L, Liebsch F, Albertin C, Bonventre JV, et al. Rapid screening of glomerular slit diaphragm integrity in larval zebrafish. Am J Physiol Renal Physiol. 2007;293(5):F1746-50.
20. Hanke N, Staggs L, Schroder P, Litteral J, Fleig S, Kaufeld J, et al. "Zebrafishing" for novel genes relevant to the glomerular filtration barrier. Biomed Res Int. 2013;2013:658270.
21. Nagata M. Podocyte injury and its consequences. Kidney Int. 2016;89(6):1221-30.
22. Kok FO, Shin M, Ni CW, Gupta A, Grosse AS, van Impel A, et al. Reverse genetic screening reveals poor correlation between morpholino-induced and mutant phenotypes in zebrafish. Dev Cell. 2015;32(1):97-108.

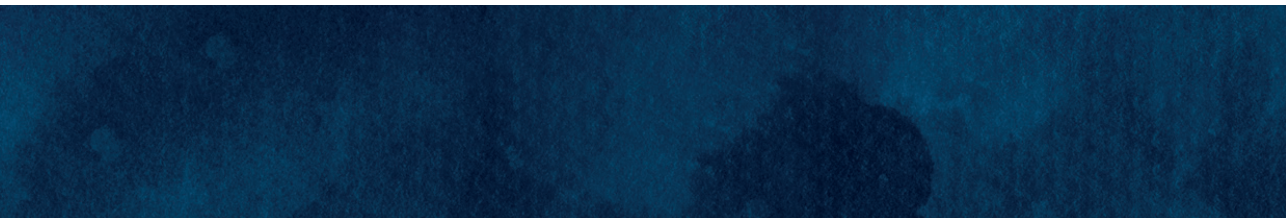

CHAPTER 7

General discussion and future perspectives

Patients with proteinuria can suffer from a myriad of diseases that cause protein to pass the glomerular filtration barrier and being insufficiently reabsorbed by the proximal tubule apparatus. These diseases include those that are histopathologically characterized by scarring and fibrosis of glomeruli, such as both primary and secondary focal segmental glomerulosclerosis, and diabetic nephropathy. Other types of diseases leading to proteinuria could be classified as auto-immune mediated, such as lupus nephritis and membraneous nephropathy. Moreover, many monogenetic diseases that cause proteinuria have been identified. Most of these display either a podocytopathy or a defect in tubular reabsorption. Although the underlying pathophysiological mechanisms differ between all of these diseases, they can share some elements in their respective pathways leading to proteinuria. As proteinuria is an independent risk factor for the progression of renal disease, cardiovascular morbidity, and overall mortality, treatments attenuating or relieving proteinuria are needed. Current treatment is mainly focused on the underlying disease and consists of reducing glomerular filtration pressure through inhibition of the renin-angiotensin-aldosterone system and, depending on whether an auto-immune or auto-inflammatory disease is involved, the addition of immunosuppressive drugs such as corticosteroids.

Elucidating the pathways leading to proteinuria is required to identify novel potential therapeutic targets for the treatment of proteinuria. Historically, the main constituents of the glomerular filtration barrier were identified through analysis of hereditary proteinuria syndromes, as also reviewed by Tryggvason *et al.*(16) For example, the slit diaphragm proteins of Nephrin (*NPHS1*) and Podocin (*NPHS2*), glomerular basement membrane protein Laminin (*LAMB2*), and transcription factors that influence podocyte gene expression (*WT1* and *ACTN4)* were all identified by investigation of monogenetic proteinuric diseases.

As eloquently said by Iain Drummond: 'unravelling the molecular pathogenesis of human disease presents many experimental challenges, not the least of which is that experiments on humans are generally frowned upon.(105)' Although experimentation on animals is also increasingly frowned upon and must rightfully adhere to rigorous ethical standards, it is currently still an indispensable element of pathophysiological research. In this thesis, a combination of cell culture, experimental animal models, histopathological examination of human tissue, and a patient cohort investigation were all employed to investigate pathways leading to proteinuria.

Nephropathic cystinosis

In chapter 2, an experimental zebrafish embryo model for the autosomal recessive disease of nephropathic cystinosis is introduced. Nephropathic cystinosis is a lysosomal storage disease where the *CTNS* gene is mutated, which leads to the accumulation of cystine in lysosomes. If left untreated, the disease is fatal.(106, 107) Currently, specific treatment is limited to cysteamine, which prevents further cystine accumulation but does not reverse the damage. Moreover, drug compliance is relatively low due to adverse effects of bad breath, skin odour, gastro-intestinal complaints such as nausea, vomiting, diarrhoea, and abdominal pain.(108-110) A *Ctns* knockout mouse has been developed, but this model lacks the glomerular changes also seen in nephropathic cystinosis.(111-113) The *ctns* -/- zebrafish mutant introduced in this study is presented as a promising model for the investigation of new therapeutic options and the pathophysiology of nephropathic cystinosis. The model displays a phenotype similar to that of the human disease, including cystine accumulation, increased glomerular permeability, and decreased proximal tubular reabsorption. They have higher mortality than wild-type animals. These last symptoms were preventable by treating mutant embryos with cysteamine. Renal and extrarenal manifestations of cystinosis have also been described in the adult model of this mutant.(114) The zebrafish cystinosis model has already been used to test novel treatment strategies for nephropathic cystinosis, such as luteolin, disulfiram, and bicalutamide-cysteamine.(115-118)

Heparan sulphate glycosaminoglycans

Chapters 3 and 4 discuss the previously held paradigm that heparan sulphate glycosaminoglycans are essential to glomerular filtration barrier function. This hypothesis was formulated by Kanwar and Farquhar several decades ago and was based on the finding that enzymatic removal of HS-GAG resulted in the loss of GFB integrity.(7, 8) Also, HS-GAG expression has been found to be reduced in various proteinuric renal diseases.(22) However, based on the results presented in chapters 3 and 4, homozygous germline mutations in zebrafish and, respectively, heterozygous mutations in humans of HS backbone elongating enzymes are shown not to result in proteinuria, nor a renal phenotype. The role of HS-GAG has long been thought to provide the GFB its charge selectivity due to the negatively charged sulphate groups of heparan sulphate. In chapter 3, we show that a significant reduction in negatively charged sites in the glomerular basement membrane does not result in proteinuria. Results from other experimental animal models with HS-GAG deficiencies are in line with this notion.(23-25, 27, 119) In chapter 4, the effect of heterozygous germline mutations on the backbone elongating

enzymes of heparan sulphate glycosaminoglycans was investigated in patients with multiple osteochondromas. Multiple osteochondroma is an autosomal dominant disease caused by a mutation in either EXT1 or EXT2 leading to the formation of, as the name implies, multiple osteochondromas.(59, 60, 69) We investigated a cohort of multiple osteochondroma patients in a cross-sectional manner and found that they did not exhibit proteinuria or an altered endothelial glycocalyx. Also, we investigated a historic cohort of patients who had both an osteochondroma resection and kidney biopsy in their medical history. Upon re-examination of the slides, no specific glomerular morphological changes were observed. One patient did show a glomerular phenotype on electron microscopy similar to that of a described case of 'MO glomerulopathy' with focal fibril deposition. (56) The rare cases of MO glomerulopathy are hypothesized to be caused by local loss of heterozygosity.

In conclusion, the results from these studies support the growing body of evidence that loss of heparan sulphate glycosaminoglycans does not result in loss of glomerular filtration barrier integrity, despite resulting in loss of negatively charged sites.

Dynamin and GTPases

One of the most promising potential therapeutic targets for the treatment of proteinuria is dynamin. Dynamin is known for its role clathrin-mediated endocytosis and synapse junction vesicle budding. Dynamin is a GTPase that forms a helical polymer around the neck of budding vesicles and causes membrane scission (120). In the kidney, it has been identified to be involved in the turnover of nephrin, direct interaction with actin and actin-regulatory proteins, and the endocytosis of albumin by podocytes. (11, 12, 14, 74) Its function depends on its oligomerization state and on whether it is cleaved by cathepsin L. (13, 14, 87, 121, 122) Schiffer *et al.* and Ono *et al.* demonstrated the potential of dynamin as a therapeutic target by treating several proteinuric animal models with Bis-T-23, which stimulates dynamin oligomerization. After administration, proteinuria decreased and the ultrastructure of podocyte foot processes was restored.(75, 76) In chapter 5, we show that glomerular dynamin mRNA expression increases before the onset of proteinuria and that both Dynamin and Cathepsin L protein expression is increased in proteinuric patients with various different underlying diseases. These results further support the suggested protective and dynamic role of dynamin in preventing the development of proteinuria through its interaction with the actin cytoskeleton and nephrin before the onset of proteinuria. As this mechanism also seems to play a role in proteinuric patients, this study further propagates the concept that dynamin and its regulation are potential therapeutic targets for the treatment of proteinuria.

Podocyte actin cytoskeletal regulation not only depends on dynamin, which is classed as a large GTPase, but also on the Rho-family of small GTPases like RhoA, Cdc42, and Rac1. They are involved in podocyte foot process motility and junctional and cytoskeletal interactions. Imbalances to the Rho GTPases are described to result in either hypo- or hypermobility of foot processes which both result in the progression of podocytopathy. (123) Rho GTPase signaling can be influenced by circulation factors such as soluble urokinase-type plasminogen activator receptor (suPAR), which activates Rac1. Inhibiting suPAR has been shown to inhibit podocyte injury *in vitro*. (124)

The results described in this thesis, combined with other literature on actin cytoskeleton regulation, expand the understanding that the GFB is not the static barrier it was once presumed to be, but rather an intricate apparatus that is dynamically regulated depending on local circumstances and circulating factors.

Transmembrane protein 14A

In chapter 6, transmembrane protein 14A (TMEM14A) is reported as another important protein in the preservation of adequate GFB function and integrity. It was previously implied to be involved in suppressing Bax mediated apoptosis.(95) Other than that, TMEM14A is a relatively unknown protein. Here, we identified it to be involved in the development of proteinuria by examining the results of a microarray study in spontaneously proteinuric Dahl SS rats. There, it was found to be significantly downregulated compared to spontaneously hypertensive, non proteinuric rats. To establish whether TMEM14A plays a direct and essential role in the development of proteinuria, a zebrafish embryo knockdown model was utilized. Results from this study shows that knocking down TMEM14A translation results in loss of GFB integrity without affecting tubular reabsorption capacity. Next, we show that both mRNA and protein expression of TMEM14A is reduced before onset of proteinuria. This study also reveals that glomerular TMEM14A expression is increased in proteinuric kidney disease, except in diabetic nephropathy. This result corresponds with *in vitro* findings, where inducing podocyte damage also increases TMEM14A expression. A protective mechanism by TMEM14A is proposed with a potential action mechanism through inhibiting podocyte apoptosis. Further studies are required to assess whether this is indeed the case. It would be of particular interest to identify up- and downstream modulators of TMEM14A expression and function.

Zebrafish embryo model

Zebrafish (*Danio rerio*) are freshwater fish originally from Southern Asia. They have become a widespread scientific model for the investigation of various pathophysiological

processes, including renal physiology. They are even part of the aquatic habitat on the International Space Station and are one of the few vertebrates to have lived a full life cycle in space.(125)

In chapters 2, 3, 5, and 6, an experimental zebrafish (*Danio rerio*) embryo model is used to assess whether knocking down mRNA translation of a single gene results in the development of proteinuria and whether tubular reabsorption mechanisms remain intact. Using this model presents several advantages compared to other experimental animal models. First, zebrafish embryos develop rapidly. Most major organs are formed within 40 hours post-fertilization. Due to their mostly transparent appearance, this development can be visualized relatively easily. Secondly, a single pair of adult zebrafish can lay over 200 eggs. Thus, in controlled conditions, it is possible to create high throughput models. The zebrafish embryo kidney consists of a pronephros with two nephrons that share a fused glomerulus in the midline of the body. Despite its simple structure compared to the more complex human metanephros, the zebrafish kidney shares many similar features with the kidneys of higher vertebrates and as such, is increasingly used as an experimental model for the study of cellular and molecular mechanisms of renal pathophysiology.(105, 126) Because of these characteristics, these animals are highly suited for investigating individual components of the pathways leading to proteinuria. (39, 40, 43, 82, 105, 126, 127)

In chapters 2 and 3, genetically mutated zebrafish were used as experimental models. In chapters 5 and 6, gene knockdown was effectuated by injecting zebrafish embryos with morpholino constructs. These constructs bind to mRNA and thus inhibit translation, leading to a functional knockdown of the targeted gene and its mRNA. In all these models, functional assays of glomerular filtration barrier integrity and tubular reabsorption were assessed by injecting a mixture of TRITC-labelled 3 kDa and FITC-labelled 70-kDa dextrans. As 3 kDa dextrans can freely pass the glomerular filtration barrier, they are reabsorbed in endosomes in the proximal tubule under physiological conditions. On the other hand, 70 kDa dextrans do not readily pass the GFB and as such, are only reabsorbed when GFB integrity is compromised. Thus, the presence of 3 kDa droplets was used to assess whether tubular reabsorption mechanism functions properly. The presence of 70 kDa was used to assess the loss of GFB integrity. This model was developed in these studies after adapting it from Hentschel *et al.* (40)

Other methods to assess GFB integrity in zebrafish embryos have also been developed by others. For example, a transgenic zebrafish expresses its main serum protein, vitamin D binding protein, bound with green fluorescent protein (EGFP). This model removes

the necessity to inject a dextran mixture but has no simultaneous assessment of tubular reabsorption function. With the introduction of this model, measuring the loss of fluorescence intensity in the zebrafish eye was also established as an indirect measurement of loss of GFB integrity. (45)

Spontaneously proteinuric rat model

Laboratory rats (*Rattus norvegicus domestica)* are perhaps the most well-known experimental animal model, after mice. The first documented experiment on rats was performed in France back in 1856 and consisted of the examination of the effects of adrenalectomy.(128) Rats were also ahead of zebrafish regarding space travel, as they had joined Soviet space dogs Belka and Strelka aboard the Sputnik 5 in 1960. In this thesis, the spontaneously proteinuric Dahl salt-sensitive rat strain was compared with nonproteinuric spontaneously hypertensive rats in chapters 5 and 6. Although these two strains have similar blood pressure levels, the Dahl rats become progressively proteinuric as they age. The cause of early onset albuminuria in Dahl rats was previously found to be a polygenic trait.(79) In that study, genome-wide linkage, and quantitative trait loci (QTL) mapping analysis was performed. These QTLs were subsequently used to identify individual genes that are involved in the development of proteinuria. This was done by microarray analysis on purified Dahl and SHR glomeruli and comparing the differential regulation in time to the previously defined QTLs. Dynamin, which is discussed in chapter 5, was one of the cytoskeleton-related genes identified in this manner. TMEM14A was one of the most markedly downregulated genes in the comparison of relative expression prior to QTL correlation.

Future perspectives

In conclusion, the work presented in this thesis adds to the knowledge of the pathways to proteinuria by both challenging the previously held tenet of a static filtration barrier and supporting the theories entailing a dynamically regulated interplay between the various layers of the glomerular filtration barrier in conjunction with the tubular reabsorption apparatus. As also reviewed by Comper *et al.*, the functionality of both the GFB and proximal tubular reabsorption seems to depend on whether proteinuric circumstances are present.(129) The expansion of comprehension of the pathophysiological mechanisms underlying pathways to proteinuria will be key to identifying new therapeutic targets. As described above, the novel zebrafish model of nephropathic cystinosis has already proven its worth for testing new therapeutic compounds whilst simultaneously offering new insights in the pathophysiology of cystinosis.

Regarding the role of negative charge and specifically, that of heparan sulphate glycosaminoglycans in the glomerular filtration barrier, it would be most interesting to investigate which proteins or circulating factors (next to the previously identified heparanase) influence its expression and degradation.(130, 131) Also, the changes in ligand binding ability of the glomerular glycocalyx might reveal more about the role of HS-GAG in maintaining GFB integrity.

Both large (dynamin) and small (Rho family) GTPases have already shown promise as therapeutic targets in preventing or even attenuating renal damage in proteinuric animal models. Compounds acting on these targets are yet to enter safety and efficacy testing for human trials but are an elegant example of translational medicine from a pathophysiological point of view. New potential targets, such as TMEM14A and its uncharted regulatory proteins, are being discovered at a high rate. As glomerular expression levels in human proteinuric kidneys in our TMEM14A experiments differed depending on etiology, it is conceivable that this particular pathway might not be of interest to all proteinuric diseases, but only a subset like diabetic nephropathy. It can be tentatively stated that the further identification of its protein-protein interactions including up- and downstream effects will reveal if this pathway to proteinuria is indeed a feasible therapeutic option.

The zebrafish experimental animal model has presented itself as an expedient model for both identifying and testing therapeutic targets. Further innovations in experimental animal models and especially in non-animal models such as organoids, will hopefully increase the rate of discovering potential targets and screening the effectiveness of therapeutic compounds. Thus, by further illuminating the pathways to proteinuria we hope to keep advancing the field towards targeted treatment of proteinuria for the benefit of our patients.

References

1. Matsushita K, van d, V, Astor BC, Woodward M, Levey AS, de Jong PE, et al. Association of estimated glomerular filtration rate and albuminuria with all-cause and cardiovascular mortality in general population cohorts: a collaborative meta-analysis. Lancet. 2010;375(9731):2073-81.
2. Group CW. KDIGO clinical practice guideline for the evaluation and management of chronic kidney disease. Kidney Int Suppl. 2013.
3. Diseases GBD, Injuries C. Global burden of 369 diseases and injuries in 204 countries and territories, 1990-2019: a systematic analysis for the Global Burden of Disease Study 2019. Lancet. 2020;396(10258):1204-22.
4. Dane MJ, van den Berg BM, Lee DH, Boels MG, Tiemeier GL, Avramut MC, et al. A microscopic view on the renal endothelial glycocalyx. American journal of physiology Renal physiology. 2015;308(9):F956-66.
5. Dane MJ, Khairoun M, Lee DH, van den Berg BM, Eskens BJ, Boels MG, et al. Association of kidney function with changes in the endothelial surface layer. Clinical journal of the American Society of Nephrology : CJASN. 2014;9(4):698-704.
6. Rennke HG, Patel Y, Venkatachalam MA. Glomerular filtration of proteins: clearance of anionic, neutral, and cationic horseradish peroxidase in the rat. Kidney Int. 1978;13(4):278-88.
7. Kanwar YS, Farquhar MG. Presence of heparan sulfate in the glomerular basement membrane. Proceedings of the National Academy of Sciences of the United States of America. 1979;76(3):1303-7.
8. Kanwar YS, Linker A, Farquhar MG. Increased permeability of the glomerular basement membrane to ferritin after removal of glycosaminoglycans (heparan sulfate) by enzyme digestion. The Journal of cell biology. 1980;86(2):688-93.
9. Esko JD, Selleck SB. Order out of chaos: assembly of ligand binding sites in heparan sulfate. Annual review of biochemistry. 2002;71:435-71.
10. Miner JH. Glomerular basement membrane composition and the filtration barrier. Pediatric nephrology. 2011;26(9):1413-7.
11. Gu C, Chang J, Shchedrina VA, Pham VA, Hartwig JH, Suphamungmee W, et al. Regulation of dynamin oligomerization in cells: the role of dynamin-actin interactions and its GTPase activity. Traffic. 2014;15(8):819-38.
12. Gu C, Yaddanapudi S, Weins A, Osborn T, Reiser J, Pollak M, et al. Direct dynamin-actin interactions regulate the actin cytoskeleton. EMBO J. 2010;29(21):3593-606.
13. Sever S, Altintas MM, Nankoe SR, Moller CC, Ko D, Wei C, et al. Proteolytic processing of dynamin by cytoplasmic cathepsin L is a mechanism for proteinuric kidney disease. J Clin Invest. 2007;117(8):2095-104.
14. Soda K, Balkin DM, Ferguson SM, Paradise S, Milosevic I, Giovedi S, et al. Role of dynamin, synaptojanin, and endophilin in podocyte foot processes. J Clin Invest. 2012;122(12):4401-11.
15. Comper WD, Hilliard LM, Nikolic-Paterson DJ, Russo LM. Disease-dependent mechanisms of albuminuria. American journal of physiology Renal physiology. 2008;295(6):F1589-600.
16. Tryggvason K, Patrakka J, Wartiovaara J. Hereditary proteinuria syndromes and mechanisms of proteinuria. The New England journal of medicine. 2006;354(13):1387-401.
17. Koop K, Eikmans M, Wehland M, Baelde H, Ijpelaar D, Kreutz R, et al. Selective loss of podoplanin protein expression accompanies proteinuria and precedes alterations in podocyte morphology in a spontaneous proteinuric rat model. Am J Pathol. 2008;173(2):315-26.
18. Jungers P, Hannedouche T, Itakura Y, Albouze G, Descamps-Latscha B, Man NK. Progression rate to end-stage renal failure in non-diabetic kidney diseases: a multivariate analysis of determinant factors. Nephrol Dial Transplant. 1995;10(8):1353-60.

19. Jeansson M, Haraldsson B. Morphological and functional evidence for an important role of the endothelial cell glycocalyx in the glomerular barrier. Am J Physiol Renal Physiol. 2006;290(1):F111-F6.
20. Brenner BM, Hostetter TH, Humes HD. Molecular basis of proteinuria of glomerular origin. N Engl J Med. 1978;298(15):826-33.
21. Holmborn K, Habicher J, Kasza Z, Eriksson AS, Filipek-Gorniok B, Gopal S, et al. On the roles and regulation of chondroitin sulfate and heparan sulfate in zebrafish pharyngeal cartilage morphogenesis. J Biol Chem. 2012;287(40):33905-16.
22. van den Born J, van den Heuvel LP, Bakker MA, Veerkamp JH, Assmann KJ, Weening JJ, et al. Distribution of GBM heparan sulfate proteoglycan core protein and side chains in human glomerular diseases. Kidney Int. 1993;43(2):454-63.
23. Goldberg S, Harvey SJ, Cunningham J, Tryggvason K, Miner JH. Glomerular filtration is normal in the absence of both agrin and perlecan-heparan sulfate from the glomerular basement membrane. Nephrol Dial Transplant. 2009;24(7):2044-51.
24. Harvey SJ, Jarad G, Cunningham J, Rops AL, van d, V, Berden JH, et al. Disruption of glomerular basement membrane charge through podocyte-specific mutation of agrin does not alter glomerular permselectivity. Am J Pathol. 2007;171(1):139-52.
25. Chen S, Wassenhove-McCarthy DJ, Yamaguchi Y, Holzman LB, van Kuppevelt TH, Jenniskens GJ, et al. Loss of heparan sulfate glycosaminoglycan assembly in podocytes does not lead to proteinuria. Kidney Int. 2008;74(3):289-99.
26. Aoki S, Saito-Hakoda A, Yoshikawa T, Shimizu K, Kisu K, Suzuki S, et al. The reduction of heparan sulphate in the glomerular basement membrane does not augment urinary albumin excretion. Nephrol Dial Transplant. 2018;33(1):26-33.
27. Sugar T, Wassenhove-McCarthy DJ, Esko JD, van Kuppevelt TH, Holzman L, McCarthy KJ. Podocyte-specific deletion of NDST1, a key enzyme in the sulfation of heparan sulfate glycosaminoglycans, leads to abnormalities in podocyte organization in vivo. Kidney Int. 2014;85(2):307-18.
28. van Det NF, van den Born J, Tamsma JT, Verhagen NA, Berden JH, Bruijn JA, et al. Effects of high glucose on the production of heparan sulfate proteoglycan by mesangial and epithelial cells. Kidney Int. 1996;49(4):1079-89.
29. Singh A, Satchell SC, Neal CR, McKenzie EA, Tooke JE, Mathieson PW. Glomerular endothelial glycocalyx constitutes a barrier to protein permeability. Journal of the American Society of Nephrology : JASN. 2007;18(11):2885-93.
30. Lee JS, von der Hardt S, Rusch MA, Stringer SE, Stickney HL, Talbot WS, et al. Axon sorting in the optic tract requires HSPG synthesis by ext2 (dackel) and extl3 (boxer). Neuron. 2004;44(6):947-60.
31. Wiweger MI, Avramut CM, de Andrea CE, Prins FA, Koster AJ, Ravelli RB, et al. Cartilage ultrastructure in proteoglycan-deficient zebrafish mutants brings to light new candidate genes for human skeletal disorders. J Pathol. 2011;223(4):531-42.
32. Clement A, Wiweger M, von der HS, Rusch MA, Selleck SB, Chien CB, et al. Regulation of zebrafish skeletogenesis by ext2/dackel and papst1/pinscher. PLoS Genet. 2008;4(7):e1000136.
33. Wiweger MI, Zhao Z, van Merkesteyn RJ, Roehl HH, Hogendoorn PC. HSPG-deficient zebrafish uncovers dental aspect of multiple osteochondromas. PloS one. 2012;7(1):e29734.
34. van Eeden FJ, Granato M, Schach U, Brand M, Furutani-Seiki M, Haffter P, et al. Genetic analysis of fin formation in the zebrafish, Danio rerio. Development. 1996;123:255-62.
35. Faas FG, Avramut MC, van den Berg BM, Mommaas AM, Koster AJ, Ravelli RB. Virtual nanoscopy: generation of ultra-large high resolution electron microscopy maps. The Journal of cell biology. 2012;198(3):457-69.

36. de Andrea CE, Prins FA, Wiweger MI, Hogendoorn PC. Growth plate regulation and osteochondroma formation: insights from tracing proteoglycans in zebrafish models and human cartilage. J Pathol. 2011;224(2):160-8.
37. Hogendoorn PC, de Heer E, Weening JJ, Daha MR, Hoedemaeker PJ, Fleuren GJ. Glomerular capillary wall charge and antibody binding in passive Heymann nephritis. The Journal of laboratory and clinical medicine. 1988;111(2):150-7.
38. Gundersen HJ, Seefeldt T, Osterby R. Glomerular epithelial foot processes in normal man and rats. Distribution of true width and its intra- and inter-individual variation. Cell Tissue Res. 1980;205(1):147-55.
39. Ebarasi L, He L, Hultenby K, Takemoto M, Betsholtz C, Tryggvason K, et al. A reverse genetic screen in the zebrafish identifies crb2b as a regulator of the glomerular filtration barrier. Developmental biology. 2009;334(1):1-9.
40. Hentschel DM, Mengel M, Boehme L, Liebsch F, Albertin C, Bonventre JV, et al. Rapid screening of glomerular slit diaphragm integrity in larval zebrafish. American journal of physiology Renal physiology. 2007;293(5):F1746-50.
41. Schurer JW, Hoedemaeker J, Molenaar I. Polyethyleneimine as tracer particle for (immuno) electron microscopy. J Histochem Cytochem. 1977;25(5):384-7.
42. Rosenzweig LJ, Kanwar YS. Removal of sulfated (heparan sulfate) or nonsulfated (hyaluronic acid) glycosaminoglycans results in increased permeability of the glomerular basement membrane to 125I-bovine serum albumin. Lab Invest. 1982;47(2):177-84.
43. Hanke N, Staggs L, Schroder P, Litteral J, Fleig S, Kaufeld J, et al. "Zebrafishing" for novel genes relevant to the glomerular filtration barrier. BioMed research international. 2013;2013:658270.
44. Laurent TC, Sundelof LO, Wik KO, Warmegard B. Diffusion of dextran in concentrated solutions. Eur J Biochem. 1976;68(1):95-102.
45. Hanke N, King BL, Vaske B, Haller H, Schiffer M. A Fluorescence-Based Assay for Proteinuria Screening in Larval Zebrafish (Danio rerio). Zebrafish. 2015;12(5):372-6.
46. Rider SA, Bruton FA, Collins RG, Conway BR, Mullins JJ. The Efficacy of Puromycin and Adriamycin for Induction of Glomerular Failure in Larval Zebrafish Validated by an Assay of Glomerular Permeability Dynamics. Zebrafish. 2018;15(3):234-42.
47. Salmon AH, Satchell SC. Endothelial glycocalyx dysfunction in disease: albuminuria and increased microvascular permeability. J Pathol. 2012;226(4):562-74.
48. Miner JH. Glomerular filtration: the charge debate charges ahead. Kidney Int. 2008;74(3):259-61.
49. Nayak BR, Spiro RG. Localization and structure of the asparagine-linked oligosaccharides of type IV collagen from glomerular basement membrane and lens capsule. J Biol Chem. 1991;266(21):13978-87.
50. Bernard MA, Hogue DA, Cole WG, Sanford T, Snuggs MB, Montufar-Solis D, et al. Cytoskeletal abnormalities in chondrocytes with EXT1 and EXT2 mutations. J Bone Miner Res. 2000;15(3):442-50.
51. Lin X, Wei G, Shi Z, Dryer L, Esko JD, Wells DE, et al. Disruption of gastrulation and heparan sulfate biosynthesis in EXT1-deficient mice. Developmental biology. 2000;224(2):299-311.
52. Xu D, Esko JD. Demystifying heparan sulfate-protein interactions. Annual review of biochemistry. 2014;83:129-57.
53. Garsen M, Rops AL, Rabelink TJ, Berden JH, van der Vlag J. The role of heparanase and the endothelial glycocalyx in the development of proteinuria. Nephrol Dial Transplant. 2014;29(1):49-55.
54. Harvey SJ, Jarad G, Cunningham J, Rops AL, van der Vlag J, Berden JH, et al. Disruption of glomerular basement membrane charge through podocyte-specific mutation of agrin does not alter glomerular permselectivity. Am J Pathol. 2007;171(1):139-52.

55. Khalil R, Lalai RA, Wiweger MI, Avramut CM, Koster AJ, Spaink HP, et al. Glomerular permeability is not affected by heparan sulfate glycosaminoglycan deficiency in zebrafish embryos. American journal of physiology Renal physiology. 2019;317(5):F1211-F6.
56. Roberts IS, Gleadle JM. Familial nephropathy and multiple exostoses with exostosin-1 (EXT1) gene mutation. Journal of the American Society of Nephrology : JASN. 2008;19(3):450-3.
57. Colvin RB, Chang A. Diagnostic Pathology: Kidney Diseases: Elsevier Health Sciences; 2015.
58. Wuyts W, Van Hul W. Molecular basis of multiple exostoses: mutations in the EXT1 and EXT2 genes. Human mutation. 2000;15(3):220-7.
59. Bovee JV. Multiple osteochondromas. Orphanet journal of rare diseases. 2008;3:3.
60. Bovee JV, Hogendoorn PC. Multiple osteochondromas. In: Fletcher CDM, Unni KK, Mertens F, editors. World Health Organization classification of tumours : pathology and genetics tumours of soft tissue and bone. Lyon: IARC Publications; 2002. p. 360–2.
61. Le Merrer M, Legeai-Mallet L, Jeannin PM, Horsthemke B, Schinzel A, Plauchu H, et al. A gene for hereditary multiple exostoses maps to chromosome 19p. Human molecular genetics. 1994;3(5):717-22.
62. Hameetman L, Bovee JV, Taminiau AH, Kroon HM, Hogendoorn PC. Multiple osteochondromas: clinicopathological and genetic spectrum and suggestions for clinical management. Hereditary cancer in clinical practice. 2004;2(4):161-73.
63. Anower EKMF, Matsumoto K, Habuchi H, Morita H, Yokochi T, Shimizu K, et al. Glycosaminoglycans in the blood of hereditary multiple exostoses patients: Half reduction of heparan sulfate to chondroitin sulfate ratio and the possible diagnostic application. Glycobiology. 2013;23(7):865-76.
64. Hecht JT, Hall CR, Snuggs M, Hayes E, Haynes R, Cole WG. Heparan sulfate abnormalities in exostosis growth plates. Bone. 2002;31(1):199-204.
65. Reitsma S, Slaaf DW, Vink H, van Zandvoort MA, oude Egbrink MG. The endothelial glycocalyx: composition, functions, and visualization. Pflugers Archiv : European journal of physiology. 2007;454(3):345-59.
66. Deanfield JE, Halcox JP, Rabelink TJ. Endothelial function and dysfunction: testing and clinical relevance. Circulation. 2007;115(10):1285-95.
67. Stam F, van Guldener C, Becker A, Dekker JM, Heine RJ, Bouter LM, et al. Endothelial dysfunction contributes to renal function-associated cardiovascular mortality in a population with mild renal insufficiency: the Hoorn study. Journal of the American Society of Nephrology : JASN. 2006;17(2):537-45.
68. Lee DH, Dane MJ, van den Berg BM, Boels MG, van Teeffelen JW, de Mutsert R, et al. Deeper penetration of erythrocytes into the endothelial glycocalyx is associated with impaired microvascular perfusion. PloS one. 2014;9(5):e96477.
69. Bovee JV, Cleton-Jansen AM, Wuyts W, Caethoven G, Taminiau AH, Bakker E, et al. EXT-mutation analysis and loss of heterozygosity in sporadic and hereditary osteochondromas and secondary chondrosarcomas. American journal of human genetics. 1999;65(3):689-98.
70. Reijnders CM, Waaijer CJ, Hamilton A, Buddingh EP, Dijkstra SP, Ham J, et al. No haploinsufficiency but loss of heterozygosity for EXT in multiple osteochondromas. Am J Pathol. 2010;177(4):1946-57.
71. Wiweger MI, de Andrea CE, Scheepstra KW, Zhao Z, Hogendoorn PC. Possible effects of EXT2 on mesenchymal differentiation--lessons from the zebrafish. Orphanet J Rare Dis. 2014;9:35.
72. Eickhoff MK, Winther SA, Hansen TW, Diaz LJ, Persson F, Rossing P, et al. Assessment of the sublingual microcirculation with the GlycoCheck system: Reproducibility and examination conditions. PloS one. 2020;15(12):e0243737.
73. Raghavan V, Rbaibi Y, Pastor-Soler NM, Carattino MD, Weisz OA. Shear stress-dependent regulation of apical endocytosis in renal proximal tubule cells mediated by primary cilia. Proceedings of the National Academy of Sciences of the United States of America. 2014;111(23):8506-11.

74. Dobrinskikh E, Okamura K, Kopp JB, Doctor RB, Blaine J. Human podocytes perform polarized, caveolae-dependent albumin endocytosis. American journal of physiology Renal physiology. 2014;306(9):F941-51.
75. Schiffer M, Teng B, Gu C, Shchedrina VA, Kasaikina M, Pham VA, et al. Pharmacological targeting of actin-dependent dynamin oligomerization ameliorates chronic kidney disease in diverse animal models. Nature medicine. 2015;21(6):601-9.
76. Ono S, Kume S, Yasuda-Yamahara M, Yamahara K, Takeda N, Chin-Kanasaki M, et al. O-linked beta-N-acetylglucosamine modification of proteins is essential for foot process maturation and survival in podocytes. Nephrol Dial Transplant. 2017;32(9):1477-87.
77. Wang J, Duncan D, Shi Z, Zhang B. WEB-based GEne SeT AnaLysis Toolkit (WebGestalt): update 2013. Nucleic acids research. 2013;41(Web Server issue):W77-83.
78. Kanehisa M, Goto S. KEGG: kyoto encyclopedia of genes and genomes. Nucleic acids research. 2000;28(1):27-30.
79. Mehr AP, Siegel AK, Kossmehl P, Schulz A, Plehm R, de Bruijn JA, et al. Early onset albuminuria in Dahl rats is a polygenetic trait that is independent from salt loading. Physiological genomics. 2003;14(3):209-16.
80. Baelde JJ, Bergijk EC, Hoedemaeker PJ, de Heer E, Bruijn JA. Optimal method for RNA extraction from mouse glomeruli. Nephrology Dialysis Transplant. 1995;9:304-8.
81. Westerfield M. The zebrafish book : a guide for the laboratory use of zebrafish (Danio rerio). [Eugene, OR]: Institute of Neuroscience, University of Oregon; 2007.
82. Kimmel CB, Ballard WW, Kimmel SR, Ullmann B, Schilling TF. Stages of embryonic development of the zebrafish. Dev Dyn. 1995;203(3):253-310.
83. FEDERA. Human Tissue and Medical Research: Code of conduct for responsible use.2011.
84. Koop K, Eikmans M, Baelde HJ, Kawachi H, De Heer E, Paul LC, et al. Expression of podocyte-associated molecules in acquired human kidney diseases. Journal of the American Society of Nephrology : JASN. 2003;14(8):2063-71.
85. Chugh SS, Clement LC, Mace C. New insights into human minimal change disease: lessons from animal models. American journal of kidney diseases : the official journal of the National Kidney Foundation. 2012;59(2):284-92.
86. Davidson A. What is damaging the kidney in lupus nephritis? Nature reviews Rheumatology. 2016;12(3):143-53.
87. Sampogna RV, Al-Awqati Q. Taking a bite: endocytosis in the maintenance of the slit diaphragm. J Clin Invest. 2012;122(12):4330-3.
88. Qin XS, Tsukaguchi H, Shono A, Yamamoto A, Kurihara H, Doi T. Phosphorylation of nephrin triggers its internalization by raft-mediated endocytosis. Journal of the American Society of Nephrology : JASN. 2009;20(12):2534-45.
89. Waters AM, Wu MY, Huang YW, Liu GY, Holmyard D, Onay T, et al. Notch promotes dynamin-dependent endocytosis of nephrin. Journal of the American Society of Nephrology : JASN. 2012;23(1):27-35.
90. Garrett MR, Dene H, Rapp JP. Time-course genetic analysis of albuminuria in Dahl salt-sensitive rats on low-salt diet. Journal of the American Society of Nephrology : JASN. 2003;14(5):1175-87.
91. Garrett MR, Joe B, Yerga-Woolwine S. Genetic linkage of urinary albumin excretion in Dahl salt-sensitive rats: influence of dietary salt and confirmation using congenic strains. Physiological genomics. 2006;25(1):39-49.
92. Siegel AK, Kossmehl P, Planert M, Schulz A, Wehland M, Stoll M, et al. Genetic linkage of albuminuria and renal injury in Dahl salt-sensitive rats on a high-salt diet: comparison with spontaneously hypertensive rats. Physiological genomics. 2004;18(2):218-25.
93. Khalil R, Koop K, Kreutz R, Spaink HP, Hogendoorn PC, Bruijn JA, et al. Increased dynamin expression precedes proteinuria in glomerular disease. J Pathol. 2019;247(2):177-85.

94. Klammt C, Maslennikov I, Bayrhuber M, Eichmann C, Vajpai N, Chiu EJ, et al. Facile backbone structure determination of human membrane proteins by NMR spectroscopy. Nature methods. 2012;9(8):834-9.
95. Woo IS, Jin H, Kang ES, Kim HJ, Lee JH, Chang KC, et al. TMEM14A inhibits N-(4-hydroxyphenyl)retinamide-induced apoptosis through the stabilization of mitochondrial membrane potential. Cancer Lett. 2011;309(2):190-8.
96. Lee SH, Yoo TH, Nam BY, Kim DK, Li JJ, Jung DS, et al. Activation of local aldosterone system within podocytes is involved in apoptosis under diabetic conditions. American journal of physiology Renal physiology. 2009;297(5):F1381-90.
97. Zhou LL, Cao W, Xie C, Tian J, Zhou Z, Zhou Q, et al. The receptor of advanced glycation end products plays a central role in advanced oxidation protein products-induced podocyte apoptosis. Kidney Int. 2012;82(7):759-70.
98. Zhou LL, Hou FF, Wang GB, Yang F, Xie D, Wang YP, et al. Accumulation of advanced oxidation protein products induces podocyte apoptosis and deletion through NADPH-dependent mechanisms. Kidney Int. 2009;76(11):1148-60.
99. Cardoso VG, Goncalves GL, Costa-Pessoa JM, Thieme K, Lins BB, Casare FAM, et al. Angiotensin II-induced podocyte apoptosis is mediated by endoplasmic reticulum stress/PKC-delta/p38 MAPK pathway activation and trough increased Na(+)/H(+) exchanger isoform 1 activity. BMC Nephrol. 2018;19(1):179.
100. Tao Y, Yazdizadeh Shotorbani P, Inman D, Das-Earl P, Ma R. Store-operated Ca(2+) entry inhibition ameliorates high glucose and Ang induced podocyte apoptosis and mitochondria damage. American journal of physiology Renal physiology. 2023.
101. Yamamoto K, Okabe M, Tanaka K, Yokoo T, Pastan I, Araoka T, et al. Podocytes are lost from glomeruli before completing apoptosis. American journal of physiology Renal physiology. 2022;323(5):F515-F26.
102. Elmonem MA, Khalil R, Khodaparast L, Khodaparast L, Arcolino FO, Morgan J, et al. Cystinosis (ctns) zebrafish mutant shows pronephric glomerular and tubular dysfunction. Sci Rep. 2017;7:42583.
103. Nagata M. Podocyte injury and its consequences. Kidney Int. 2016;89(6):1221-30.
104. Kok FO, Shin M, Ni CW, Gupta A, Grosse AS, van Impel A, et al. Reverse genetic screening reveals poor correlation between morpholino-induced and mutant phenotypes in zebrafish. Dev Cell. 2015;32(1):97-108.
105. Drummond IA. Kidney development and disease in the zebrafish. Journal of the American Society of Nephrology : JASN. 2005;16(2):299-304.
106. Gahl WA, Thoene JG, Schneider JA. Cystinosis. The New England journal of medicine. 2002;347(2):111-21.
107. Town M, Jean G, Cherqui S, Attard M, Forestier L, Whitmore SA, et al. A novel gene encoding an integral membrane protein is mutated in nephropathic cystinosis. Nat Genet. 1998;18(4):319-24.
108. Dohil R, Fidler M, Barshop BA, Gangoiti J, Deutsch R, Martin M, et al. Understanding intestinal cysteamine bitartrate absorption. J Pediatr. 2006;148(6):764-9.
109. Besouw M, Blom H, Tangerman A, de Graaf-Hess A, Levtchenko E. The origin of halitosis in cystinotic patients due to cysteamine treatment. Molecular genetics and metabolism. 2007;91(3):228-33.
110. Ariceta G, Lara E, Camacho JA, Oppenheimer F, Vara J, Santos F, et al. Cysteamine (Cystagon(R)) adherence in patients with cystinosis in Spain: successful in children and a challenge in adolescents and adults. Nephrol Dial Transplant. 2015;30(3):475-80.
111. Cherqui S, Sevin C, Hamard G, Kalatzis V, Sich M, Pequignot MO, et al. Intralysosomal Cystine Accumulation in Mice Lacking Cystinosin, the Protein Defective in Cystinosis. Molecular and Cellular Biology. 2002;22(21):7622-32.

112. Gaide Chevronnay HP, Janssens V, Van Der Smissen P, N'Kuli F, Nevo N, Guiot Y, et al. Time course of pathogenic and adaptation mechanisms in cystinotic mouse kidneys. Journal of the American Society of Nephrology : JASN. 2014;25(6):1256-69.
113. Nevo N, Chol M, Bailleux A, Kalatzis V, Morisset L, Devuyst O, et al. Renal phenotype of the cystinosis mouse model is dependent upon genetic background. Nephrol Dial Transplant. 2010;25(4):1059-66.
114. Berlingerio SP, He J, De Groef L, Taeter H, Norton T, Baatsen P, et al. Renal and Extra Renal Manifestations in Adult Zebrafish Model of Cystinosis. Int J Mol Sci. 2021;22(17).
115. Taranta A, Elmonem MA, Bellomo F, De Leo E, Boenzi S, Janssen MJ, et al. Benefits and Toxicity of Disulfiram in Preclinical Models of Nephropathic Cystinosis. Cells. 2021;10(12).
116. Jamalpoor A, van Gelder CA, Yousef Yengej FA, Zaal EA, Berlingerio SP, Veys KR, et al. Cysteamine-bicalutamide combination therapy corrects proximal tubule phenotype in cystinosis. EMBO molecular medicine. 2021;13(7):e13067.
117. Jamalpoor A, Othman A, Levtchenko EN, Masereeuw R, Janssen MJ. Molecular Mechanisms and Treatment Options of Nephropathic Cystinosis. Trends Mol Med. 2021;27(7):673-86.
118. De Leo E, Elmonem MA, Berlingerio SP, Berquez M, Festa BP, Raso R, et al. Cell-Based Phenotypic Drug Screening Identifies Luteolin as Candidate Therapeutic for Nephropathic Cystinosis. Journal of the American Society of Nephrology : JASN. 2020;31(7):1522-37.
119. Wijnhoven TJ, Lensen JF, Wismans RG, Lamrani M, Monnens LA, Wevers RA, et al. In vivo degradation of heparan sulfates in the glomerular basement membrane does not result in proteinuria. J Am Soc Nephrol. 2007;18(3):823-32.
120. Praefcke GJ, McMahon HT. The dynamin superfamily: universal membrane tubulation and fission molecules? Nat Rev Mol Cell Biol. 2004;5(2):133-47.
121. Reiser J, Oh J, Shirato I, Asanuma K, Hug A, Mundel TM, et al. Podocyte migration during nephrotic syndrome requires a coordinated interplay between cathepsin L and alpha3 integrin. J Biol Chem. 2004;279(33):34827-32.
122. Yaddanapudi S, Altintas MM, Kistler AD, Fernandez I, Moller CC, Wei C, et al. CD2AP in mouse and human podocytes controls a proteolytic program that regulates cytoskeletal structure and cellular survival. J Clin Invest. 2011;121(10):3965-80.
123. Kistler AD, Altintas MM, Reiser J. Podocyte GTPases regulate kidney filter dynamics. Kidney Int. 2012;81(11):1053-5.
124. Rashmi P, Sigdel TK, Rychkov D, Damm I, Da Silva AA, Vincenti F, et al. Perturbations in podocyte transcriptome and biological pathways induced by FSGS associated circulating factors. Ann Transl Med. 2023;11(9):315.
125. Ijiri K. Life-cycle experiments of medaka fish aboard the international space station. Adv Space Biol Med. 2003;9:201-16.
126. Drummond IA, Majumdar A, Hentschel H, Elger M, Solnica-Krezel L, Schier AF, et al. Early development of the zebrafish pronephros and analysis of mutations affecting pronephric function. Development. 1998;125(23):4655-67.
127. Ebarasi L, Oddsson A, Hultenby K, Betsholtz C, Tryggvason K. Zebrafish: a model system for the study of vertebrate renal development, function, and pathophysiology. Current opinion in nephrology and hypertension. 2011;20(4):416-24.
128. Modlinska K, Pisula W. The Norway rat, from an obnoxious pest to a laboratory pet. Elife. 2020;9.
129. Comper WD, Vuchkova J, McCarthy KJ. New insights into proteinuria/albuminuria. Front Physiol. 2022;13:991756.
130. Garsen M, Rops AL, Rabelink TJ, Berden JH, van d, V. The role of heparanase and the endothelial glycocalyx in the development of proteinuria. Nephrol Dial Transplant. 2014;29(1):49-55.
131. Gil N, Goldberg R, Neuman T, Garsen M, Zcharia E, Rubinstein AM, et al. Heparanase is essential for the development of diabetic nephropathy in mice. Diabetes. 2012;61(1):208-16.

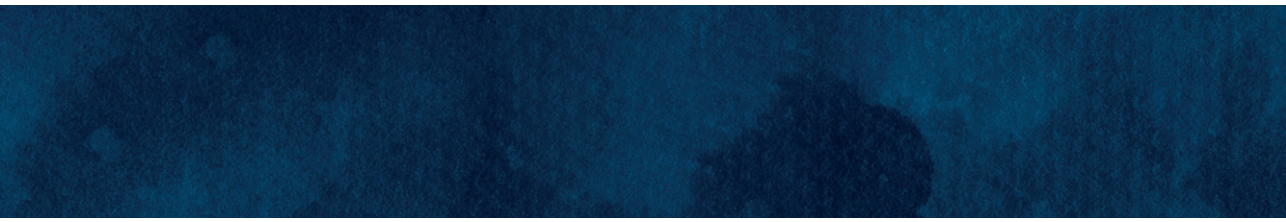

Appendices

Nederlandse samenvatting

Curriculum vitae

List of publications

Dankwoord

Nederlandse Samenvatting

Proteïnurie en chronische nierinsufficiëntie

Proteïnurie, het uitplassen van eiwit in de urine, is een onafhankelijke risicofactor van toename van schade aan de nier, ontwikkelen van cardiovasculaire ziekten en sterfte. In normale, fysiologische omstandigheden hebben mensen geen aanhoudende proteïnurie. Er komt pas eiwit in de urine wanneer deze door de filtereenheid van de nier, de glomerulus, gaat en vervolgens niet wordt opgenomen in de tubulus van de nier. Als een van deze onderdelen beschadigd raakt, kan dat leiden tot proteïnurie.

De glomerulaire filtratiebarrière

In afbeelding 1 wordt een schematisch overzicht getoond van de anatomie van de nier in verschillende niveaus van detail. In de afbeelding links boven is de locatie van de nieren zichtbaar, samen met een dwarsdoorsnede van een nier. Een menselijke nier bevat ongeveer een miljoen functionele eenheden die nefronen worden genoemd. Onder de dwarsdoorsnede van een nier staat een schematische voorstelling van twee nefronen. Elk nefron bestaat uit een capillaire vaatkluwen, of glomerulus, waar de filtratie plaats vindt. Deeltjes die groot zijn of een negatieve lading hebben, passeren minder gemakkelijk dan kleinere deeltjes of deeltjes die positief geladen zijn. De glomerulus wordt begrensd door de glomerulaire filtratiebarrière (GFB), wat de grens vormt tussen het bloed en de pre urine. Rechtsboven is een detail van een glomerulus te zien. In de afbeeldingen daaronder zijn een doorsnede van een capillair en een detail van de GFB weergeven. Elk vaatkluwen wordt overdekt door gespecialiseerde cellen die de vaatjes bedekken met uitlopers die ook 'voetuitlopers' worden genoemd. Daarom heten deze cellen ook wel podocyten, van het Griekse ποδος (voet) en κύτος (container, cel). Tussen deze podocyten en de cellen die het capillair vormen, de glomerulaire endotheelcellen, zit een gel-achtige laag die door beide cellen wordt gemaakt. Dat is de glomerulaire basaalmembraan (GBM). De endotheelcellen van het capillair zijn gespecialiseerde cellen. Ze worden bedekt door een laag met suikerketens (de glycocalyx) en zijn gefenestreerd. In het onderste detail zijn de verschillende lagen zichtbaar die samen de glomerulaire filtratiebarrière (GFB) vormen.

In het onderste detail van afbeelding 1 zijn de aparte lagen van de GFB schematisch weergeven. Van onder naar boven (of van bloed naar pre urine) zijn dit de glomerulaire endotheliale glycocalyx (paars), gefenestreerde endotheelcellen (rood), glomerulaire basaalmembraan (grijs) en de viscerale epitheelceelcellen – of podocyten – inclusief de voetuitlopers hiervan (geel/groen).

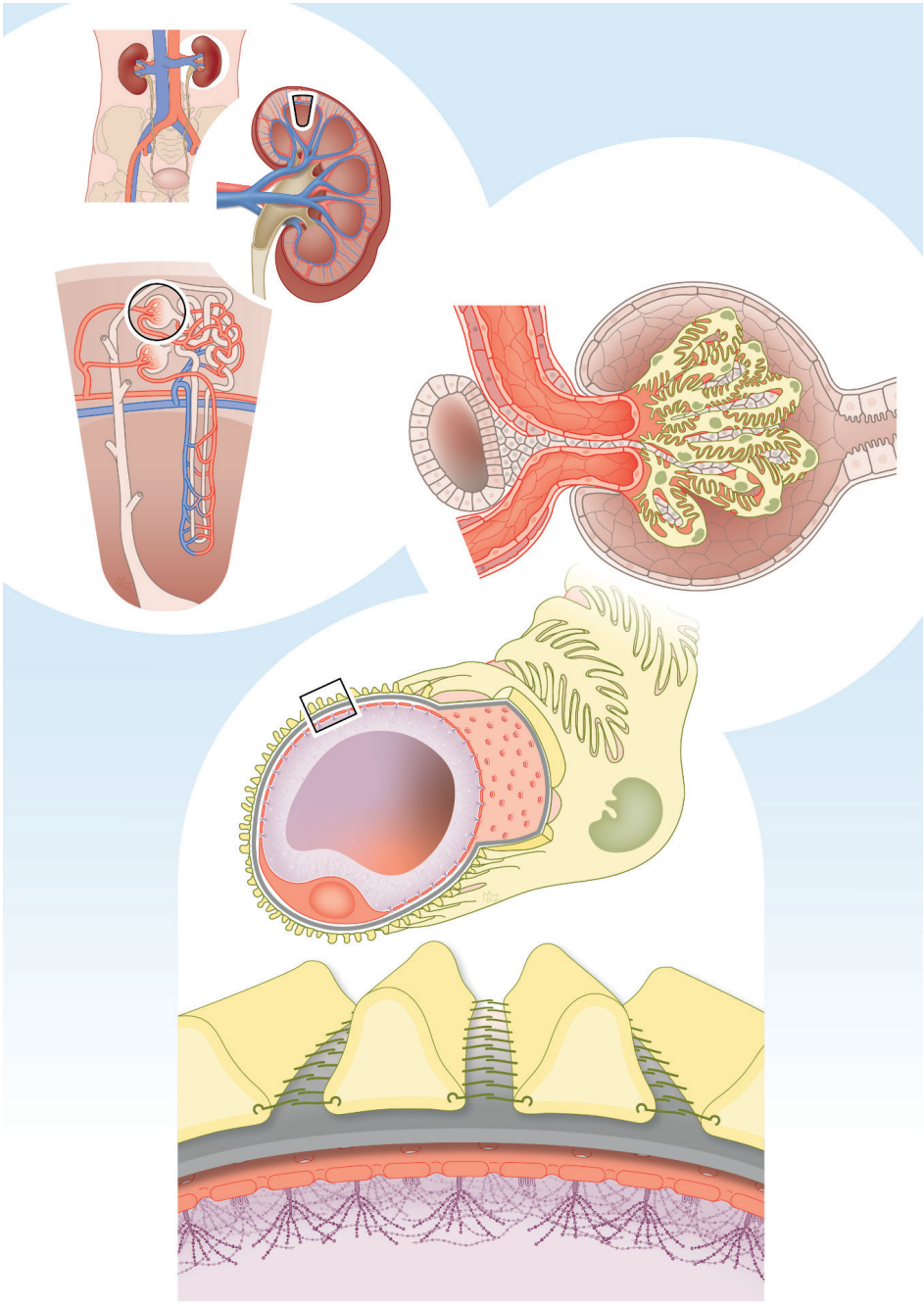

Afbeelding 1. De anatomie van de nier, het nefron, de glomerulus en de glomerulaire filtratiebarrière.

De pathofysiologische processen die ten grondslag liggen aan verschillende met proteïnurie gepaard gaande nierziekten, kunnen ver uiteen liggen. Zo zijn er aandoeningen die vooral gekenmerkt worden door verlittekening van glomeruli, zoals focale segmentale focale glomerulosclerose en diabetische nefropathie. Andere ziektes worden juist weer vooral als auto-immuun aandoeningen geclassificeerd, zoals lupus nefritis en membraneuze nefropathie. Daarnaast zijn er ook verschillende monogenetische aandoeningen die gepaard gaan met proteïnurie. In deze ziektes is er vaak sprake van een podocytopathie of probleem in de tubulaire reabsorptiecapaciteit. Hoewel de onderliggende pathofysiologische mechanismen tussen deze ziektes van elkaar verschillen, kunnen ze toch overlappende kenmerken hebben in de wijze waarop proteïnurie ontstaat.

Gezien proteïnurie een onafhankelijke risicofactor is voor progressie van schade aan de nier, cardiovasculaire ziektes en sterfte, is het verminderen (of voorkómen) van proteïnurie een van de doelen in het behandelen van patiënten met chronische nierinsufficiëntie. De behandeling van chronische nierinsufficiëntie richt zich tot op heden vooral nog op algemeen (cardio)vasculair risicomanagement, zoals het verlagen van de bloeddruk en het cholesterol, maar er is nog geen behandeling die zich specifiek op de proteïnurie richt. Om dat mogelijk te kunnen maken, is een beter begrip vereist van de mechanismen die leiden tot het ontstaan van proteïnurie. In dit proefschrift wordt een combinatie van experimenten in celkweek, experimentele diermodellen, histopathologisch onderzoek en een patiënt cohort onderzoek toegepast om de paden leidend tot proteïnurie verder te onderzoeken.

Nefropathische cystinose

In hoofdstuk 2 wordt een experimenteel zebravissenembryo model van de erfelijke aandoening 'nefropathische cystinose' geïntroduceerd. Nefropathische cystinose is een monogenetische aandoening. Een mutatie in het *CTNS* gen leidt tot stapeling van cystine in lysosomen, wat kristalvorming en schade aan weefsels veroorzaakt. Zonder behandeling is nefropathische cystinose een dodelijke aandoening. De behandeling is nu nog beperkt tot het gebruik van cysteamine. Dit middel voorkomt nieuwe schade, maar kan bestaande schade niet herstellen. Daarnaast kent het vele bijwerkingen, zoals misselijkheid, braken en diarree. Het hier geïntroduceerde model van een zebravisembryo met homozygote *ctns* mutatie vertoont veel overeenkomsten met het fenotype van nefropathische cystinose in de mens. De gemuteerde zebravissenembryo's ontwikkelen stapeling van cystine, vertraagde ontwikkeling en glomerulaire en tubulaire dysfunctie. Behandeling met cysteamine kon deze schade deels voorkomen. Hiermee wordt aangetoond dat dit een geschikt experimenteel model is voor het onderzoeken van de pathofysiologie en eventuele nieuwe behandelingen van nefropathische cystinose.

Heparan sulfaat glycosaminoglycanen

In hoofdstukken 3 en 4 worden heparan sulfaat glycosaminoglycanen onderzocht. Heparan sulfaat glycosaminoglycanen (HS-GAG) bestaan uit aggregaten van negatief geladen, gesulfateerde suikerketens die vastzitten aan een kerneiwit. Deze aggregaten bevinden zich in de glomerulaire basaalmembraan en glycocalyx. Verschillende enzymen en co-polymerases zijn vereist om HS-GAG te kunnen vormen, waaronder EXT1 en EXT2. Lang werd gedacht dat HS-GAG essentieel is voor het behoud van de barrière in de glomerulus. De hypothese was dat dit zowel door hun vorm als negatieve lading kwam. Recente studies trekken deze theorie echter in twijfel. In hoofdstuk 3 en 4 wordt beschreven dat mutaties in genen die essentieel zijn voor de vorming van HS-GAG niet leiden tot proteïnurie. Hoofdstuk 3 gebruikt hiervoor het *dackel* zebravissenembryo model. De in dit model onderzochte zebravis embryo's hebben een homozygote kiembaan mutatie in 1 van 2 co-polymerases die essentieel zijn in de vorming van HS-GAG. Ondanks dat de hoeveelheid negatieve lading in de glomerulaire basaalmembraan verminderd is, wordt er in dit model geen proteïnurie geobserveerd. In hoofdstuk 4 wordt de rol van HS-GAG verder onderzocht in patiënten met het autosomaal dominant overervende ziektebeeld van 'multipele osteochondromen,' voorheen ook bekend als hereditaire multipele exostosen. Mensen met deze aandoening hebben in meer dan 85% van de gevallen een heterozygote kiembaan mutatie in het EXT1 of EXT2 gen. De ziekte wordt gekenmerkt door de vorming van meerdere osteochondromen. In hoofdstuk 4 wordt in een dwarsdoorsnede onderzoek van mensen met multipele osteochondromen aangetoond dat zij niet vaker proteïnurie of veranderingen aan de glycocalyx hebben dan mensen zonder multipele osteochondromen. Ook wordt in dit hoofdstuk een historisch cohortonderzoek beschreven. Dit cohort bestaat uit patiënten die ooit een resectie van een osteochondroom en nierbiopt hebben gehad. De pathologieverslagen en nierbiopten van deze patiënten zijn opnieuw onderzocht en er werden geen specifieke glomerulaire morfologische afwijkingen gezien. Wel werd in 1 patiënt een beeld gezien dat past bij een eerder beschreven casus van 'MO glomerulopathie', bestaande uit depositie van fibrillen. De zeldzame casus van MO glomerulopathie worden toegeschreven aan lokaal verlies van heterozygositeit.

De resultaten van hoofdstukken 3 en 4 komen overeen met andere studies waaruit blijkt dat verlies van HS-GAG niet leidt tot verlies van integriteit van de glomerulaire filtratiebarrière, ondanks dat er wel verlies is van negatieve lading.

Dynamin en GTPases

Dynamin is wellicht een van de meest veelbelovende potentiële therapeutische doelen voor de behandeling van proteïnurie. Dynamin is een eiwit dat vooral bekend is in

clathrin-gemedieerde endocytose en afsplitsing van vesikels in de synapsspleet. Deze processen zijn veel onderzocht in neuronen. Dynamin is een GTPase dat een helix-vormige polymeer om de hals van afsplitsende vesikels kan vormen om deze te splitsen van de onderliggende membraan. Van dynamin is beschreven dat het in de nier betrokken is bij de verwerking van nephrin, directe interactie met het cytoskelet van de podocyt via actin en actin-reguleerde eiwitten en in endocytose van albumine door podocyten. De functie van dynamin hangt af van de vorm, of staat van oligomerizatie, waar het zich in bevindt. Daarnaast kan dynamin inactief gemaakt worden door Cathepsin L. In twee recente studies wordt in verschillende experimentele proteïnurische diermodellen Bis-T-23 gebruikt als behandeling. Bis-T-23 stimuleert het oligomerizeren van dynamin. In deze experimenten leidde toediening van dit middel tot minder proteïnurie.

In hoofdstuk 5 wordt beschreven dat expressie van dynamin en Cathepsin L verhoogd is in patiënten met proteïnurische nierziekten. Ook wordt in een experimenteel model met een spontaan proteïnurische rat aangetoond dat de expressie van dynamin al verhoogd is voordat er proteïnurie optreedt. Deze resultaten ondersteunen de hypothese dat dynamin een beschermende rol heeft in de glomerulaire filtratiebarrière en een veelbelovend aangrijpingspunt is voor het behandelen van proteïnurie.

Transmembrane protein 14A

In hoofdstuk 6 wordt transmembrane protein 14A (TMEM14A) beschreven als een essentieel onderdeel van de glomerulaire filtratiebarrière. Van TMEM14A is bekend dat het mogelijk betrokken is bij het voorkomen van Bax-gemedieerde apoptose. Verder is het een relatief onbekend eiwit. In dit onderzoek wordt TMEM14A geïdentificeerd in de spontaan proteïnurische rat die ook in hoofdstuk 5 gebruikt is. Het lijkt vooral tot expressie te komen in podocyten. De expressie van TMEM14A blijkt significant lager te zijn in spontaan proteïnurische ratten dan in niet-proteïnurische ratten. Dit is al het geval voordat er proteïnurie optreedt. In een zebravissenembryo knockdown model wordt de translatie van de zebravissen homoloog van TMEM14A geblokkeerd, wat leidt tot verhoogde permeabiliteit van de glomerulaire filtratiebarrière. Vervolgens wordt aangetoond dat TMEM14A expressie verlaagd is in verschillende proteïnurische nierziekten in mensen, behalve bij diabetische nefropathie.

De resultaten van dit hoofdstuk introduceren TMEM14A als een element dat van belang is voor het intact houden van de glomerulaire filtratiebarrière. Meer onderzoek is nodig om vast te stellen hoe dit effect tot stand komt en of dit potentieel van andere factoren afhankelijk is.

Conclusie

Het doel van het onderzoek in dit proefschrift is om de paden leidend tot proteïnurie verder in kaart te brengen. De glomerulaire filtratiebarrière is niet een statische zeef. Het is een dynamisch gereguleerde machine, waarbij de verschillende onderdelen van zowel de filtratiebarrière als de tubulaire reabsorptie samenwerken. Het vergroten van het begrip van deze samenwerkende onderdelen zal de sleutel zijn tot het identificeren en ontwikkelen van nieuwe gerichte behandelingen van proteïnurie, die hopelijk zullen leiden tot een lagere ziektelast en betere gezondheid van onze patiënten.

Curriculum Vitae

Ramzi Khalil werd geboren in 1991 te Leiden. In 2009 behaalde hij het gymnasiumdiploma aan het Stedelijk Gymnasium Leiden, waar hij ook het Pre-University College doorliep van 2007 tot en met 2009.

In 2009 begon hij met de studie Geneeskunde in het Leids Universitair Medisch Centrum. Tijdens zijn studie nam hij deel aan het Honours College, waar hij als bachelor student begon met de eerste experimenten die al onderdeel waren van zijn promotieonderzoek (promotoren prof. P.C.W. Hogendoorn en prof. A.J. Rabelink, co-promotor J.J. Baelde). Van 2014 tot en met 2016 deed hij fulltime onderzoek in het kader van het MD-PhD programma van het Honours College. Hier begon hij op de afdeling Pathologie en werkte samen met de afdelingen Nierziekten, Moleculaire Celbiologie en Biologie. Van 2016 tot en met 2018 doorliep hij zijn co-schappen in de Leidse regio. Hij behaalde het artsexamen in 2018.

Tijdens zijn studie en onderzoek heeft Ramzi verschillende bestuursfuncties bekleed, waaronder Voorzitter der Medische Faculteit der Leidse Studenten in (2012 – 2013) , LUMC Studentenraad (2013 – 2014) , secretaris, vice-voorzitter en external affairs officer van de LUMC Association for PhD Candidates (2014 – 2016) alwaar hij ook plaats nam in de UMC werkgroep van het Promovendi Netwerk Nederland.

In 2020 begon Ramzi met de opleiding tot internist in het HagaZiekenhuis. In 2024 begon hij aan de differentiatie tot internist-nefroloog in het LUMC.

List of publications

Bavelaar, K.,* **Khalil, R.**,* Mutikainen, I. et al. A dinuclear silver compound with 5,6,7-trimethyl-[1,2,4]triazolo[1,5-a]pyrimidine with a short Ag–Ag bond. Synthesis, characterization, single-crystal structure analysis and cytostatic activity. *Inorganica Chica Acta* 2011, 366: 81-84

Elmonem, M., **Khalil, R.**, Khodaparast, L. et al. Cystinosis (ctns) zebrafish mutant shows pronephric glomerular and tubular dysfunction. *Scientific Reports* 2017, 7, 42583.

Khalil, R., Lalai, R.A., Wiweger, M.I., *et al.* Glomerular permeability is not affected by heparan sulfate glycosaminoglycan deficiency in zebrafish embryos. *American Journal of Physiology-Renal Physiology*. 2019, 317:5, F1211-F1216

Khalil, R., Boels, M.G.S., PALGA Group. *et al.* Mutations in the heparan sulfate backbone elongating enzymes EXT1 and EXT2 have no major effect on endothelial glycocalyx and the glomerular filtration barrier. *Molecular Genetics and Genomics* 2022, 297, 397–405

Khalil, R., Koop, K., Kreutz, R., Spaink, H.P., et al. Increased dynamin expression precedes proteinuria in glomerular disease. *Journal of Pathology* 2019, 247: 177-185.

Khalil, R., Bonnemaijer, J. D. D., Kreutz, *et al.* Transmembrane protein 14A protects glomerular filtration barrier integrity. *Physiological Reports* 2023, 11, e15847

Dankwoord

Van beginnend student geneeskunde tot arts in opleiding tot internist-nefroloog heb ik het voorrecht gehad om onderdeel te kunnen zijn van een geweldig team in wisselende samenstellingen. Mijn dank gaat uit naar eenieder die betrokken is geweest bij dit onderzoek. Hieronder zijn enkele personen die ik in het bijzonder wil bedanken.

Geachte professor Hogendoorn, beste Pancras, ik zal je altijd dankbaar voor je inzet om mijn opleiding tot onderzoeker succesvol af te ronden en ook voor je inzet voor alle opleidingen en studenten van het LUMC.

Geachte professor Rabelink, beste Ton, dank voor de fijne samenwerking en dat je voor mij en het team klaar hebt gestaan. Ik kijk uit naar onze verdere samenwerking in mijn opleiding tot nefroloog.

Geachte dr. Baelde, beste Hans, ik heb enorme bewondering voor al jouw kennis en vaardigheden en voel me bevoorrecht dat ik van je heb mogen leren.

Geachte professor Bruijn, beste J.A., dank voor je begeleiding en mentorschap tijdens het Honours College.

Geachte professor Spaink, beste Herman, dank voor het verbreden van mijn horizon en het begeleiden van mijn spreekwoordelijke sprong in het diepe bij het Instituut Biologie Leiden.

Geachte professor Levtchenko, beste Elena, bedankt voor de gastvrijheid in Leuven en de genomen moeite om van een idee op een congres samen een succesvol project te maken.

Beste Bart, Marion, Ron, Ingeborg en professor van Es, ik ben jullie dankbaar voor de waardevolle bijdragen in onze werkbesprekingen, waarin een groot deel van mijn wetenschappelijke vorming plaats vond.

Beste Kimberley, Cristina, Ulrike, Dave, Brendy, Peter en Frans, zonder jullie verschillende expertises had ik nooit zoveel verschillende labtechnieken kunnen leren en toepassen.

Een speciaal woord van dank wil ik wijden aan Nierstichting Nederland, die mij reeds als student hebben ondersteund om dit onderzoek mogelijk te maken.

Ook wil ik in het bijzonder de HME-MO vereniging Nederland bedanken voor de samenwerking en de gelegenheid meermaals op de landelijke dag aanwezig te zijn, waar ik weer kon zien waar al ons onderzoek uiteindelijk voor bedoeld is.

Beste coauteurs, dank voor het vertrouwen en jullie harde werk. Ik ben trots op onze samenwerking.

Dank aan mijn collega's en opvolgers in commissies en besturen van de M.F.L.S., LAP, het PNN en meer. Goed georganiseerde en democratische vertegenwoordiging is een groot goed om je voor in te zetten.

Lieve NePa's, beste Arda, Malu, Celine, Emilie, Chinar, Emma, Cleo, Nina, Tessa, Ling, Maria, Manon, Danielle, Suzanne en Marlies, ik heb ervan genoten met jullie samen te werken en jullie te zien floreren.

Niels, Lisa, Patrick en Maartje, honderd woorden van waardering zijn niet genoeg om jullie te bedanken voor jullie vriendschap.

Jamie en Pascal, jullie maakten van de reis een avontuur en in ons avontuur liggen vast nog veel reizen besloten.

Lieve Suzanne, dank voor je liefde, steun en inspiratie. Het mooiste hoofdstuk schrijven we samen.

Nadir en Sarah, mijn tweelingbroer en grote zus, ik zal altijd dankbaar naar jullie op blijven kijken.

Lieve papa en mama, ik ben hier, omdat jullie er altijd en onvoorwaardelijk voor ons zijn geweest. Dank jullie wel.